Coordination Chemistry Reviews 253 (2009) 1793–1832

Contents lists available at ScienceDirect

Coordination Chemistry Reviews

journal homepage: www.elsevier.com/locate/ccr

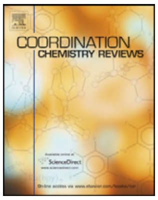

Review

Classification of P,N-binucleating ligands for hetero- and homobimetallic complexes

Simona Maggini

Universita' degli Studi di Milano, Dipartimento di Chimica Strutturale e Stereochimica Inorganica, Via G. Venezian 21, 20133 Milano, Italy

E-mail address: simona.maggini@unimi.it.

doi:10.1016/j.ccr.2009.01.030

ARTICLE INFO

Article history:
Received 12 November 2008
Accepted 27 January 2009
Available online 5 February 2009

This paper is dedicated to Nada e Luigi Poggiali.

Keywords:
Binuclear systems
Multidentate ligands
Multimetallic catalysts
Crystal engineering
Supramolecular chemistry

ABSTRACT

This review focuses on P,N-ligands capable of establishing binucleating interactions and on the resulting bimetallic complexes.

The work is grouped by the type of P,N-binucleating ligand backbones which are closely responsible for the chemistry of their correspondent bimetallic complexes. The P,N-binucleating ligands are classified according to their length (the number of atoms between the N- and P-donor), their backbone structure (the relative disposition of the N- and P-donor), and the presence or not of additional donor atoms.

Similarities between the structures of the bimetallic complexes obtained with P,N-ligands inside each group are highlighted. Based on the analysis of the different groups, the structure of new metallo/P,N-ligand complexes not yet synthesized can be hypothesized. A summary of the few examples of P,N-binucleating ligand based bimetallic complexes that have catalytic activity is given.

1. Introduction

The impetus for this review is the potential of bimetallic systems in catalysis combined with the successful[1] application of P,N-ligands in a wide range of monometallic catalytic processes, particularly asymmetric catalysis [1].

Bimetallic catalysts benefit from advantages such as metallic cooperation, a well-defined geometry, and new reactivity patterns [2–4]. However, only a limited number of man-made bimetallic catalysts are known and their catalytic potential has been only partially explored. Even fewer examples of successful bimetallic complexes containing P,N-ligands capable of establishing binucleating interactions (called P,N-binucleating ligands) exist.

The absence of a list of P,N-binucleating ligands and their bimetallic complexes synthesized to date, suggests the need for a review. The amount of literature available is large enough that it is possible to do a fairly comprehensive review based around structure. On the other hand, there is too much data available to discuss each complex in depth. Because of the possible importance of these ligands for catalysis, a summary of the catalytic results obtained is reported in the last section of the paper.

The choice of ligands was restricted. In the case of P,N-binucleating ligands with no additional donor atoms, only bimetallic complexes containing two P,N-binucleating ligands are discussed. Where P,N-binucleating ligands contain additional donor atom(s), only bimetallic complexes where each metal is P,N-coordinated are considered. No discussion of other binucleating ligands or of man-made bimetallic catalysts adopting ligands different from P,N-binucleating types will be given in this paper. For reference to these topics, reviews are cited [2–7].

2. Classification of P,N-binucleating ligands by their backbone unit

Ligands capable of forming bimetallic complexes are usually differentiated by the number and type of donor atoms possessed, and the length and the flexibility of the bridging unit. In a bimetallic complex, the structure of the bridging unit of the binucleating ligand is responsible for keeping the donor atoms of the ligand at a specific distance and for determining the relative disposition of the unsaturated coordinative sites around the two metal centers. This determines the Metal–Metal separation which affects the electronic interaction between the two metal centers and consequentially the chemistry of the correspondent bimetallic complex.

Since the backbone of the bridging unit is such an important parameter, a classification of P,N-binucleating ligands present in literature according to their different types of backbone units seems reasonable. In Table 1, a summary of the different class of backbone units treated in this review is shown along with a scheme of the correspondent bimetallic complex(es). For convenience only one P,N-binucleating ligand of the complex is shown in the scheme.

In the table, entry 1 refers to simple P,N-binucleating ligands differentiated by the number of atoms between their P- and N-donor. Entries 2–4, 5–6 and 7 refer to P,N-binucleating ligands containing respectively one, two, or four additional donor atoms. The presence of additional donor atom(s) can modify considerably the structure of the resulting bimetallic complex and increases the chance for the formation of multiple coordination modes of the P,N-ligand.

3. Discussion of bimetallic complexes containing two P,N-binucleating ligands: structural variation

This section discusses the main variations of structure within the bimetallic complexes. The basic terminology concerning structure here is applied in the rest of the review.

When considering the structural variation of a bimetallic complex containing two P,N-binucleating bridging ligands, the asymmetry of the ligands needs to be taken into account. For example, P,N-ligands bridging two metal centers, besides being arranged *cis* or *trans* to each other, can assume two possible configurations: head-to-tail and head-to-head. An example is given in Fig. 1, where the two type of structures are reported for *trans*,*trans*-$[\{PdCl\}_2(\mu\text{-}\mathbf{3}\text{-}\kappa N,\kappa P)_2]$ (for ligand **3** see Table 2) [8–10].

If the complex is heterobimetallic, then two head-to-head complexes can exist depending on the placement of the two metals in the different coordination sites. Based on the relative hardness/softness of the metals involved, different ratios of head-to-head and head-to-tail heterobimetallic complexes result. Hard metals bind more strongly with small electronegative donor

---

[1] The success of P,N-ligands is due to steric factors and their electronic asymmetry. P,N-ligands can stabilise metal ions in a variety of oxidation states. The π-acceptor character of the phosphorus stabilizes metal centers in low oxidation states, while the nitrogen σ-donor facilitates oxidative addition reactions on the metallic centre. The nitrogen donor is weakly coordinated to soft metal centers and can allow an open coordination site which is important for catalysis.

Table 1
Classification of P,N-binucleating ligands by backbone unit.

N.r	Bridging unit	Spacer atoms (n, m)	Metal binding mode
1	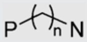	$n = 1$–5	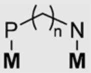
2	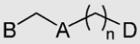	$n = 1$	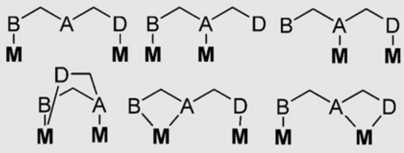
		$n = 2$	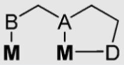
3		$n = 2$	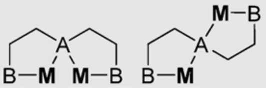
		$n = 3$	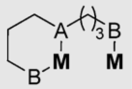
4	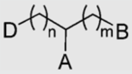	$n = 0$, $m = 0$	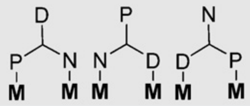
		$n = 0$, $m = 1$	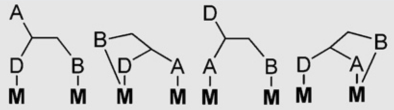
		$n = 1$, $m = 1$	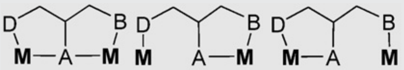
5	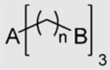	$n = 1$	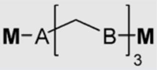
6	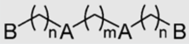	$n = 1$, $m = 1$	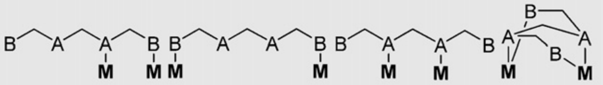
		$n = 1$, $m = 2, 3$	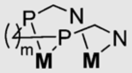
		$n = 2, 3$, $m = 0$–4	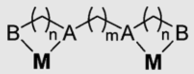
7	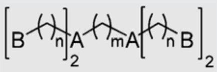	$n = 1$, $m = 2$	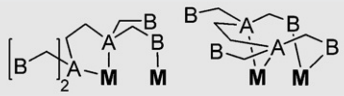
		$n = 2$, $m = 1$	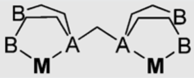
		$n = 2$, $m = 2, 5, 6$	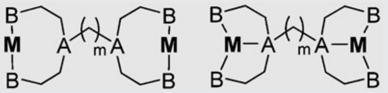

Key: A and B can be either N- or P-donor atoms but are dissimilar for the same molecule. If all coordination modes of the molecule are represented clearly using the symbols P and N, they are used instead of A and B. D is a generic additional donor atom, including but not limited to P or N. M represents a metal atom. Lower case *n* and *m* represent the number of atoms in a particular bridge.

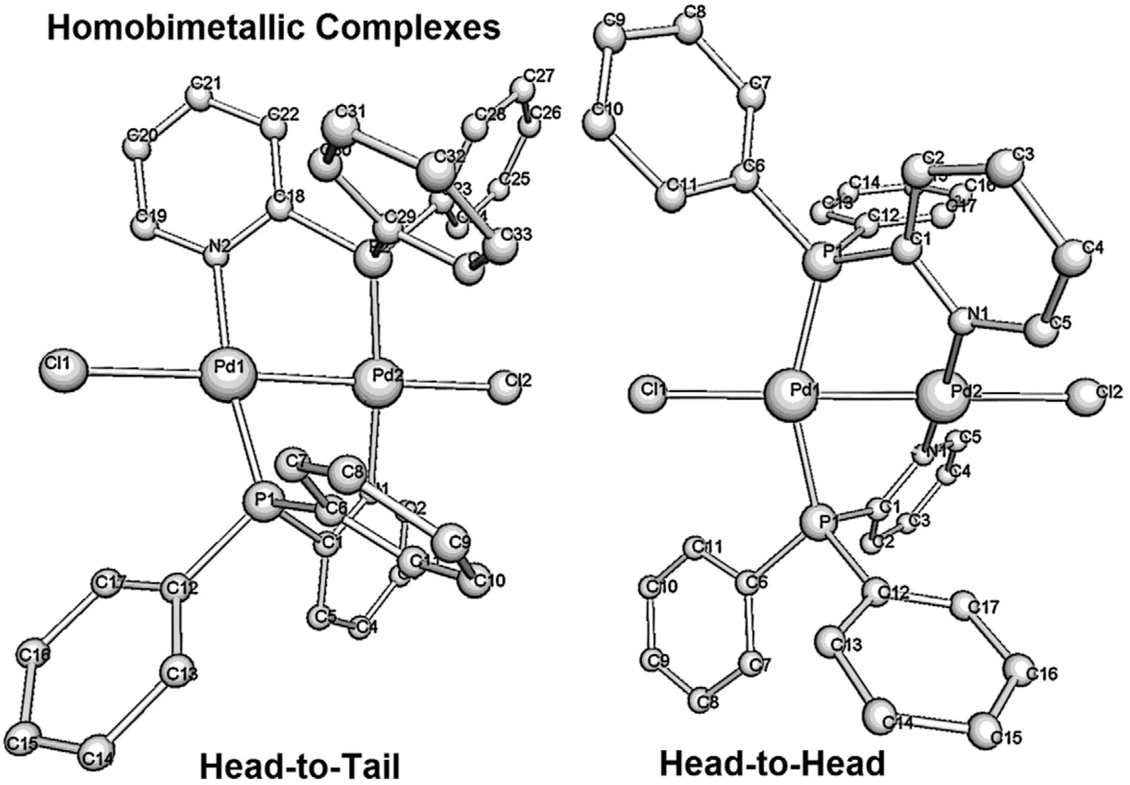

Fig. 1. Head-to-tail and head-to-head arrangement for *trans*,*trans*-[{PdCl}$_2$(μ-**3**-κ*N*,κ*P*)$_2$] (for ligand **3** see Table 2).

atoms (such as N) while soft metals have a greater affinity for less electronegative and more polarisable donor atoms (such as P). If one metal is much harder, the mixture is almost exclusively head-to-head. As the metals become more similar in character, the ratio changes until with two very similar metals, head-to-tail is dominant.

In homobimetallic systems, the tendency is for head-to-tail configurations. There are exceptions but often the exceptions occur when the two metallic centers have a different oxidation state. For example, in the stable complex [(CO)Co(μ-**3**-κ*N*,κ*P*)$_2$(μ-CO)CoCl] (Fig. 2), it is the different oxidation state of the two cobalt atoms (Co and Co^{I}) that favours the head-to-head configuration of the two P,N-binucleating ligands [11]. In other cases, the head-to-head homobimetallic complex is the kinetic product of the reaction but isomerises spontaneously to the thermodynamic product head-to-tail. In the kinetic product *cis*,*trans*-[Me$_2$Pt(μ-**3**-κ*N*,κ*P*)$_2$PtMe](CF$_3$CO$_2$) (Fig. 3), the electronic instability and internal strain, mostly due to the severe distortions from the ideal

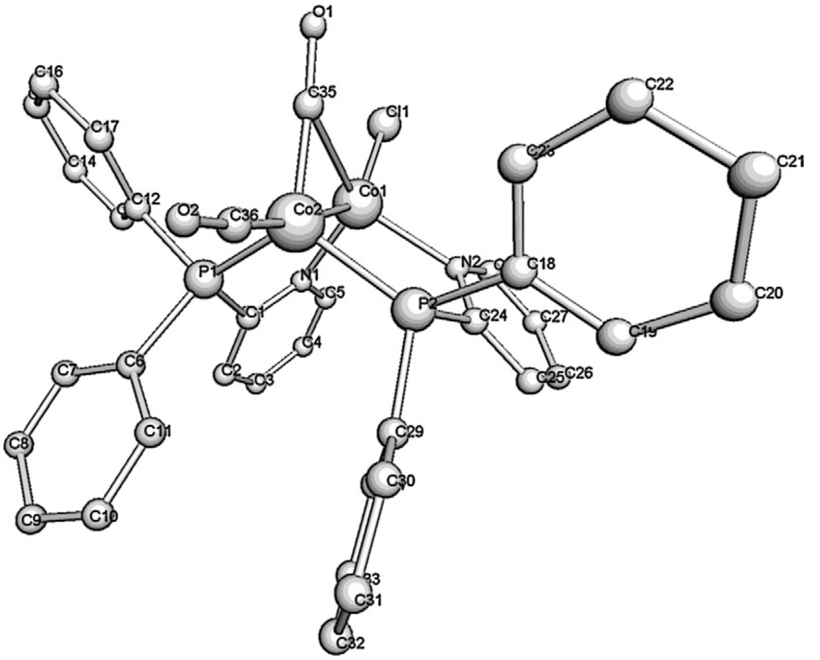

Fig. 2. Example of head-to-head homobimetallic complex with metals of different oxidation states: [(CO)Co(μ-**3**-κ*N*,κ*P*)$_2$(μ-CO)CoCl] (for ligand **3** see Table 2).

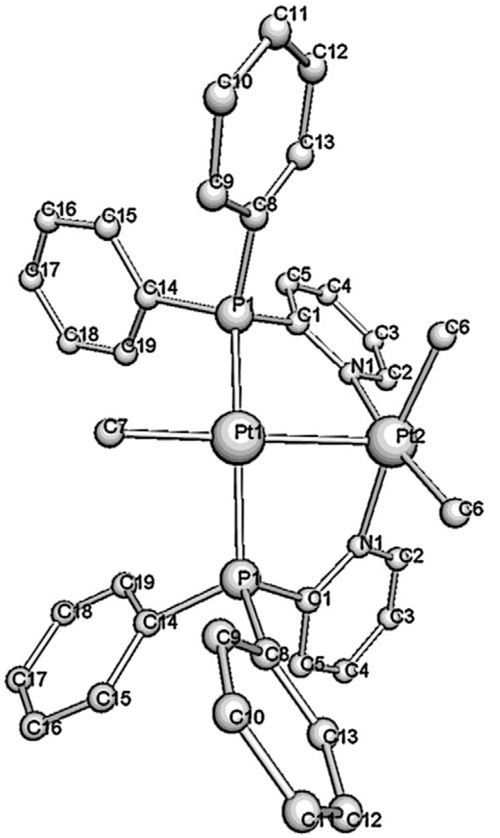

Fig. 3. Example of head-to-head homobimetallic complex obtained as kinetic product: *cis*,*trans*-[$Me_2Pt(\mu$-**3**-κ*N*,κ*P*$)_2PtMe](CF_3CO_2)$ (for ligand **3** see Table 2).

square planar geometry around the P-bound Pt center, seem to be the causes of its spontaneous isomerisation to the more stable head-to-tail structure [10,12].

Besides the two P,N-bridging ligands, the disposition of the other ligands in the bimetallic complex leads to additional structural classifications. In A-frame bimetallic complexes a bridging unit composed by one or more atoms is present between the two metallic centers. In *trans*,*trans*-[$\{RhCl\}_2(\mu$-**7**-κ*N*,κ*P*$)_2(\mu$-CO)] (for ligand **7** see Table 2), a CO unit bridges the two rhodium atoms giving a classic A-frame structure (Fig. 4) [13].

In side-by-side structures, such as in *trans*,*trans*-[$\{Pd(O_2CCH_3$-κ*O*$)\}_2(\mu$-**3**-κ*N*,κ*P*$)_2$], the additional ligands bound to the two metallic centers, like the acetate ligands in this case, are disposed on opposite sides (Fig. 5) [14].

In face-to-face structures, as in *trans*,*trans*-[$\{MoCl_2\}_2(\mu$-**8**-κ*N*,κ*P*$)_2$] (for ligand **8** see Table 2), the additional ligands bound to the metallic centers occupy both faces of the structure (Fig. 6) [15].

4. P,N-binucleating ligand structures

For clarity, the discussion of the complexes that result from each P,N-binucleating ligand will be divided into homo- and heterobimetallic complexes. This pattern is repeated for all the types of backbone units treated.

4.1. Structure 1: only one P- and one N-donor atom

See Table 2.

4.1.1. Homobimetallic complexes

This chapter deals with ligands containing only one P- and one N-donor separated by *n* equal to 0, 1, 2, 3 or more atoms.

4.1.1.1. n = 0. Ligand **2** was reacted with an equimolar amount of [$Zn(N(SiMe_3)_2)_2$] to give the bimetallic complex [$\{Zn(N(SiMe_3)_2\}_2$(**2**-κ*N*,κ*P*$)_2$] (**2a**) (Fig. 7, Table 3). In **2a** the two Zn centers bond with the two ligands to form a 6-membered ring that assumes a distorted boat conformation. The P–N distance in the ligand suggests a partial P=N double bond character [16].

A relatively flat 6-membered ring is formed by the two Pd centers and the two **1** (R = Ph) ligands in [$\{Pd(PPh_3)\}_2$(**1**-κ*N*,κ*P*$)_2$] (**1a**) (Fig. 7, Table 3). Here the two Pd centers are at a binding distance [17].

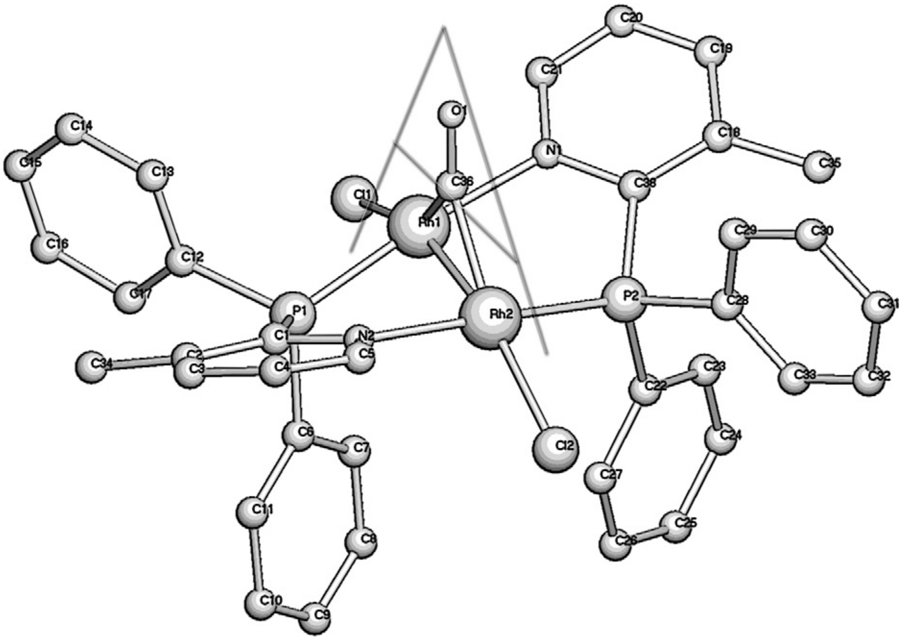

Fig. 4. Example of A-Frame structure: *trans*,*trans*-[$\{RhCl\}_2(\mu$-**7**-κ*N*,κ*P*$)_2(\mu$-CO)] (for ligand **7** see Table 2).

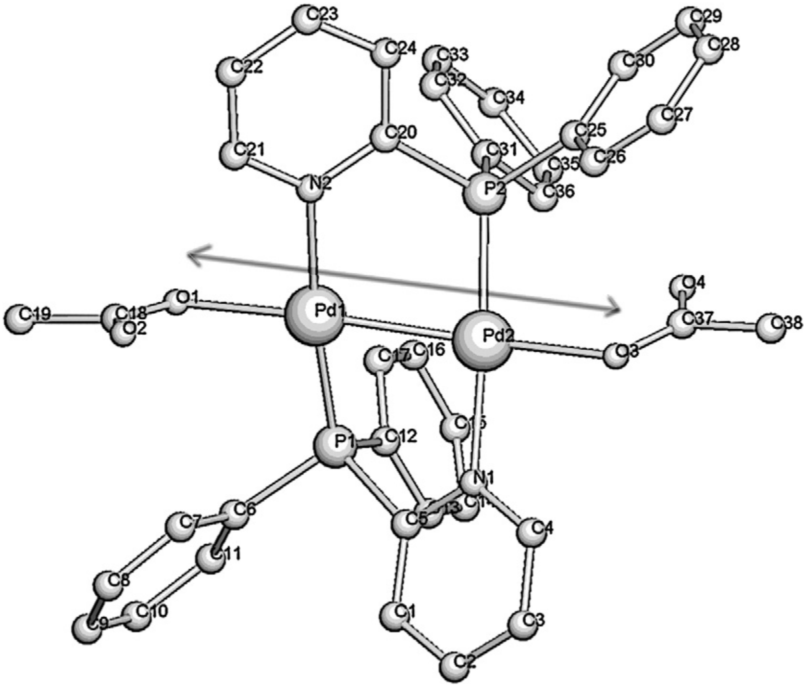

Fig. 5. Example of side-by-side structure: *trans*,*trans*-[{Pd(O_2CCH_3-κ*O*)}$_2$(μ-**3**-κ*N*,κ*P*)$_2$] (for ligand **3** see Table 2).

Table 2
Ligands discussed, classified by the number of atoms between the P- and N- donors.

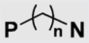	P,N-ligand
n = 0	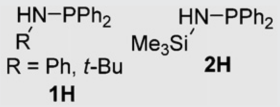 R = Ph, *t*-Bu **1H** **2H**
n = 1	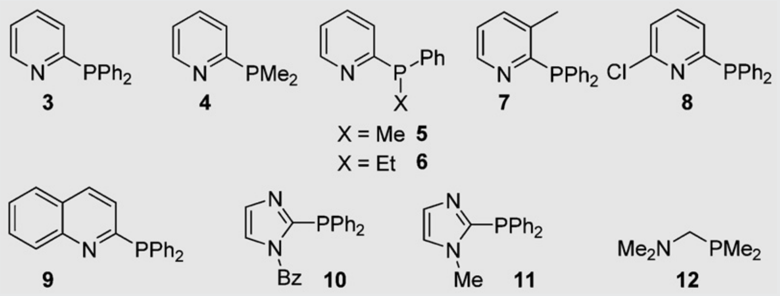 **3** **4** **7** **8** X = Me **5** X = Et **6** **9** **10** **11** **12**
n = 2	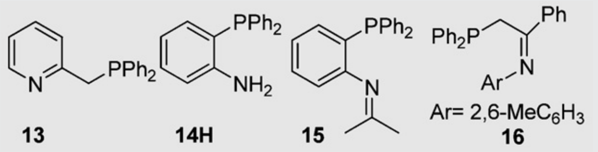 Ar= 2,6-MeC_6H_3 **13** **14H** **15** **16**
n = 3	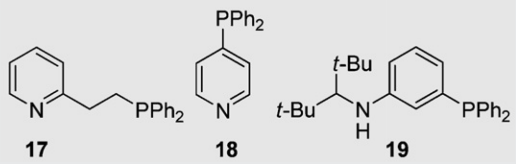 **17** **18** **19**
n > 3	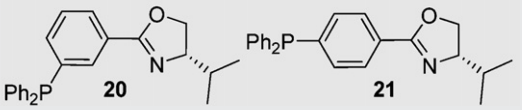 **20** **21**

Key: lower case n represents the number of spacer atoms in the bridge.

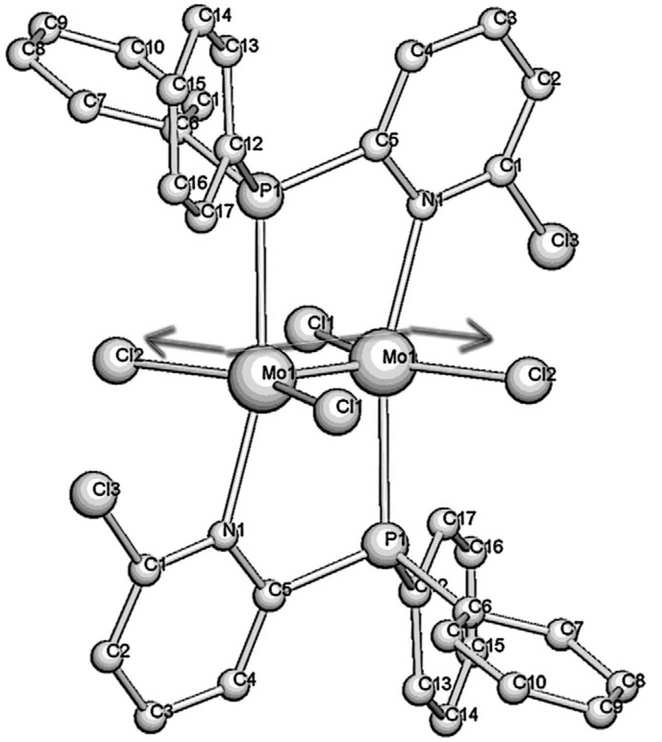

Fig. 6. Example of face-to-face structure: *trans*,*trans*-[$\{MoCl_2\}_2(\mu$-8-κ*N*,κ*P*$)_2$] (for ligand **8** see Table 2).

Table 3
Geometric parameters of the bimetallic complexes.

Complex	P–Metal–Metal–N	P–Metal–N	Metal–Metal
1a	3°	154°	2.59 Å
2a	16°	110°	3.80 Å
3a	7°	166°	2.19 Å
3b	33°, 38°	173°, 170°	2.59 Å
3c	43°	117°	4.06 Å
10a	20°	157°	3.10 Å
12a	2°, 0°	178°	2.61 Å
13a	48°	132°	2.92 Å
14a	70°, 66°	157°, 84°	2.55 Å
14b	78°	96°, 82°	3.27 Å
15a	4.5°	173°	2.84 Å
16a	12°	166°	2.70 Å
17a	14°	166°	5.08 Å
18a	7°	88°	7.74 Å
20a	56°, 53°	169°, 168°	4.91 Å
21a	6°, 5°	176°, 175°	7.12 Å

In both complexes the two P,N-ligands assume a head-to-tail arrangement.

4.1.1.2. n = 1. This situation, where the P- and N-donor are separated by only one atom, is the most common. In this category **3** is the most representative and widely used P,N-binucleating ligand [18–22]. Similar ligands but with a less bulky and more basic P-donor moiety, such as **4**, **5**, **6**, or with a slightly different electronic character of the pyridine ring, such as **7**, **8**, **9**, have been introduced successively. In other cases, the pyridine is replaced by an imidazole (**10**, **11**) or by an amine group (**12**).

The successful application of P,N-ligands with n = 1 for the synthesis of bimetallic complexes is due to the higher stability of the 5-membered ring obtained through the coordination of the P- and

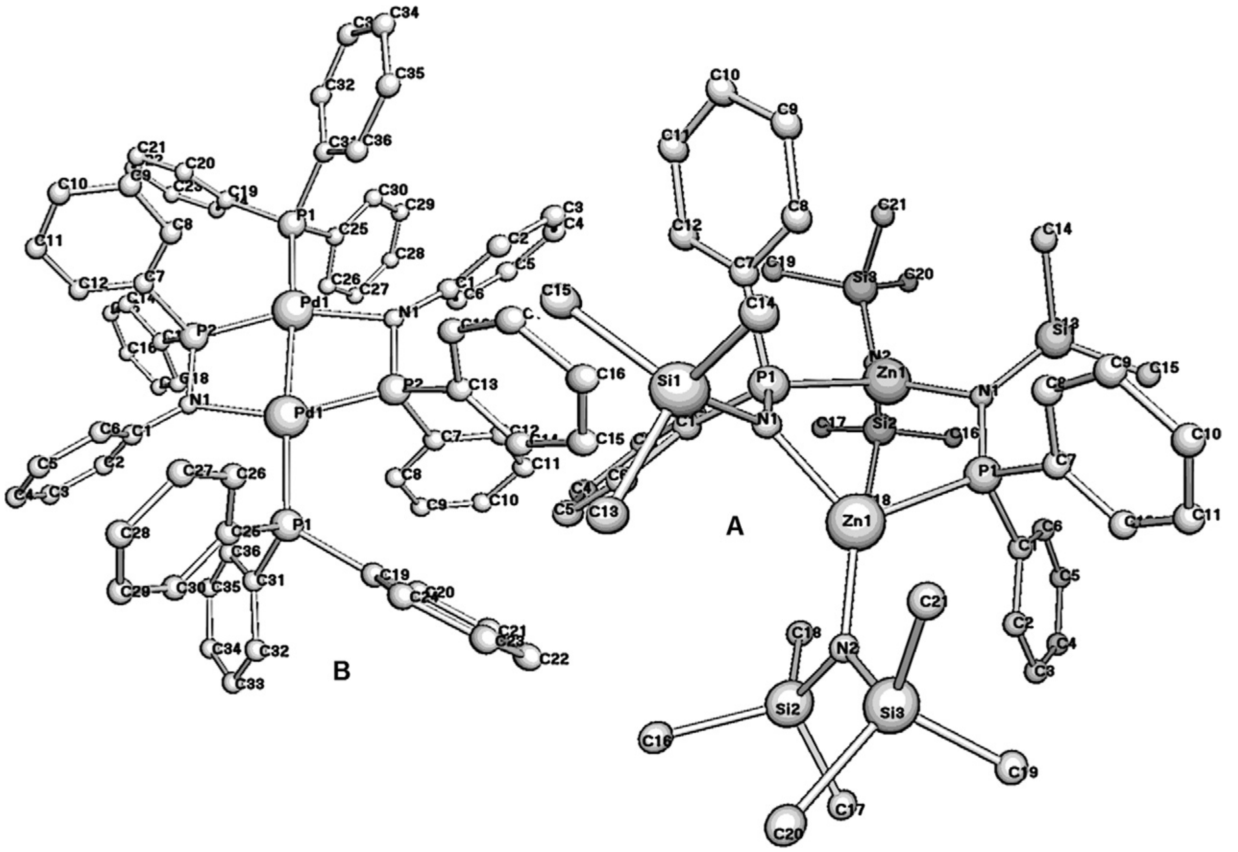

Fig. 7. Homobimetallic complexes: (A) [$\{Zn(N(SiMe_3)_2\}_2$(**2**-κ*N*,κ*P*$)_2$] (**2a**) and (B) *trans*,*trans*-[$\{Pd(PPh_3)\}_2$(**1**-κ*N*,κ*P*$)_2$] (**1a**).

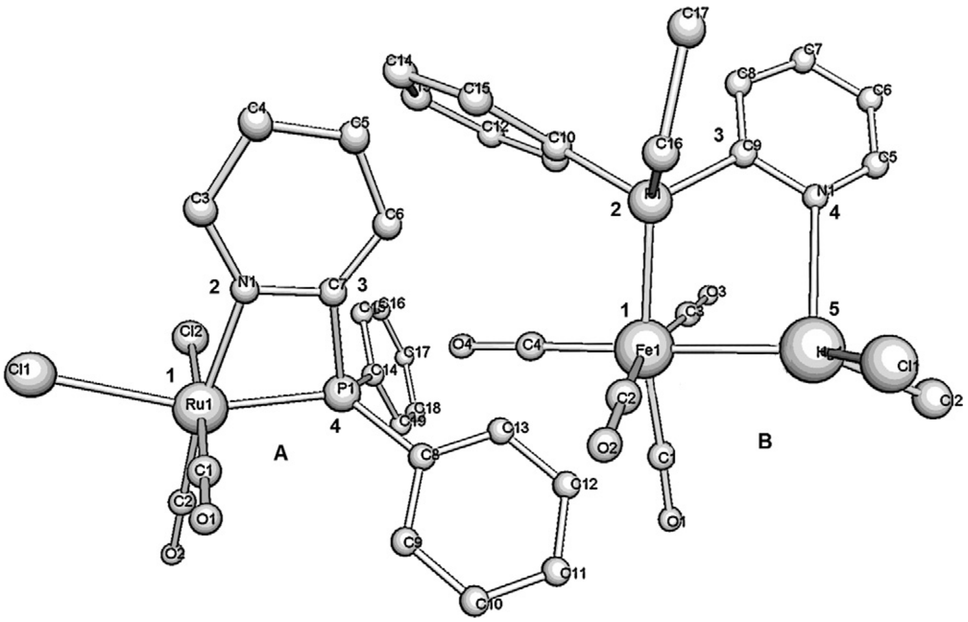

Fig. 8. Comparison of a 4-membered ring metallocycle versus a 5-membered ring bimetallocycle obtained respectively with ligands **3** and **6**: (A) [Ru(CO)$_2$Cl$_2$(**3**-κ*N*,κ*P*)] and (B) [(CO)$_4$Fe(μ-**6**-κ*N*,κ*P*)HgCl$_2$].

N-donor to two metallic centers (as opposed to the strained 4-membered ring formed with only one metal center) (Fig. 8).

P,N-ligands with n = 1 do not allow a large Metal. . .Metal separation in their correspondent bimetallic complexes. Only the adoption of a skewed conformation by the Metal–P–C–N–Metal 5-membered ring, which corresponds to higher values of the N–Metal–Metal–P torsional angles, allows a minimum variation in the distance between the two metal centers (Fig. 9). Consequentially, the formation of Metal–Metal bonds in their bimetallic complexes is usually strongly induced unless steric factors or the presence of bridging atoms between the two metallic centers prevent the bond [23–25,12,26–34].

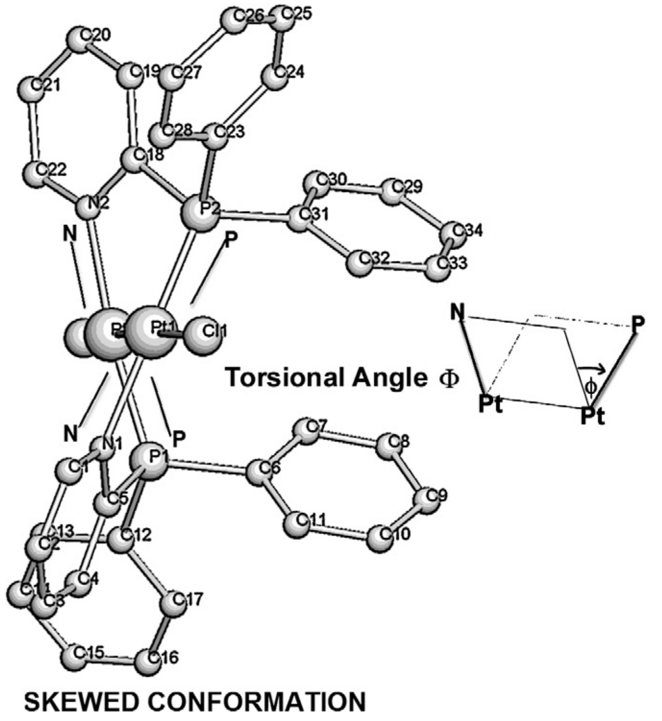

Fig. 9. Example of skewed conformation showing relation to torsional angle: *trans*,*trans*-[{PtCl}$_2$(μ-**3**-κ*N*,κ*P*)$_2$].

In homobimetallic complexes containing two **3** bridging ligands, the Metal–Metal separation ranges from 2.2 Å to 4.4 Å, with N–Metal–Metal–P torsional angles ranging from ~1° to 60°. Similar parameters are found for the homobimetallic complexes obtained with **4**, **5**, **6**, **7**, **8**, and **9**.

When a triple [35,36] or a quadruple [37,38,15] Metal–Metal bond is involved in the bimetallic complex, an eclipsed conformation of the two metallic centers is preferred in order to maximize the Metal–Metal bonding; this is reflected by the low values of N–Metal–Metal–P torsional angles. Complex *trans*,*trans*-[{MoCl}$_2$(μ-**3**-κ*N*,κ*P*)$_2$(μ-O$_2$CCH$_3$-κ^2*O*,*O*′)$_2$] (**3a**) (Fig. 10, Table 3) is a typical example of this case, where the Mo$_2$$^{\mathrm{II}}$ quadruple bond favours an almost eclipsed conformation [37].

In general, homobimetallic complexes obtained with **10**, **11**, and **12** are similar to those obtained with **3** but have smaller N–Metal–Metal–P torsional angles (ranging from ~1° to 25° for the imidazole ligands). For example, in *trans*,*trans*-[{PdCl}$_2$(μ-**12**-κ*N*,κ*P*)$_2$] (**12a**) the Pd–Pd single bond is slightly longer than in *trans*,*trans*-[{PdCl}$_2$(μ-**3**-κ*N*,κ*P*)$_2$] (**3b**), and the two **12** ligands are closer to being coplanar with the two Pd centers almost eclipsed (Fig. 11, Table 3) [39,40].

The limited number of bimetallic complexes obtained with the non-rigid aminophosphine ligands, such as ligand **12**, it has been explained by considering the nearly planar configuration of the free amino N-donor which precludes the coordination to a metal center [41–43].

Ligand **3** and its close derivatives support several coordination geometries around their metallic centers: octahedral [44–50,36,47], square pyramidal [35], trigonal bipyramidal [15,51,52,18,19,35], square planar [52,53,40,53,54], trigonal planar [26,55], tetrahedral [11], and linear [55]. This is not as well documented for ligands **10** and **11**. However, since the bimetallic complexes known with **10** and **11** have similar geometries to those obtained with **3**, this leads to the assumption of similar characteristics. For example, similar structural variations, resulting from the different coordination modes of the anions, were reported for the bimetallic complexes obtained by reacting **3**, **10** and **11** ligands with different Ag salts (Fig. 12) [31,56,57,58,31,59,60]. In

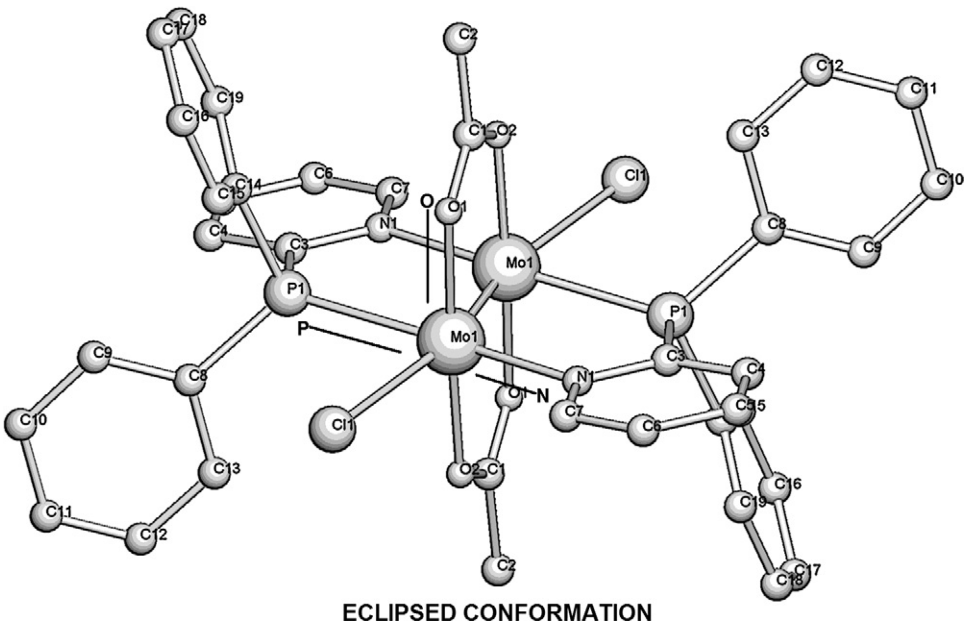

Fig. 10. Example of eclipsed conformation: *trans,trans*-[{MoCl}$_2$(μ-**3**-κ*N*,κ*P*)$_2$(μ-O$_2$CCH$_3$-κ^2*O*,*O*′)$_2$] (**3a**).

[{Ag(O$_2$N-κ^2*O*,*O*′)}$_2$(μ-**3**-κ*N*,κ*P*)$_2$] (**3c**) and [{Ag(O$_2$N-κ^2*O*,*O*′)}$_2$(μ-**10**-κ*N*,κ*P*)$_2$] (**10a**) (Fig. 12, Table 3), the two Ag centers are chelated by the anions, adopting a pseudotetrahedral coordination [31]. In all the complexes obtained with **10** or **11**, the Metal. . .Metal separations indicate strong argentophilic interactions in contrast to **3c** where the two Ag centers are at the non-binding distance. Ligands **10** and **11** maintain a hemilabile character but their N-donor is a stronger base compared to the N-donor of ligand **3** [61].

4.1.1.3. n = 2. When there are two atoms between the P- and N-donor, chelation of the P,N-ligand with one metal center is strongly favoured by the formation of a stable 5-membered ring. However the formation of the correspondent bimetallic complex (6-membered rig) can be favoured by the structure of the ligand itself, by the coordination geometry of the metallic centers involved or by the stabilizing effects of a Metal. . .Metal interaction.

For example, normally **13** do not form bimetallic complexes. However, in the bimetallic complex [{Ag(O$_3$N-κ^2*O*,*O*′)}$_2$(μ-**13**-κ*N*,κ*P*)$_2$] (**13a**) (Fig. 13, Table 3), the Ag are held in close proximity by the two **13** ligands which results in Ag. . .Ag interaction and a distorted tetrahedral geometry of the Ag. The **13** ligands assume in this case a proper P,N-bridging mode [62].

The **14H** and **15** ligands act in most cases as chelating ligands. In the homobimetallic complexes [M$_2$(μ-**L**-κ*N*,κ*P*)$_2$] X$_2$ (L = **14H** M = Ag X = OTf, ClO$_4$; L = **14H** M = Cu X = OTf; L = **14H**, **15** M = Au X = ClO$_4$) [63], the linear geometry required by the two metallic

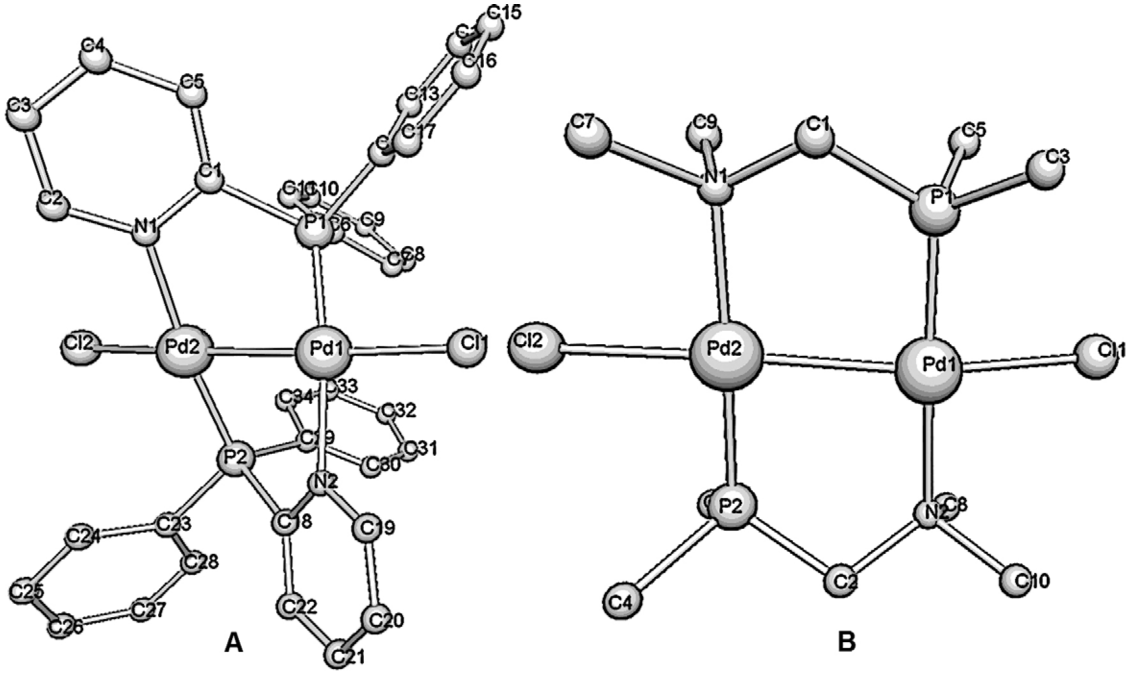

Fig. 11. Comparison between the two palladium complexes obtained with ligands **3** and **12**: (A) *trans,trans*-[{PdCl}$_2$(μ-**3**-κ*N*,κ*P*)$_2$] (**3b**) and (B) *trans,trans*-[{PdCl}$_2$(μ-**12**-κ*N*,κ*P*)$_2$] (**12a**).

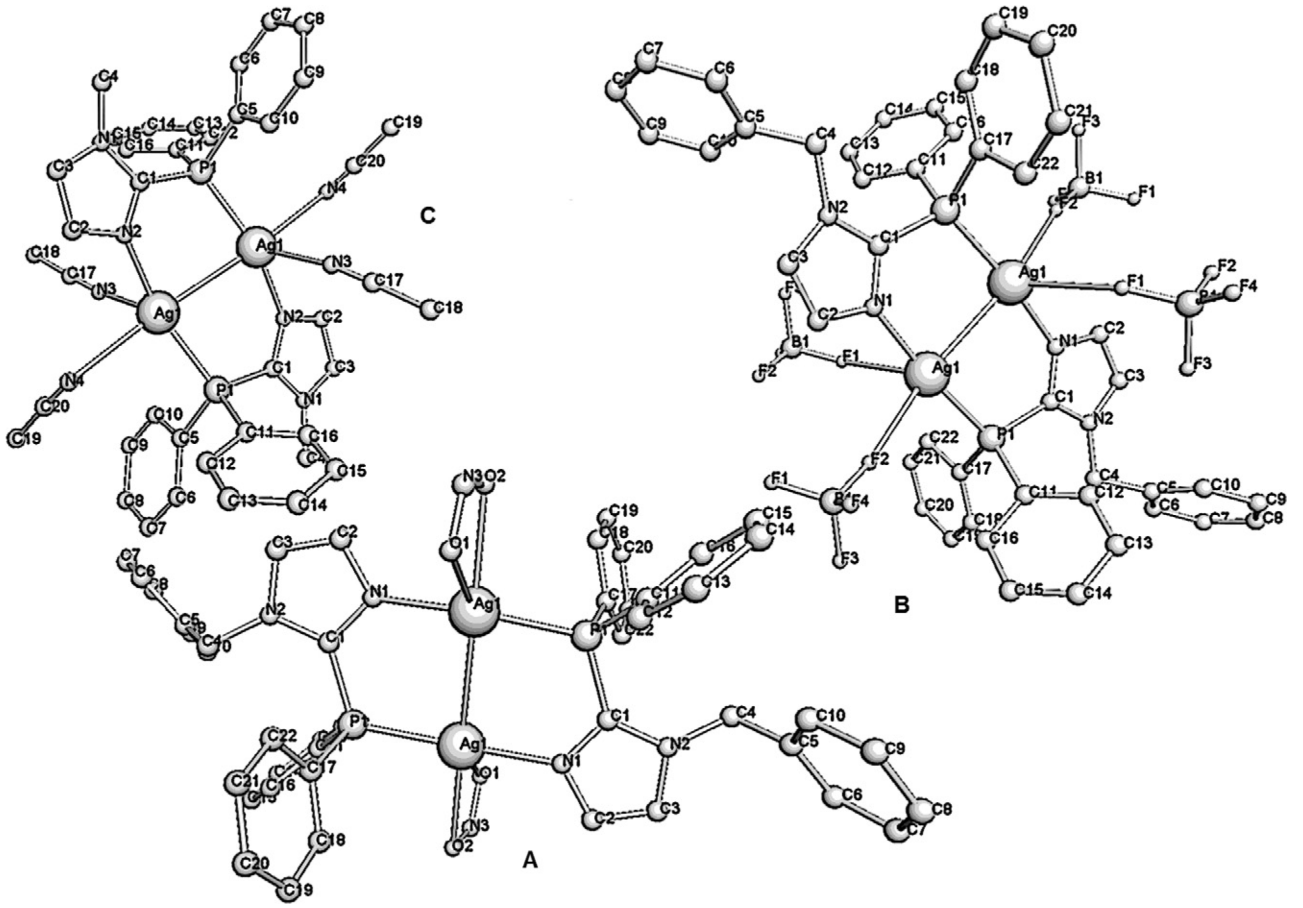

Fig. 12. Examples of structural variations obtained by reacting AgX (X = NO_2, BF_4, ClO_4) with ligand **10** or **11**: (A) $[\{Ag(O_2N\text{-}\kappa^2 O,O')\}_2(\mu\text{-}\mathbf{10}\text{-}\kappa N,\kappa P)_2]$ (**10a**), (B) $[Ag_2(\mu\text{-}\mathbf{10}\text{-}\kappa N,\kappa P)_2(BF_4\text{-}\kappa F)_2]$ (**10b**) and (C) $[\{Ag(NCCH_3)_2\}_2(\mu\text{-}\mathbf{11}\text{-}\kappa N,\kappa P)_2](ClO_4)_2$ (**11a**).

centers leads to a P,N-bridging mode of the two **14H** or **15** ligands, as shown in $[Au_2(\mu\text{-}\mathbf{15}\text{-}\kappa N,\kappa P)_2](ClO_4)_2$ (**15a**), Fig. 14.

A pseudo-P,N-bridging coordination mode is adopted by **14** in $[\{Rh(CO)X\}_2(\mu\text{-}\mathbf{14}\text{-}\kappa^2 N,\kappa P)_2]$ (X = Cl (**14a**), Br, or I) [64] and in $[\{Mn(CO)_2\}_2(\mu\text{-}\mathbf{14}\text{-}\kappa^2 N,\kappa P)_2]$ [65] (**14b**) (Fig. 15, Table 3), where each **14** ligand coordinates one metal center by chelation through its P- and N-donor and bridges the other metal center through its N-donor. In **14b**, the Mn_2N_2 core is planar, while the 5-membered Mn-P-C-C-N ring has a slightly folded envelope conformation. In **14a**, the Rh_2N_2 core is folded.

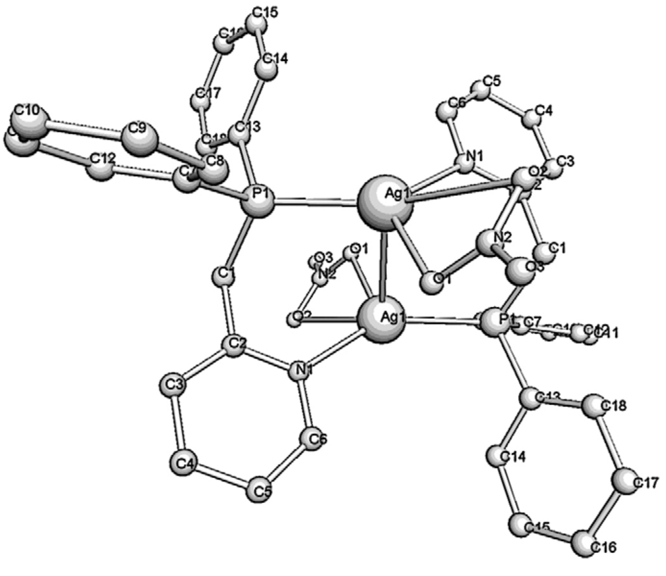

Fig. 13. Homobimetallic complex $[\{Ag(O_3N\text{-}\kappa^2 O,O')\}_2(\mu\text{-}\mathbf{13}\text{-}\kappa N,\kappa P)_2]$ (**13a**).

This type of pseudo-P,N-bridging coordination mode seems to be an alternative for ligands with n = 2 because of the formation of the stable 5-membered chelated ring. Equally, in $[Pd_2(\mu\text{-}\mathbf{16}\text{-}\kappa C^{23-24},\kappa N,\kappa^2 P)_2](BF_4)_2$ (**16a**) (Fig. 16, Table 3), the PPh_2 units of the imidophosphine ligands bridge the two Pd centers disposed from each other by a single bond. The two 5-membered rings formed are almost planar [66].

4.1.1.4. n = 3.

For P,N-ligands where the P- and N-donors are separated by three atoms the formation of the 7-membered ring bimetallic complex is still less favoured than the formation of the 6-membered ring monometallic complex.

Ligand **17** acts either as a chelating or a P-monodentate ligand. The sole example of bimetallic structure is $[Ag_2(\mu\text{-}\mathbf{17}\text{-}\kappa N,\kappa P)_2](OAc)_2$ (**17a**) (Fig. 17, Table 3), where the Ag^I ions lie in a distorted linear environment at the non-bonding Ag. . .Ag distance.

In the case of **18**, the geometry of the ligand does not allow chelation. In the homobimetallic complex *cis,cis*-$[\{W(CO)_4\}_2(\mu\text{-}\mathbf{18}\text{-}\kappa N,\kappa P)]$ (**18a**) the two tungsten centers are in a slightly distorted octahedral environment and the two **18** P,N-bridging ligands are disposed parallel to each other (Fig. 18, Table 3). The face-to-face π-stacking interaction between the two pyridyl rings is characterized by a quite short distance (~3.29 Å), and is probably one of the forces that drive the formation of the bimetallic complex [67].

4.1.1.5. n = 4.

Increasing the number of the atoms between the N- and P-donor of the P,N-ligand increases the size of the metallocycle

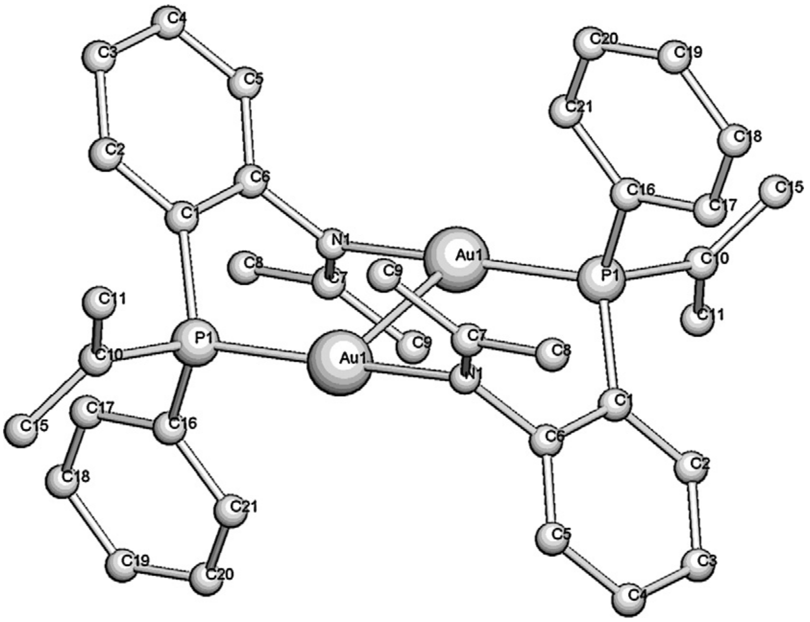

Fig. 14. Homobimetallic complex $[Au_2(\mu\text{-}\mathbf{15}\text{-}\kappa N,\kappa P)_2](ClO_4)_2$ (**15a**).

formed by the P,N-ligand and the two metallic centers. In general, rings larger than 6 are less favoured because their formation decreases the configurational entropy of the molecule. Reducing the configurational entropy by limiting the possibility of bond rotation and having the donor atoms already tied into the optimal positions for complex formation are important in order to enhance the formation of large cycles.

An example is given by the **20** and the **21** ligands, where the N- and P-donor are rigidly spaced. When reacted with several Pd^{II} salts, the ligands favour only the formation of the 14- or 16-membered ring bimetallic complexes (Fig. 19, Table 3) [68].

4.1.2. Heterobimetallic complexes

The synthesis of heterobimetallic complexes is usually performed by reacting an organometallic fragment (metallo-ligand complex) with a second metal. This procedure allows better control over synthesis and is usually adopted for the preparation of early–late heterometallic complexes. The hard/soft character of the

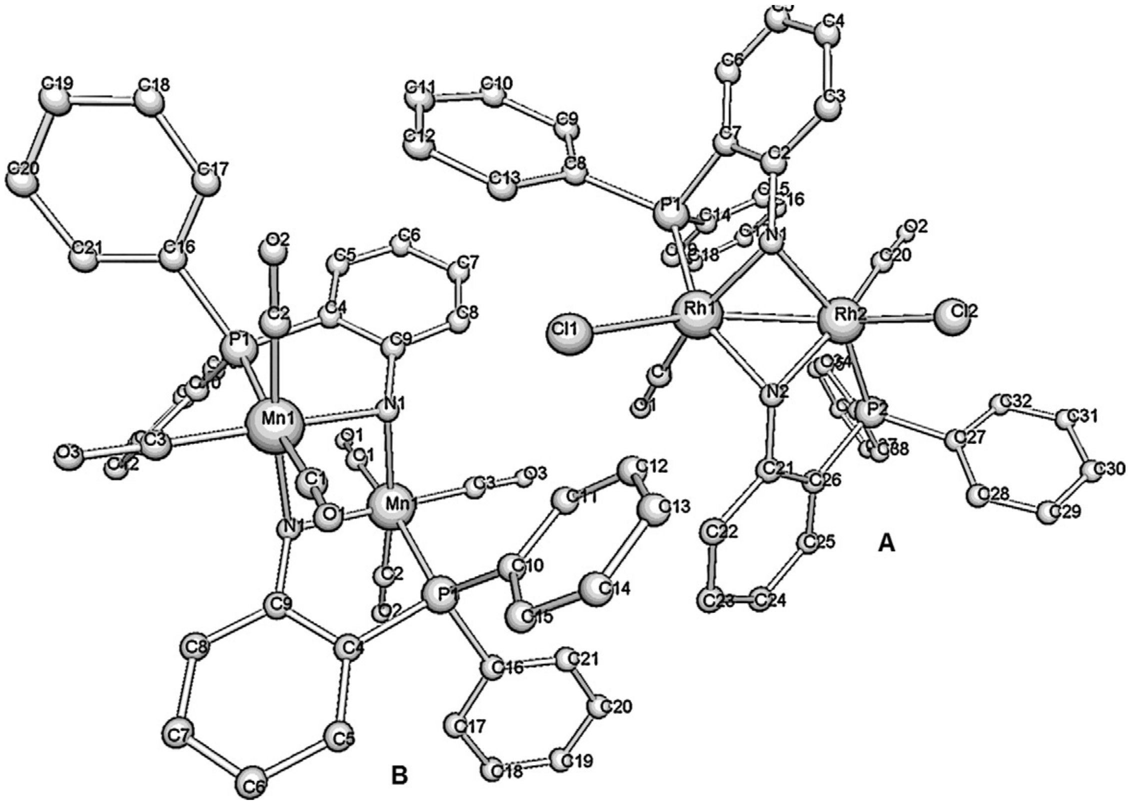

Fig. 15. Pseudo-PN-bridging mode of ligand **14** in the homobimetallic complexes: (A) $[\{Rh(CO)Cl\}_2(\mu\text{-}\mathbf{14}\text{-}\kappa^2N,\kappa P)_2]$ (**14a**) and (B) $[\{Mn(CO)_2\}_2(\mu\text{-}\mathbf{14}\text{-}\kappa^2N,\kappa P)_2]$ (**14b**).

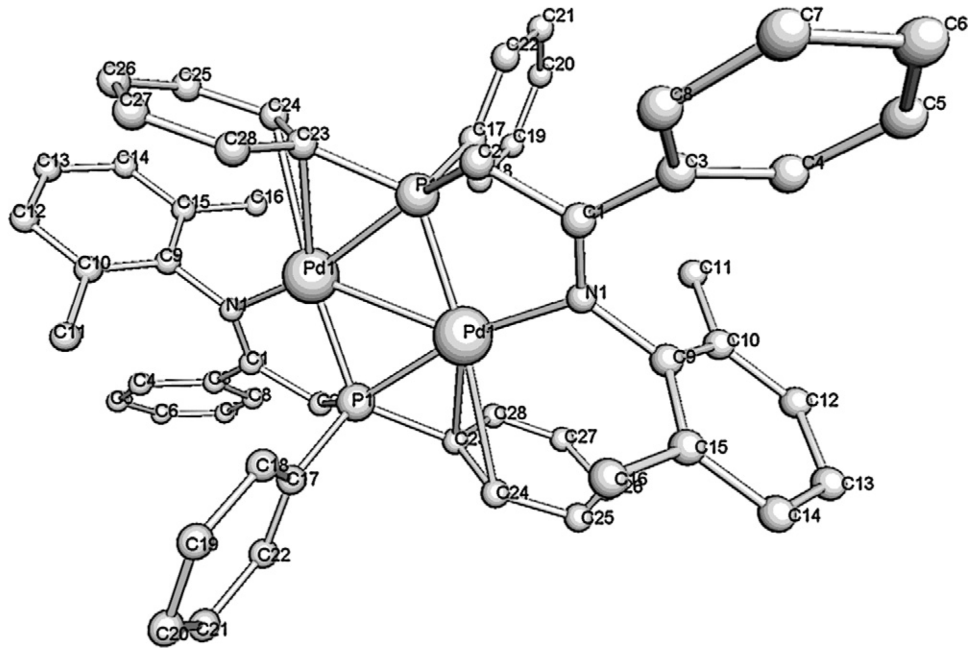

Fig. 16. Homobimetallic complex $[Pd_2(\mu\text{-}\mathbf{16}\text{-}\kappa C^{23-24},\kappa N,\kappa^2 P)_2](BF_4)_2$ (**16a**).

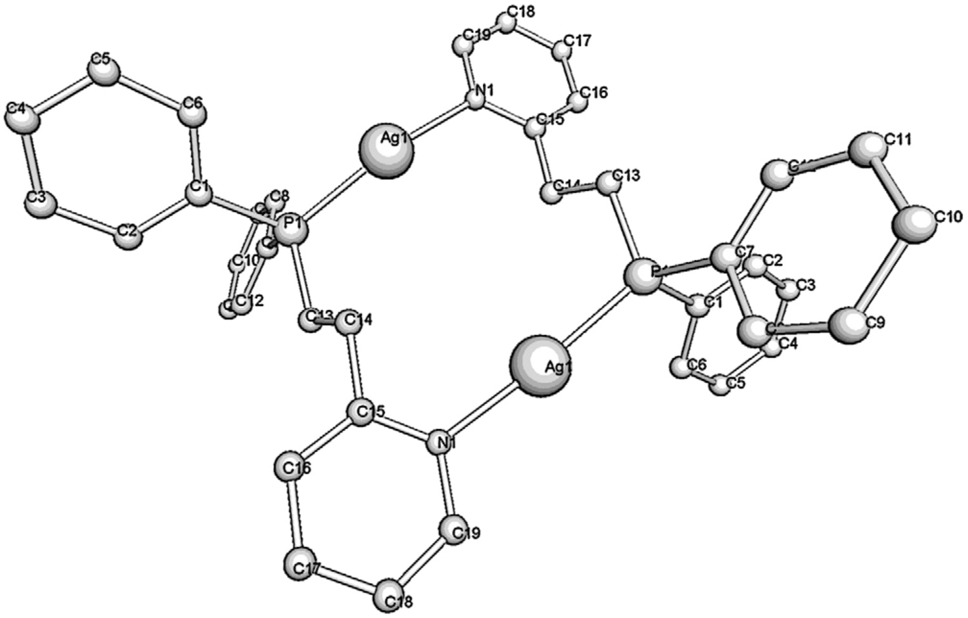

Fig. 17. Homobimetallic complex $[Ag_2(\mu\text{-}\mathbf{17}\text{-}\kappa N,\kappa P)_2](OAc)_2$ (**17a**).

P- and N-donor in P,N-binucleating ligands is optimal for the application of this type of synthesis.

The metallo-ligand $[TiCl_2(\mathbf{1}\text{-}\kappa N)_2]$ complex was (**1**, R = *t*-Bu) reacted with organoplatinum to afford *cis*,*cis*-$[Cl_2Ti(\mu\text{-}\mathbf{1}\text{-}\kappa N,\kappa P)_2PtXY]$ (X = Y = Cl (**1b**), X = Cl Y = Me, X = Cl Y = *p*-Tol, X = Y = Me) (Fig. 20, Table 4). In the complexes, the N-donors of the two **1** ligands are bound to Ti and the P-donors are bound to the Pt. The Ti–N–P–Pt–P–N 6-membered ring adopts a boat conformation. The coordination geometry around the Pt is square planar while the titanium is in pseudo-trigonal bipyramidal geometry. The structures present a Ti–Pt dative bond that is cleaved and re-formed in solution to allow dynamic conformation change [69].

Similarly, by reacting $[TiCl_2(\mathbf{1}\text{-}\kappa N)_2]$ (**1**, R = *t*-Bu) with $[Cp^*RuCl]_4$, the early–late heterobimetallic complex $[Cp^*Ru(\mu\text{-}Cl)(\mu\text{-}\mathbf{1}\text{-}\kappa N,\kappa P)_2Ti(O)]$ (**1c**) was obtained (Scheme 1). In the complex, both the Ru and the Ti adopt a pseudo-tetrahedral coordination geometry. In this case there is no dative bond between the two metal centers; instead, the bridging Cl atom donates a lone pair to the Ti [70].

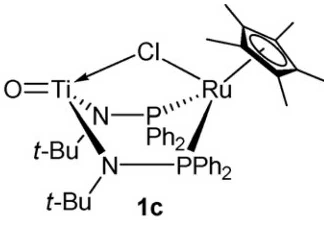

Scheme 1.

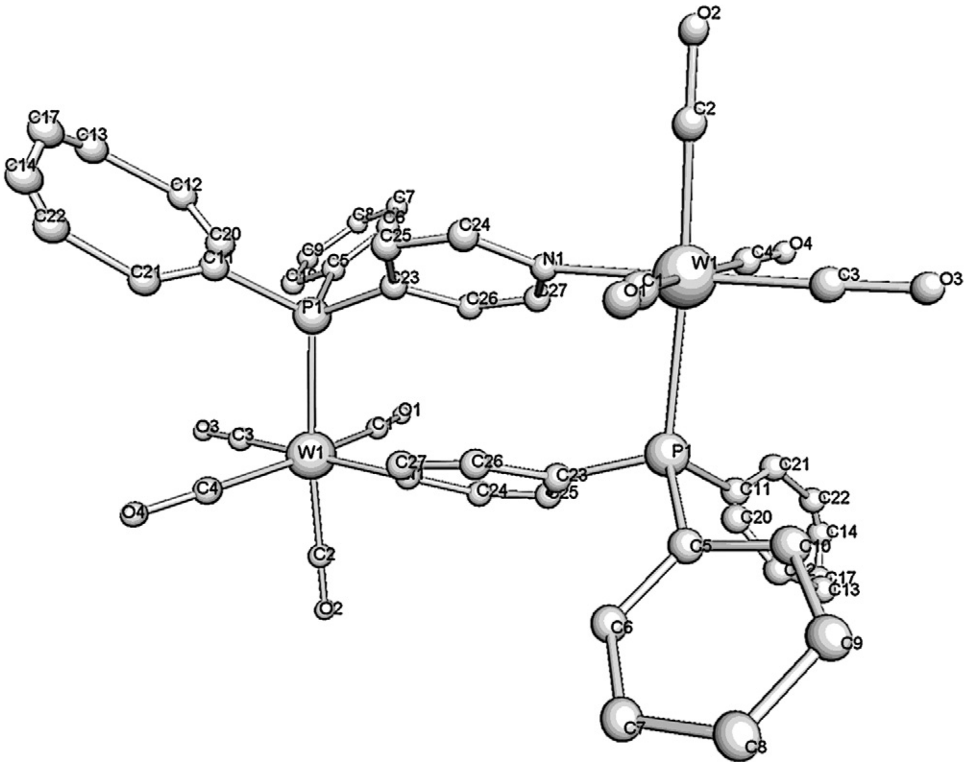

Fig. 18. Homobimetallic complex *cis*,*cis*-[{W(CO)$_4$}$_2$(μ-**18**-κ*N*,κ*P*)] (**18a**).

Several heterobimetallic complexes were synthesized by reacting the organometallic fragments: *trans*-[Fe(CO)$_3$(PR$_3$-κ*P*)$_2$] (PR$_3$ = **3** [71–74], **5** [75–77], **6** [75–77]) *trans*-[Ru(CO)$_3$(**3**-κ*P*)$_2$] [78,79], *trans*-[Ir(CO)Cl(**3**-κ*P*)$_2$] [80–82] and *trans*-[Rh(CO)Cl(PR$_3$-κ*P*)$_2$] (PR$_3$ = **3** [81], **9** [52]) with a number of Lewis acids (Scheme 2).

The reactions produced selectively head-to-head heterobimetallic complexes with the exception of [(CO)Cl$_2$Rh(μ-**10**-κ*N*,κ*P*)$_2$PdCl] (**10c**) [52], which led to head-to-head and head-to-tail isomers in a ratio close to one-to-one (Scheme 3).

Table 4
Geometric parameters of the bimetallic complexes.

Complex	P–Metal–Metal–N	P–Metal–P	N–Metal–N	Metal–Metal
1b	0.4°, 6°	103°	113°	2.76 Å
1c	2°	93°, 94°	113°	3.07 Å, 3.09 Å
14c	5°	168°	175°	2.99 Å
19a	13°, 17°	99°	115°	7.70 Å

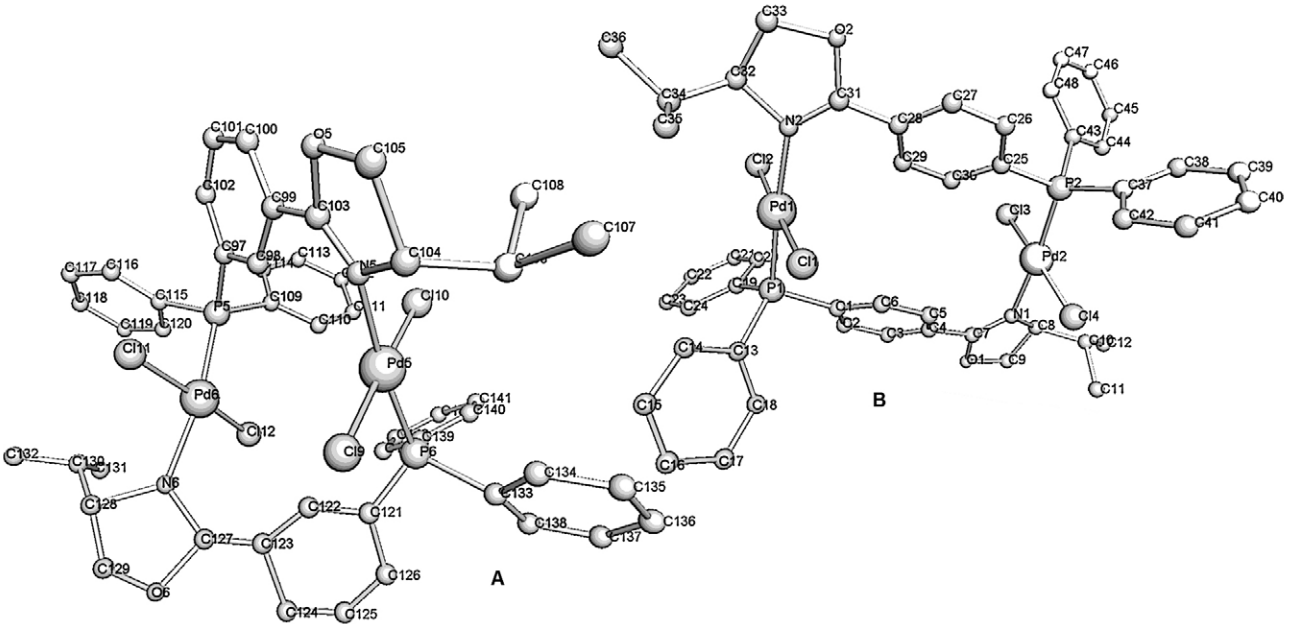

Fig. 19. Examples of Pd homobimetallic complexes obtained with ligands **20** and **21**: (A) *trans*,*trans*-[{PdCl$_2$}$_2$(μ-**20**-κ*N*,κ*P*)$_2$] (**20a**) and (B) *trans*,*trans*-[{PdCl$_2$}$_2$(μ-**21**-κ*N*,κ*P*)$_2$] (**21a**).

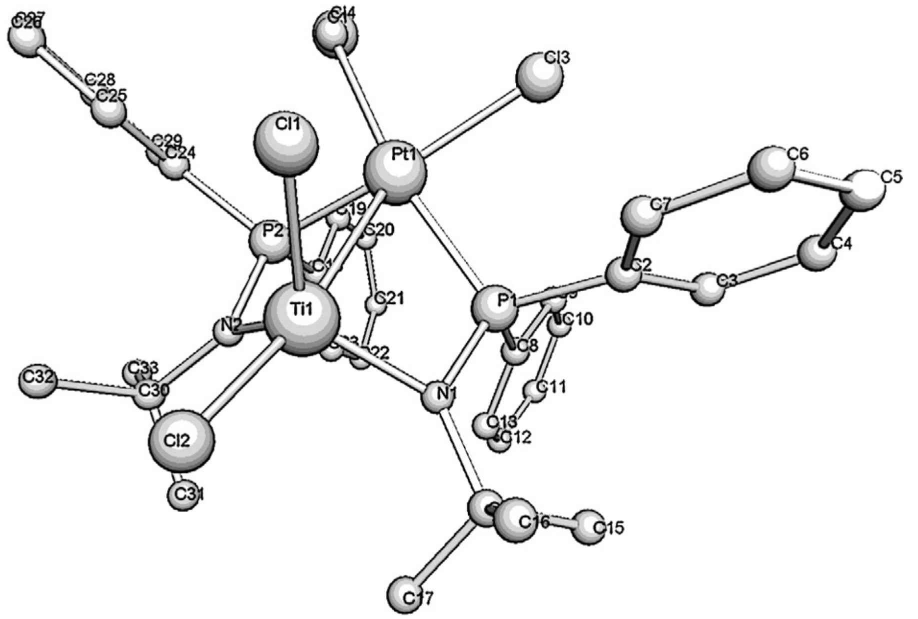

Fig. 20. Heterobimetallic complex *cis*,*cis*-[$Cl_2Ti(\mu$-**1**-κ*N*,κ*P*$)_2PtCl_2$] (**1b**).

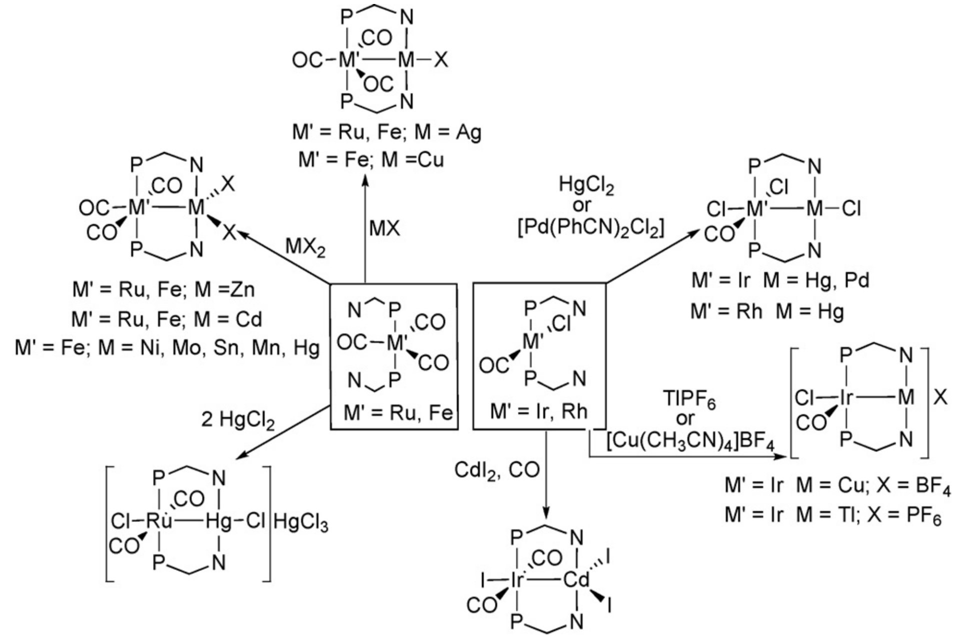

Scheme 2.

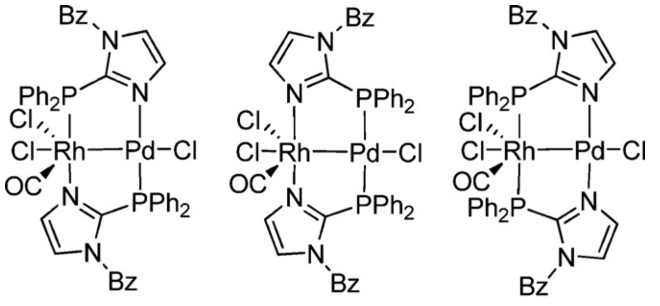

10c

Scheme 3.

In other heterobimetallic complexes, the head-to-head isomers were identified as transient species [10,83,84]. Thermal isomerisation reactions from head-to-head to head-to-tail were observed for [$XPt(\mu$-PR_3-κ*N*,κ*P*$)_2PdX$] (PR_3 = **3**, **4**; X = Cl, Br, I). The rate of the isomerisation varies according to the metal and halide ligands employed, but was always faster for **4** than for **3**, which is probably due to the stronger basicity [85] and consequentially the higher reactivity of **4** towards a second metal [9,54,86].

Heterobimetallic complexes [$Au(\mu$-**14H**-κ*N*,κ*P*$)_2M](OTf)_2$ (M = Ag (**14c**), Cu) were prepared by treating [Au(**14H**-κ*P*$)_2$](OTf) with Ag(OTf) or Cu(OTf) [63]. In the complexes, the two **14H** ligands adopt a head-to-head configuration with the Au center always coordinated to the P-donors of the two **14H** ligands. In **14c** (Fig. 21, Table 4), the Au and Ag metallic centers are

Fig. 21. Heterobimetallic complex $[\{Au(\mu\text{-}\mathbf{14H}\text{-}\kappa N,\kappa P)_2Ag\}_2(\mu\text{-}O_3SCF_3\text{-}\kappa^2 O,O')_2]$ (**14c**).

linearly coordinated and show a Metal...Metal distance characteristic of a bonding interaction. The structure is almost planar.

In *cis*-$[Cl_2Ti(\mu\text{-}\mathbf{19}\text{-}\kappa N,\kappa P)_2MX_2]$ (M = Pt, Pd X = Cl, Me (**19a**)) complexes (Fig. 22, Table 4), Ti possesses a distorted tetrahedral geometry while Pd/Pt possesses a square planar geometry [87]. The two metallic centers are held apart at a non-bonding distance. The rigid structures adopted by the compounds maximise both intramolecular Ti–Cl...H–Ar hydrogen bonding and aryl–aryl π-stacking interactions.

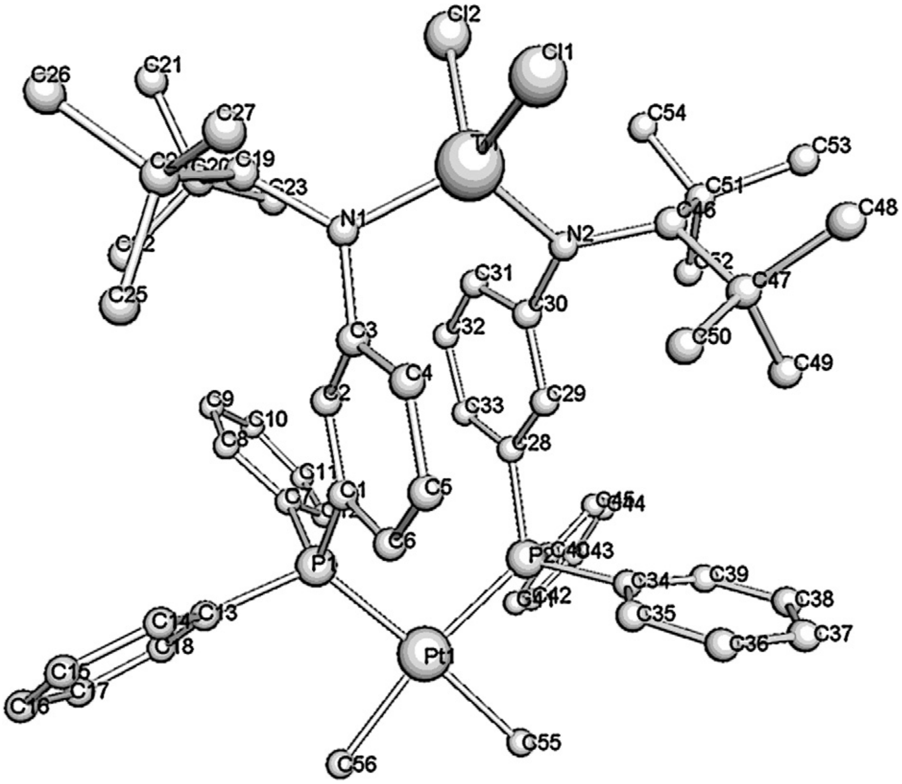

Fig. 22. Heterobimetallic complex *cis*-$[Cl_2Ti(\mu\text{-}\mathbf{19}\text{-}\kappa N,\kappa P)_2PtMe_2]$ (**19a**).

Table 5
Ligands discussed, classified by type and separation of a third donor atom.

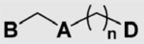	P,N-ligand
n = 1, D = P (A = N, B = P)	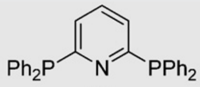 **22**
n = 1, D = N (A = N, B = P)	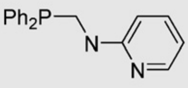 **23** 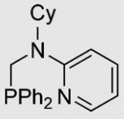 **24**
n = 1, D = N (A = P, B = N)	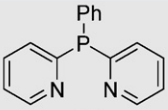 **25** 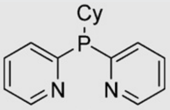 **26**
n = 1, D = O (A = N, B = P)	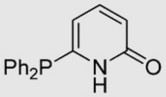 **27H**
n = 2, D = O (A = N, B = P)	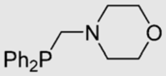 **28**
n = 2, D = N (A = N, B = P)	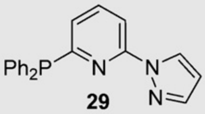 **29** 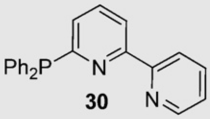 **30**

Key: A and B can be either N- or P-donor atoms but are dissimilar for the same molecule. D is a generic additional donor atom, including but not limited to P or N. Lower case *n* represents the number of spacer atoms in the bridge between A and D.

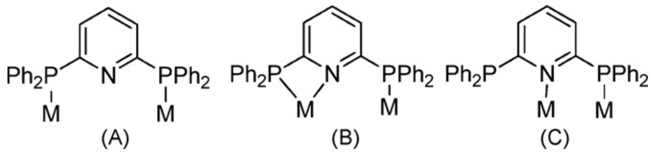

Scheme 4.

Table 6
Geometric parameters of the bimetallic complexes.

Complex	P–Metal–N	Metal–Metal
22a	167°	2.15 Å
22b	169°, 167°	2.23 Å
22c	177°	2.55 Å
23a	177°	4.59 Å
24a	170°, 23°	2.89 Å
25a	165°, 90°	2.69 Å
25b	116°	3.74 Å
26a	122°, 115°, 127°, 117°	3.33 Å
27a	160°	2.62 Å
27b	93°	4.36 Å
28a	169°, 168°	2.57 Å
29a	166°, 97°	2.15 Å
30a	n.a.	3.94 Å

4.2. Structure 2: linear chain of a P-donor, an N-donor, and a third donor atom

See Table 5.

4.2.1. Homobimetallic complexes

This section deals with P,N-binucleating ligands containing a linear chain with a P-donor, an N-donor, and a third donor atom. The P- and N-donor are separated by a single atom while the third donor can be separated by one or more atoms. With these ligands, the primary variation is the type of additional donor atom and its affinity with the metallic centers involved. Also important are the number of atoms dividing the additional donor and the geometry of the spacer.

4.2.1.1. n = 1. When the donors are separated from each other by a single atom then there is a direct competition between the three donors for the binding to the metallic centers. If the geometry of the ligand will not play a determining role then the affinity between the donors and the metallic centers employed to build the bimetallic complex will likely be the determining factor.

For example, ligand **22** presents three bimetallic coordination modes (Scheme 4). The most common coordination mode when the ligand is reacted with transition metals is A [20,88], and the more rare cases are B and C [89,90].

Only the limited flexibility of **22** and the required short Metal–Metal separation for the $\mathrm{Mo_2}^{\mathrm{II}}$ and $\mathrm{Re_2}^{\mathrm{II}}$ cores, as well as the harder character of the metals involved lets the ligand adopt a C coordination mode in the bimetallic complexes $[\{\mathrm{MoCl_2}\}_2(\mu\text{-}\mathbf{22}\text{-}\kappa N,\kappa P)_2]$ (**22a**) and $[\{\mathrm{ReCl_2}\}_2(\mu\text{-}\mathbf{22}\text{-}\kappa N,\kappa P)_2]$ (**22b**) (Table 6) [90]. Similarly, in $[\mathrm{Pd_2}(\mu\text{-}\mathbf{22}\text{-}\kappa N,\kappa^2 P,P')_2](\mathrm{ClO_4})_2$ (**22c**) (Fig. 23, Table 6), the adoption of a B coordination mode by the two **22** ligands is related to the formation of a single Pd–Pd bond which stabilises the resulting complex [91]. The rigidity of **22** leads to bimetallic complexes with P–Metal–Metal–N torsional angles lower than 10° in either the B or C coordination mode.

In *trans*,*trans*-$[\{\mathrm{PdCl_2}\}_2(\mu\text{-}\mathbf{23}\text{-}\kappa N,\kappa P)_2]$ (**23a**) (Fig. 24, Table 6), the two Pd centers are in a slightly distorted square-planar geometry and are held at the non-bonding distance through the P- and N(pyridyl)-donor of the two **23** ligands [92]. In this case, in ligand **23**, the better donor character of the N(pyridyl) group prevails over the secondary amino N-donor, which does not participate in the coordination to the metallic centers.

This is not true in the cationic homobimetallic fragment of complex $[\mathrm{Ag_2}(\mu\text{-}\mathbf{24}\text{-}\kappa^2 N,N',\kappa P)_2][\mathrm{Ag}(\mathbf{24}\text{-}\kappa N,\kappa P)_2](\mathrm{ClO_4})_3$ (**24a**), where the two **24** ligands assume a P,N(pyridyl)-bridging mode with the tertiary amino N-donor also weakly coordinated to Ag (Fig. 25, Table 6). The decreased free rotation of the amino moiety in **24** compared with **23** as well as the stabilising Ag. . .Ag interaction could be responsible for the coordination of the tertiary amino N-donor to Ag [92].

In the homobimetallic complexes of $\mathrm{Rh^{II}}$ [93], $\mathrm{Co^{II}}$ [94], $\mathrm{Cu^{I}}$ [94,95], and $\mathrm{Ag^{I}}$ [94], **25** and **26** ligands coordinate through all three of their P,N,N donors, binding one metal center through their P-donor and N,N-chelating the other metal center. On each $\mathrm{Rh^{II}}$ atom in $[\{\mathrm{RhCl_2}\}_2(\mu\text{-}\mathbf{25}\text{-}\kappa^2 N,N',\kappa P)_2]$ (**25a**) (Fig. 26, Table 6), one N-donor of **25** is on almost the same coordination plane as the P-donor of the other **25** ligand while the other N-donor is perpendicular. Each $\mathrm{Rh^{II}}$ center is in an octahedral environment and there is a single Rh–Rh bond. In the $\mathrm{Cu^{I}}$, $\mathrm{Ag^{I}}$, and $\mathrm{Co^{II}}$ homobimetallic complexes, the metallic centers adopt a distorted tetrahedral geometry. In the complexes obtained with **26**, the two metal centers are held together in close proximity as in the case of complex $[\{\mathrm{CuI}\}_2(\mu\text{-}\mathbf{26}\text{-}\kappa^2 N,N',\kappa P)_2]$ (**26a**) (Fig. 27, Table 6) [94]. In $[\{\mathrm{CuCl}\}_2(\mu\text{-}\mathbf{25}\text{-}\kappa N,\kappa P)_2](\mathrm{ClO_4})_2$ (**25b**) the two $\mathrm{Cu^{I}}$ centers are at a longer distance (Table 6) [95].

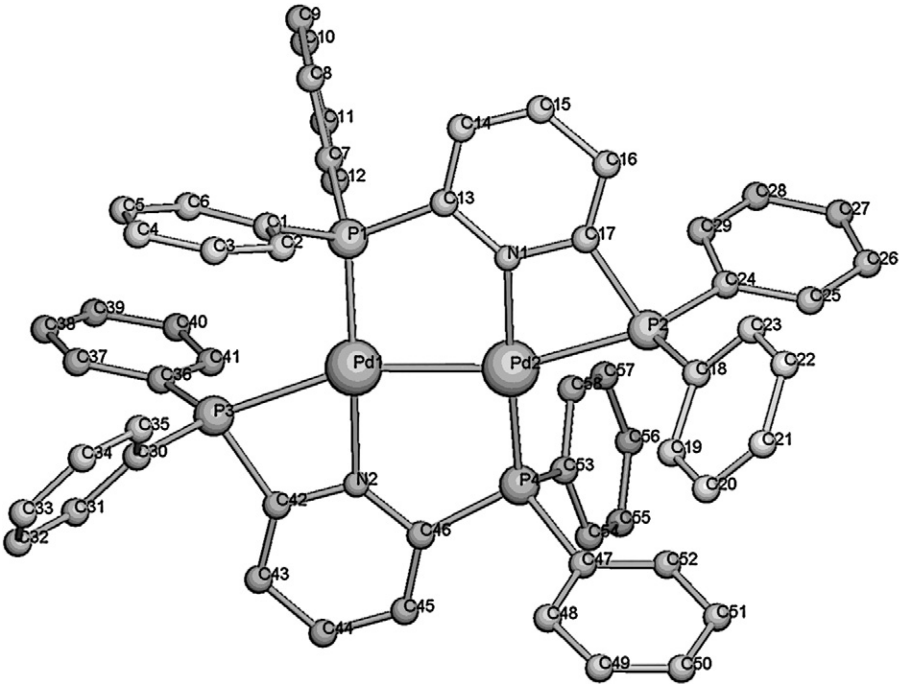

Fig. 23. Homobimetallic complex [$Pd_2(\mu$-**22**-$\kappa N,\kappa^2 P,P')_2](ClO_4)_2$ (**22c**).

If the additional donor atom is an oxygen, because of the different hard/soft character of the P-, N-, O-donor, the ligand can selectively coordinate three different kinds of metals.

For example, N,O- P,N- or P,N,O- coordination modes were obtained with **27H** ligand and its correspondent anionic structure **27**, according to the type of metals involved. Ligand **27** preferentially adopt a N,O-bridging coordination mode with Mo^{II} [96] and Cr^{II} [97], and a N,P-bridging coordination mode with Re^{II} [98], Pt^{II} and Pd^{I}. In *trans,trans*-[{Pd(**27H**-κ*P*)}$_2$(μ-**27**-κ*N*,κ*P*)$_2$] (**27a**) (Fig. 28, Table 6), the Pd^{I} centers are at a bonding distance in a pseudo square planar geometry with the two **27** anionic ligands P,N-bridging the two metals in a *trans* configuration. Each **27H** neutral ligand is P-coordinated to one metal center. The structure is stabilized by the intramolecular hydrogen bonding between the NH group of the two neutral **27H** ligands and the carbonyl oxygen of the two **27** anionic ligands and by the Pd–Pd single bond [99].

In *cis,cis*-[{Pt(**27**-κ*N*,κ*P*)}$_2$(μ-**27**-κ*N*,κ*P*)$_2$] (**27b**) (Fig. 29, Table 6), the presence of the two **27** chelated ligands cause a *cis* arrangement of the two **27** P,N-bridging ligands and lead to a non-bonding distance between the two platinum centers [99].

4.2.1.2. n = 2. When the additional donor is separated from one of the other donors by two atoms, unless geometry strongly interferes, the ligands manifest a bridging behaviour accompanied by chelation of one metal center.

In *trans,trans*-[{PdCl}$_2$(μ-**28**-κ*N*,κ*P*)$_2$] (**28a**), the two Pd centers are P,N-bridged by the two **28** ligands at a single bond distance (Fig. 30, Table 6). In this case, ligand **28** involves in coordination only

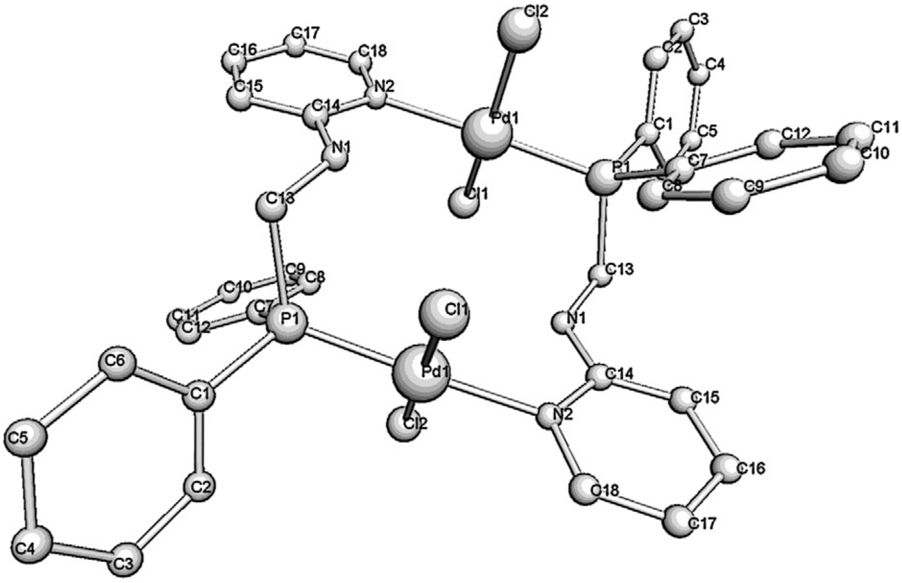

Fig. 24. Homobimetallic complex *trans,trans*-[{$PdCl_2$}$_2$(μ-**23**-κ*N*,κ*P*)$_2$] (**23a**).

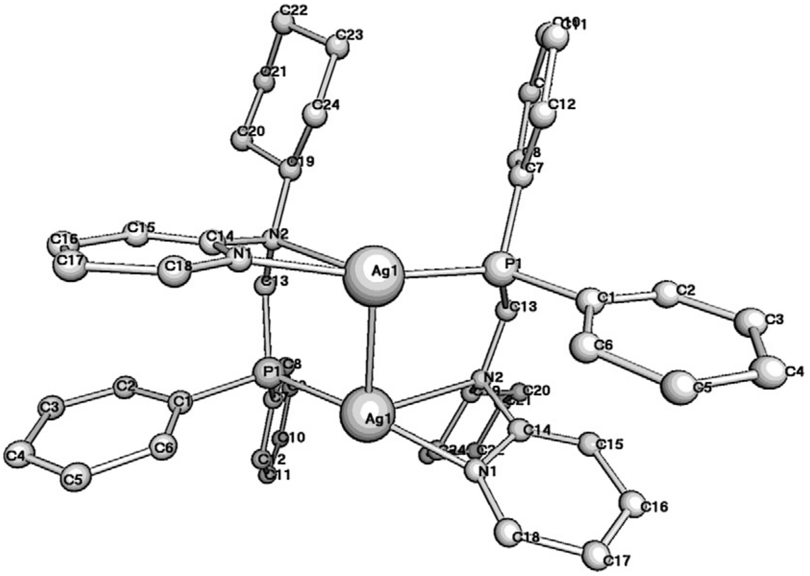

Fig. 25. Cationic fragment $[\mathrm{Ag_2}(\mu\text{-}\mathbf{24}\text{-}\kappa^2N,N',\kappa P)_2]$ of complex **24a**.

its P- and N-donor atoms since the conformation of the morpholine ring does not favour oxygen binding. The complex adopts a side-by-side structure with the **28** ligand in a skewed conformation [100].

In their Mo [101], $\mathrm{Ru^I}$ [49], $\mathrm{Ag^I}$ [102], and $\mathrm{Cu^I}$ [103–106] homobimetallic complexes **29** and **30** ligands coordinate one metal center through their P-donor and chelate the other metal center through their two N-donors.

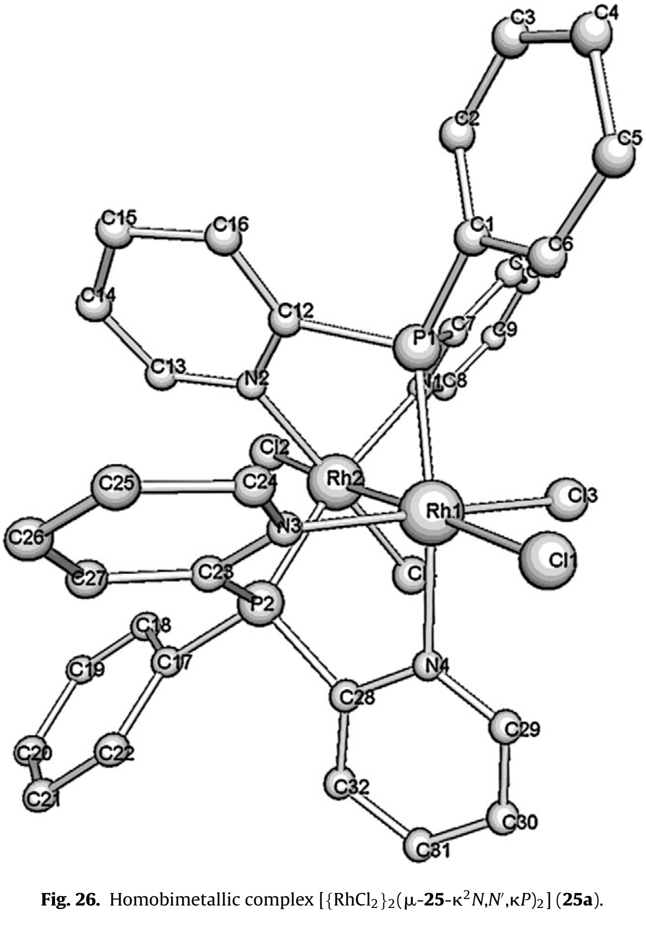

Fig. 26. Homobimetallic complex $[\{\mathrm{RhCl_2}\}_2(\mu\text{-}\mathbf{25}\text{-}\kappa^2N,N',\kappa P)_2]$ (**25a**).

In $[\mathrm{Mo_2}(\mu\text{-}\mathbf{29}\text{-}\kappa^2N,N',\kappa P)_2(\mu\text{-}\mathrm{O_2CCH_3}\text{-}\kappa^2O,O')_2](\mathrm{BF_4})_2$ (**29a**) (Fig. 31, Table 6), the quadruple bonded $\mathrm{Mo_2^{II}}$ core is bridged by two **29** ligands through their P- and N(pyridyl)-donors, while the N(pyrazole)-donors complete the octahedral coordination of the Mo [101].

In $[(\text{bipyridyl-}\kappa^2N,N')\mathrm{Cu}(\mu\text{-}\mathbf{30}\text{-}\kappa^2N,N',\kappa P)_2\mathrm{Cu}](\mathrm{PF_6})_2$ (**30a**) (Fig. 32, Table 6), the two $\mathrm{Cu^I}$ centers present a pseudotetrahedral geometry [106]. The complex is the sole example where the two **30** P,N-bridging ligands possess a head-to-head configuration; this is probably due to the steric hindrance of the bipyridyl molecule bonded to one of the copper centers.

4.2.2. Heterobimetallic complexes

Heterobimetallic complexes were obtained by reacting the fragment *trans*-$[\mathrm{Fe(CO)_3}(\mathbf{24}\text{-}\kappa P)_2]$ (**24b**) with $\mathrm{Cu^I}$ and *trans*-$[\mathrm{Fe(CO)_3}(\mathbf{28}\text{-}\kappa P)_2]$ (**28b**) with $\mathrm{Hg^{II}}$, $\mathrm{Cd^{II}}$, $\mathrm{Cu^I}$, and $\mathrm{Ag^I}$ salts (Scheme 5) [107]. In all the heterobimetallic complexes of this class, the two P,N-binucleating ligands adopt a head-to-head configuration with the two P-donors coordinated to the Fe and *trans* to each other; the Fe is in a trigonal bipyramidal geometry and there is a dative Fe–Metal bond. The coordination modes of the two nitrogen atoms of the two P,N-binucleating ligands vary with the hardness of the different metal ions. Thus there is only weak interaction between the N-donor of one of the two **28** ligands and the $\mathrm{Hg^{II}}$ center, though there is a proper bond with $\mathrm{Cd^{II}}$ (**28c**) (Fig. 33, Table 7) [107]. In *trans*-$[\mathrm{(CO)_3Fe}(\mu\text{-}\mathbf{28}\text{-}\kappa N,\kappa P)_2\mathrm{Cu}]\mathrm{ClO_4}$ (**28d**) and *trans*-$[\mathrm{(CO)_3Fe}(\mu\text{-}\mathbf{24}\text{-}\kappa N,\kappa P)_2\mathrm{Cu}]\mathrm{ClO_4}$ (**24c**) [108], both the N-donor of the two P,N-binucleating ligands coordinate with the $\mathrm{Cu^I}$ center (Figs. 33 and 34, Table 7). In the case of **24c** there is a coordination of the two N-donors of the pyridine rings and a close interaction with

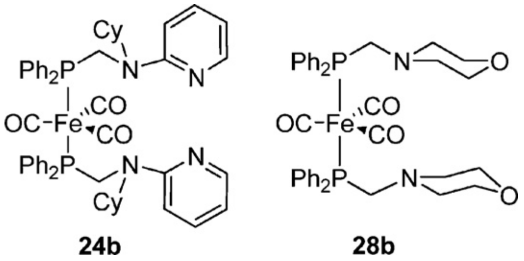

Scheme 5.

Fig. 27. Homobimetallic complex $[\{CuI\}_2(\mu\text{-}\mathbf{26}\text{-}\kappa N,\kappa P)_2]$ (**26a**).

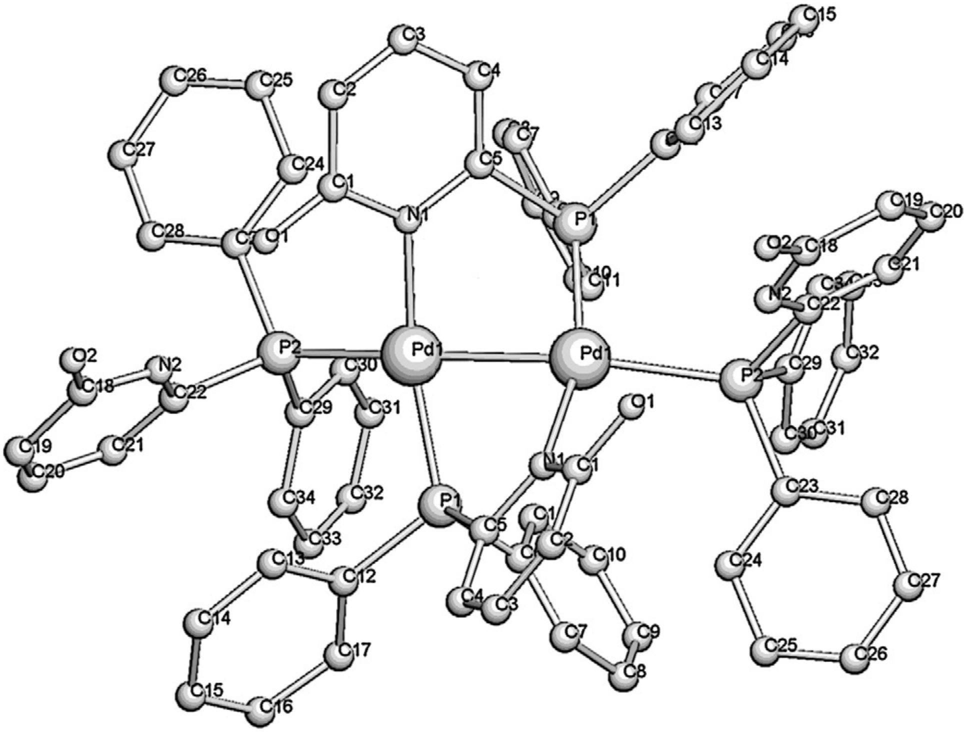

Fig. 28. Homobimetallic complex *trans,trans*-$[\{Pd(\mathbf{27H}\text{-}\kappa P)\}_2(\mu\text{-}\mathbf{27}\text{-}\kappa N,\kappa P)_2]$ (**27a**).

Table 7
Geometric parameters of the bimetallic complexes.

Complex	P–Metal–N	P–Metal–P	N–Metal–N	Metal–Metal
24c	n.a.	177°	113°	2.46 Å
25c	165°, 95° for Pd 135°, 107° for Cu	n.a.	n.a.	3.28 Å
28c	n.a.	176°	n.a.	2.74 Å
28d	n.a.	171°	154°	2.55 Å

one N-donor of the CyN amine (Fig. 34). The metal–metal bond is not in tension.

The sole heterobimetallic complex obtained with two **25** ligands in a P,N-bridging coordination mode is $[ClPd(\mu\text{-}\mathbf{25}\text{-}\kappa^2 N,N',\kappa P)_2CuCl]ClO_4$ (**25c**) (Fig. 35, Table 7). The structure resembles that of **25a**, with each **25** ligand in a head-to-tail arrangement, but in this case there is no bonding between the two metal centers [109].

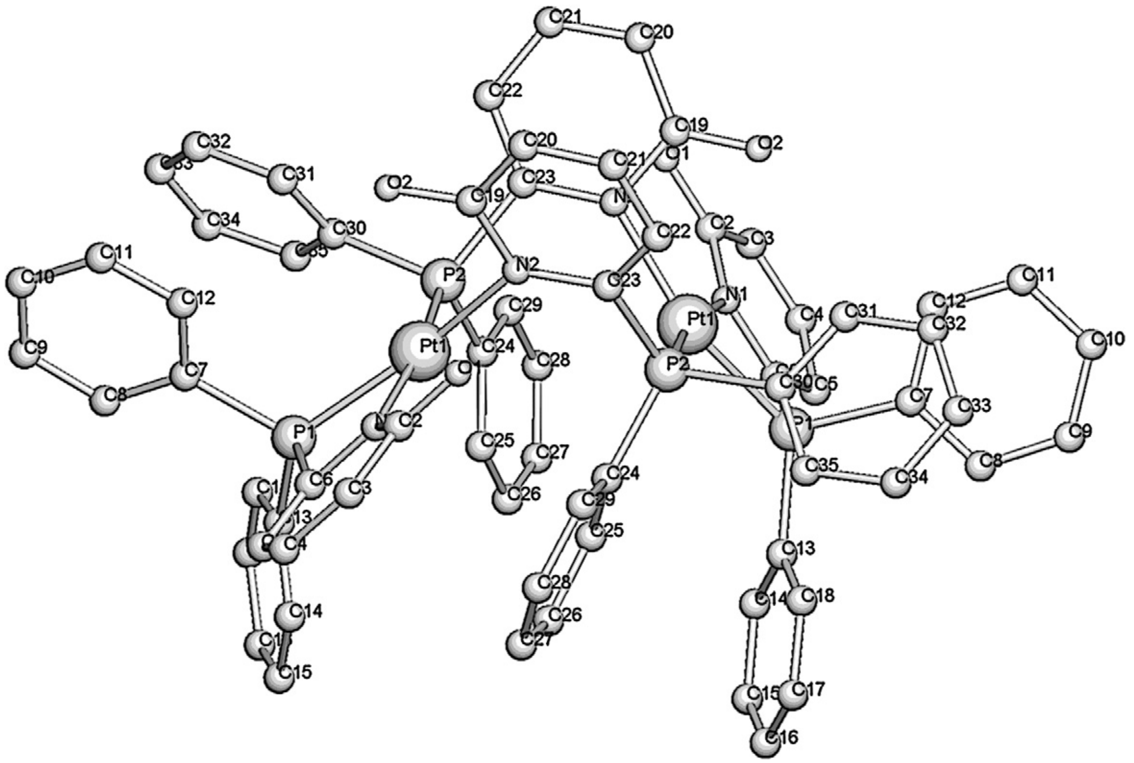

Fig. 29. Homobimetallic complex *cis,cis*-[{Pt(**27**-κ*N*,κ*P*)}$_2$(μ-**27**-κ*N*,κ*P*)$_2$] (**27b**).

4.3. Structure 3: symmetric PNP or NPN ligand with varying numbers of atoms in chain

See Table 8.

4.3.1. Homobimetallic complexes

The most important factors for these ligands is which donor atoms A and B represent and how many atoms occur between them.

4.3.1.1. n = 2.

When the A and B donors are separated by two atoms, the nature of the central donor A and the type of metallic centers involved in the bimetallic complex determine the strength of the A coordination. However, the A coordination is favoured by the formation of two 5-membered rings involving the external donors (B), the two metal centers and the central donor (A).

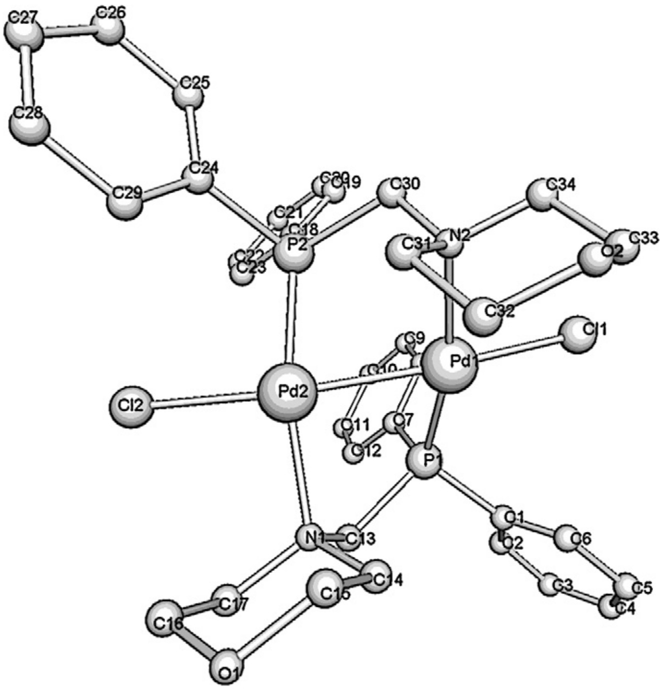

Fig. 30. Homobimetallic complex *trans,trans*-[{PdCl}$_2$(μ-**28**-κ*N*,κ*P*)$_2$] (**28a**).

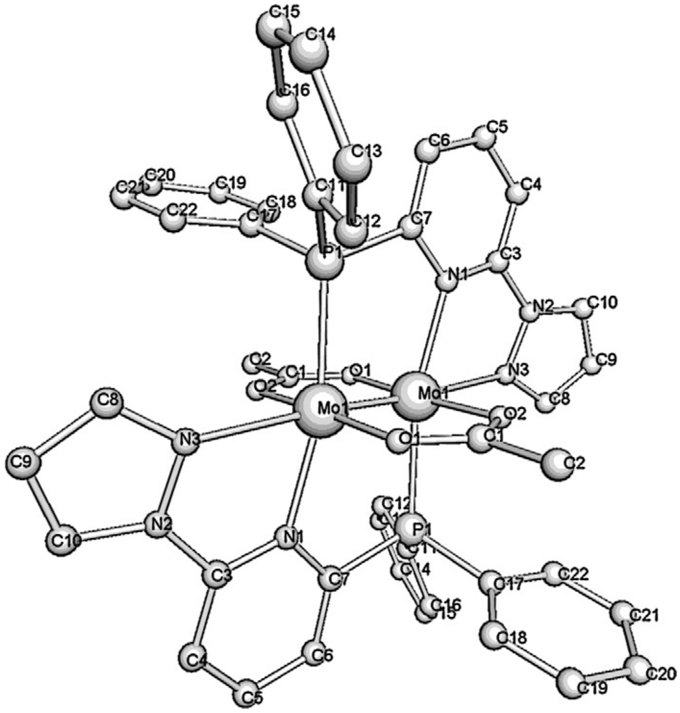

Fig. 31. Homobimetallic complex [Mo$_2$(μ-**29**-κ^2*N*,*N'*,κ*P*)$_2$(μ-O$_2$CCH$_3$-κ^2*O*,*O'*)$_2$] (BF$_4$)$_2$ (**29a**).

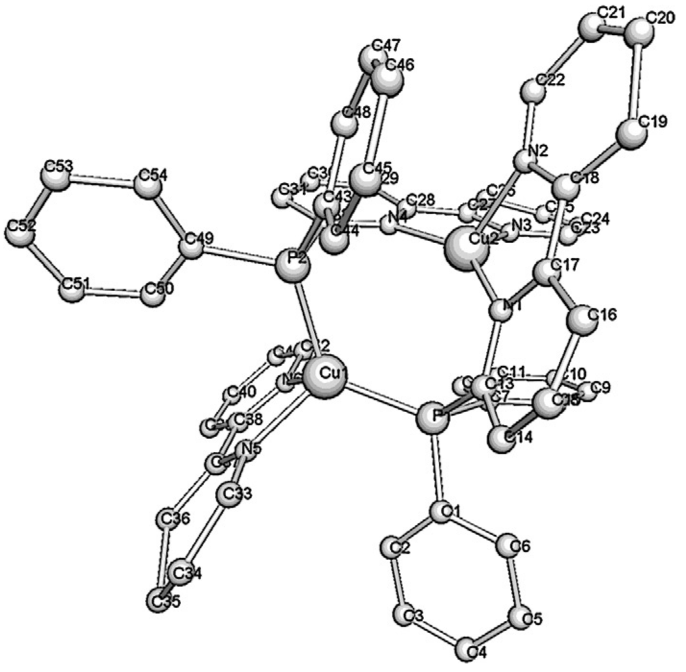

Fig. 32. Homobimetallic complex [(bipyridyl-κ^2N,N')Cu(μ-**30**-κ^2N,N',κP)$_2$Cu](PF$_6$)$_2$ (**30a**).

This type of coordination is usually accompanied by Metal–Metal bonding.

The only examples of bimetallic complexes where A is an N-donor involve phosphino amido ligands, where the negative charge on the N-donor enhances its coordination ability.

In [Cl$_2$Cr(μ-**31**-κ^2N,κ^2P,P')(μ-**31**-κC,κ^2N,κ^2P,P')CrCl] (**31a**) [110] (Fig. 36, Table 9), and [{NbCl$_2$}$_2$(μ-**31**-κ^2N,κ^2P,P')(μ-Cl)$_2$] (**31b**) [111] (Fig. 37, Table 9), the two **31** ligands bridge the two metallic centers through their amido-nitrogen atom, and coordinate through each P-donor one of the two metallic centers. A homobimetallic complex like **31a** was obtained with ligand **32** [110].

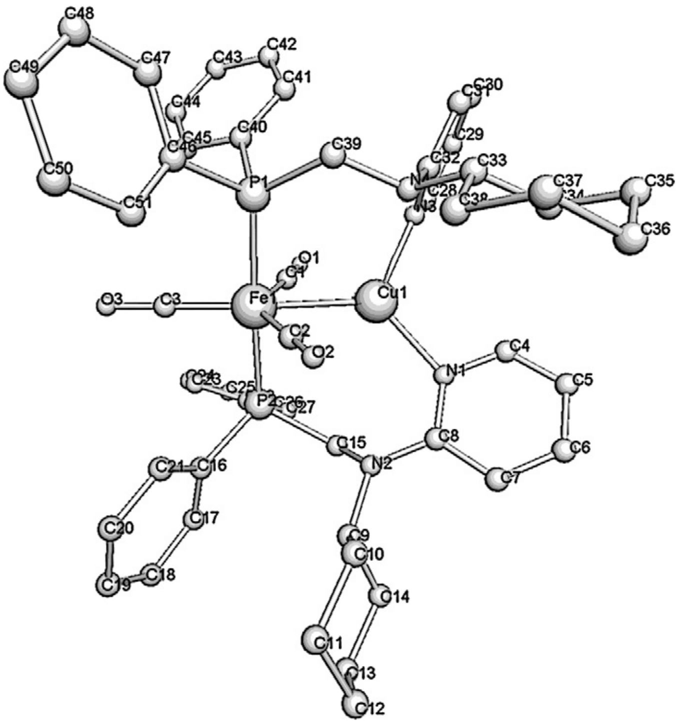

Fig. 34. Heterobimetallic complex *trans*-[(CO)$_3$Fe(μ-**24**-κN,κP)$_2$Cu]ClO$_4$ (**24c**).

A similar coordination is also shown by the two **33** ligands in [Cu$_2$(μ-**33**-κ^2N,κ^2P,P')$_2$] (**33a**), where the two Cu centers present a distorted tetrahedral geometry (Fig. 38, Table 9) [112].

In **34** and **35** ligands, A is a P-donor and is actively involved in the coordination of both metallic centers in several stable Pd$^{\text{I}}$ and Cu$^{\text{I}}$ homobimetallic complexes. In the homobimetallic complexes [Pd$_2$(μ-**L**-κ^2N,N',κ^2P)$_2$]X$_2$ (**L** = **34** X = SbF$_6$, PF$_6$ (**34a**), **L** = **35** X = PF$_6$), the two Pd$^{\text{I}}$ centers possess a slightly distorted square-planar geometry and nearly coplanar coordination planes, while the

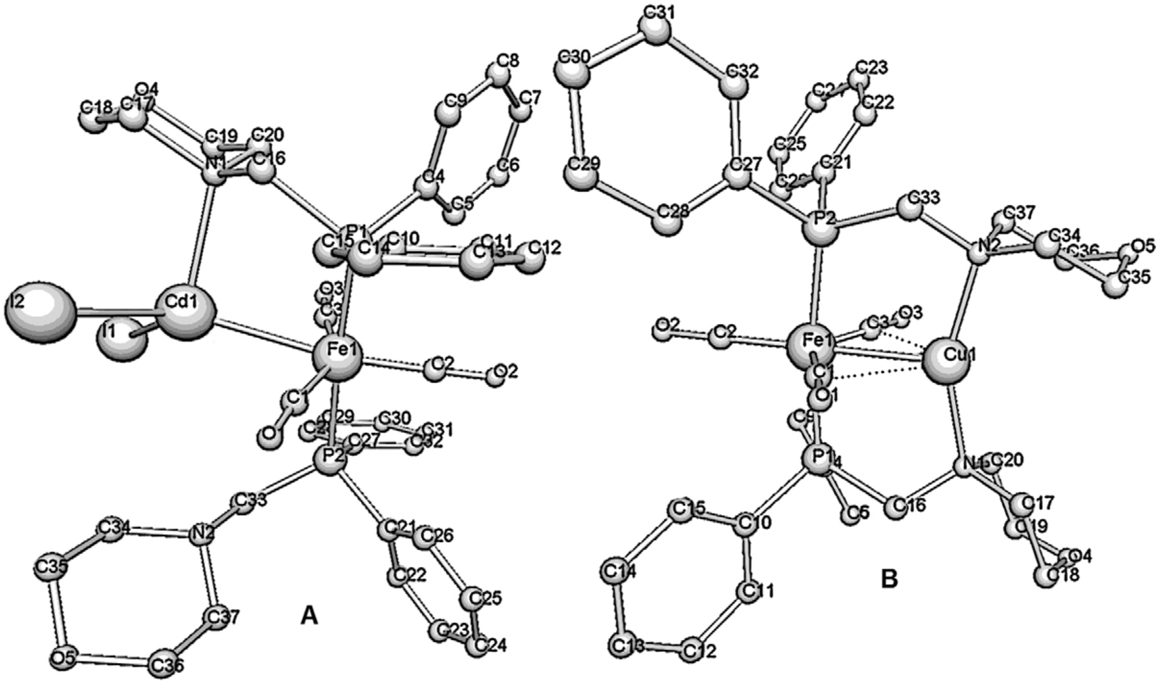

Fig. 33. Heterobimetallic complexes: (A) *trans*-[(CO)$_3$(**28**-κP)Fe(μ-**28**-κN,κP)CdI$_2$] (**28c**) and (B) *trans*-[(CO)$_3$Fe(μ-**28**-κN,κP)$_2$Cu]ClO$_4$ (**28d**).

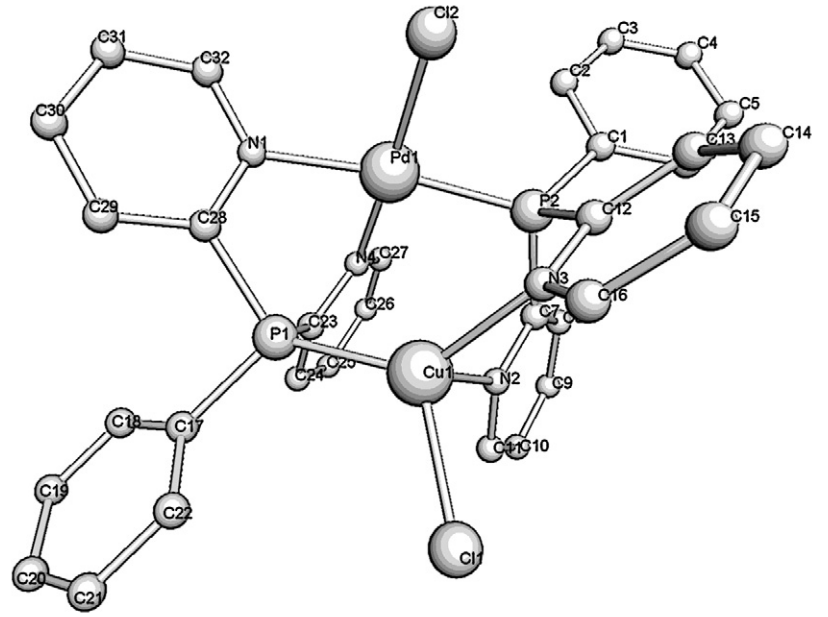

Fig. 35. Heterobimetallic complex [ClPd(μ-**25**-$\kappa^2N,N',\kappa P)_2$CuCl]ClO_4 (**25c**).

Table 8
Ligands discussed arranged by PNP versus NPN and number of spacing atoms.

$B(\ )_nA(\ )_nB$	P,N-ligand
n = 2 A = N, B = P	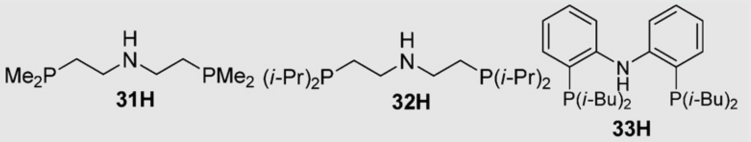 **31H** **32H** **33H**
n = 2 A = P, B = N	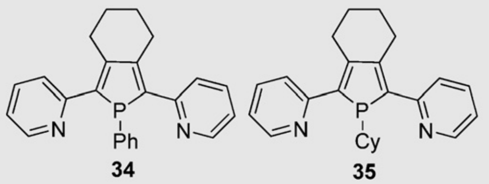 **34** **35**
n = 3 A = P, B = N	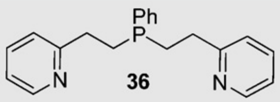 **36**

Key: A and B can be either N- or P-donor atoms but are dissimilar for the same molecule. Lower case *n* represents the number of spacer atoms in a particular bridge.

Pd–N–C–C–P 5-membered metallocycles adopt a slightly distorted envelope conformation with the P atoms out of the Pd–N–C–C planes (Fig. 39, Table 9) [113,114].

In the complex [{Cu($NCCH_3$)}$_2$(μ-**34**-κ^2N,N',κ^2P)(μ-**34**-$\kappa N,\kappa^2P$)](PF_6)$_2$ (**34b**), there is a *cis* disposition of the two **34** ligands (Fig. 40, Table 9). One of the two Cu^I center is involved in a distorted tetrahedral coordination geometry while the other adopts a pseudo-pyramidal square geometry [115,116].

Increasing the number of carbons between the A and B donors, increases the distance between the two metallic centers and decreases the possibility of the A donor acting as bridging atom.

Table 9
Geometric parameters of the bimetallic complexes.

Complex	P–Metal–N	N–Metal–N	P–Metal–P	Metal–Metal
31a	167°, 109°, 102°, 96°, 83°, 76°	83°	175°, 96°	2.99 Å, 2.97 Å
31b	143°, 141°, 75°	108°	127°, 125°	2.72 Å
33a	122, 119, 117, 116, 89, 88	107°, 104°	138°, 133°	2.62 Å
34a	170°, 81°, 80°	91°	108°	2.78 Å
34b	149°, 117°, 82°, 86°	101°	108°	2.55 Å
36a	175°, 90°	n.a.	n.a.	5.26 Å

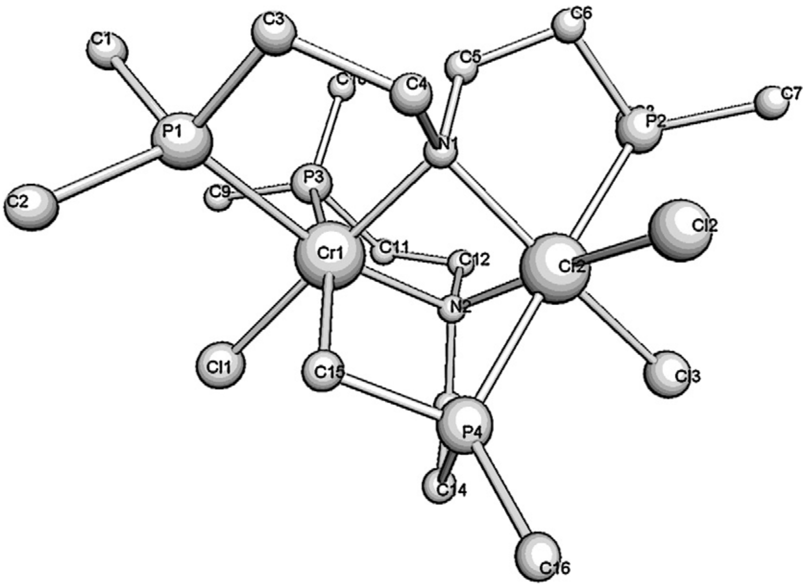

Fig. 36. Homobimetallic complex [$Cl_2Cr(\mu$-**31**-κ^2N,κ^2P,P')(μ-**31**-$\kappa C,\kappa N,\kappa^2P,P'$)CrCl] (**31a**).

4.3.1.2. n = 3. Ligand **36** acts in the isostructural complexes [{Pd(R)}$_2$(μ-**36**-$\kappa^2N,N',\kappa P)_2$]($BF_4)_2$ (R = $C_6Cl_2F_3$ (**36a**), C_6F_5) and [{Rh(CO)}$_2$(μ-**36**-$\kappa^2N,N',\kappa P)_2$]($BF_4)_2$, as P,N-chelating and P,N-bridging units, with the P-donor that coordinates only one metal center [117–120]. The two metallic centers are held at a non-bonding distance. In **36a** (Fig. 41, Table 9) each palladium atom is in a square planar environment, and the two palladium coordination planes are parallel. The two N-donors coordinated to each Pd are *cis* [120].

4.3.2. Heterobimetallic complexes

The presence of the two P,N-pockets in ligands **34** and **35** favours the formation of stable heterobimetallic complexes with metals that possess a similar hard/soft character. The heterobimetallic complex [Pd(μ-**34**-$\kappa^2N,N',\kappa P)_2$Pt](OTf)$_2$ (**34c**) was synthesized through the stepwise method reported in Scheme 6 [115]. **34c** contains two square-planar metal centers with geometrical parameters almost identical to **34a**. The major difference is represented by the position of the μ-P-donors which bind the two metal centers in a nonsymmetrical manner.

4.4. Structure 4: branched chain with one additional donor atom

See Table 10.

4.4.1. Homobimetallic complexes

In these type of P,N-ligands a third donor atom is disposed on a branched chain.

4.4.1.1. n = 0, m = 0. In the **37H** ligand, only one carbon divides the P- and N-donors, and this carbon is directly bound to a S-donor. The geometry of the ligand does not allow, in bimetallic complexes, the coordination of all the three donors, but P,N- P,S- or N,S- coor-

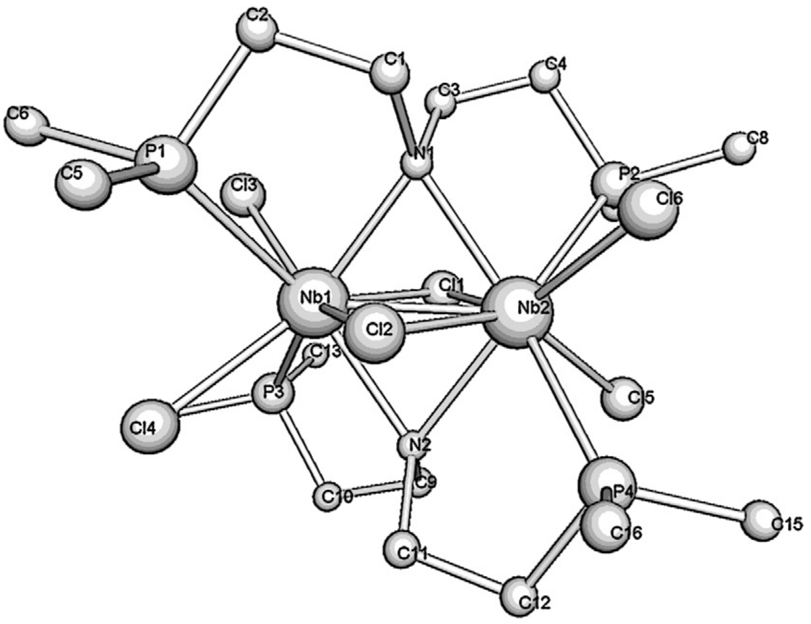

Fig. 37. Homobimetallic complex [{$NbCl_2$}$_2$(μ-**31**-κ^2N,κ^2P,P')(μ-Cl)$_2$] (**31b**).

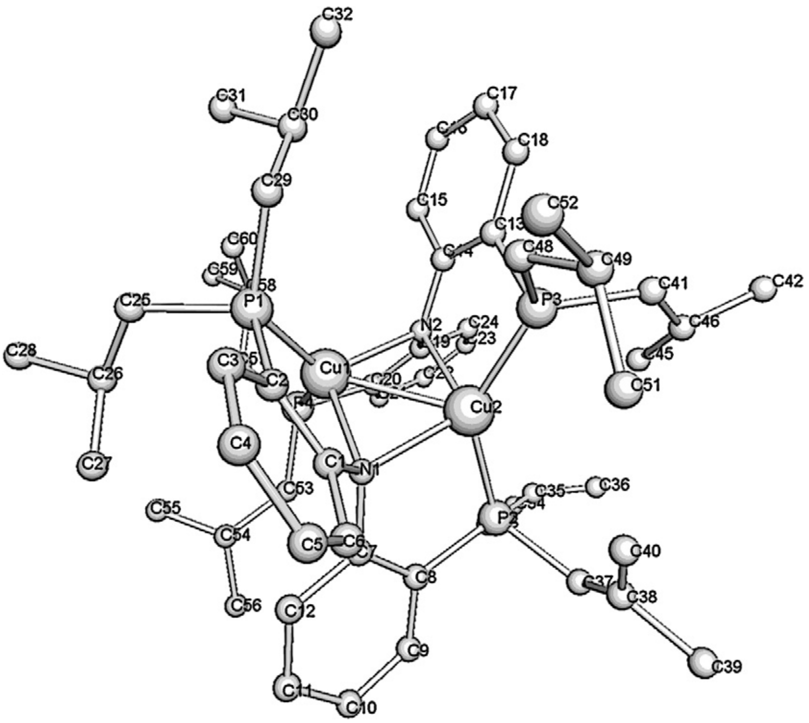

Fig. 38. Homobimetallic complex $[\mathrm{Cu}_2(\mu\text{-}\mathbf{33}\text{-}\kappa^2N,\kappa^2P,P')_2]$ (**33a**).

dination modes are possible. In $[\mathrm{Mo}_2(\mu\text{-}\mathbf{37}\text{-}\kappa N,\kappa S)_2(\mu\text{-}\mathbf{37}\text{-}\kappa N,\kappa P)_2]$ (**37a**), four **37** ligands bridge the quadruply bonded $\mathrm{Mo}_2{}^{\mathrm{II}}$ unit, two of the ligands involve their N- and S-donor while the other two involve their N- and P-donor [121]. Ligands **37** that adopt the same bonding mode are *trans* to each other and present a head-to-tail arrangement. In refluxing EtOH, **37a** slowly converts to the more stable isomer $[\mathrm{Mo}_2(\mu\text{-}\mathbf{37}\text{-}\kappa N,\kappa S)_4]$ (**37b**) containing all the four **37** ligands in a S,N-coordination mode (Scheme 7).

4.4.1.2. n = 0, m = 1. When the P- and N-donors are separated by two atoms, P,N-chelation of one metallic center to form a 5-membered ring cycle is usually preferred. The additional donor atom is involved or not in the binding of a second metallic center according to its affinity with the metals employed.

In **38**, the additional donor atom is a P-donor. Investigation of the reactivity of the **38** ligand towards several metals in groups 6–12 showed a preferential N,P-, P,P- or N,P,P-chelating binding mode for the **38** ligand towards one metallic center [122]. Exceptions are the homobimetallic complexes: $[\{\mathrm{Rh(CO)}\}_2(\mu\text{-}\mathbf{38}\text{-}\kappa N,\kappa^2P,P')_2](\mathrm{PF}_6)_2$ (**38a**) (Fig. 42, Table 11) [123,124], $[\{\mathrm{Ir(CO)}\}_2(\mu\text{-}\mathbf{38}\text{-}\kappa N,\kappa^2P,P')_2(\mu\text{-CO})](\mathrm{BF}_4)_2$ (**38b**) (Fig. 43, Table 11) [123], $[\{\mathrm{Cu(THF)}\}_2(\mu\text{-}\mathbf{38}\text{-}\kappa N,\kappa^2P,P')_2](\mathrm{BF}_4)_2$ (**38c**) (Fig. 44,

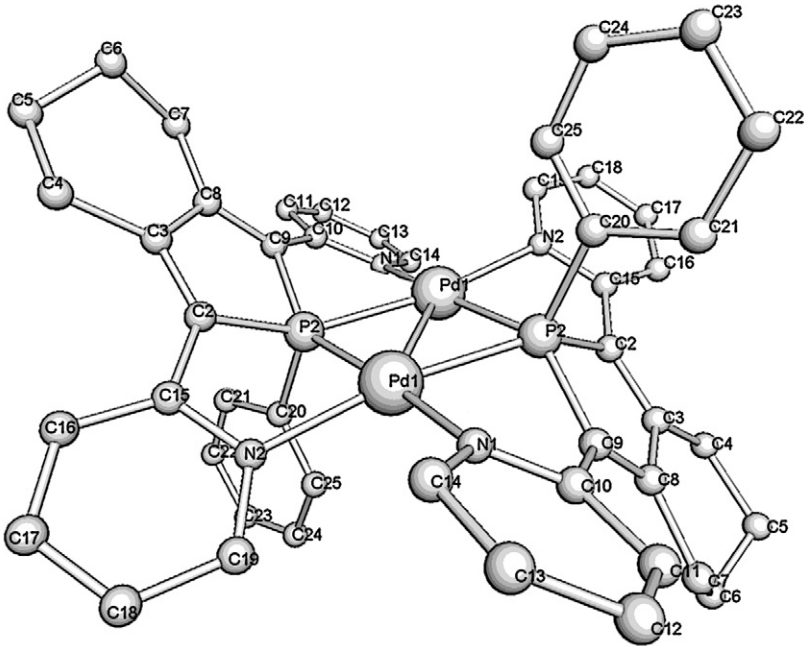

Fig. 39. Homobimetallic complex $[\mathrm{Pd}_2(\mu\text{-}\mathbf{34}\text{-}\kappa^2N,N',\kappa^2P)_2](\mathrm{PF}_6)_2$ (**34a**).

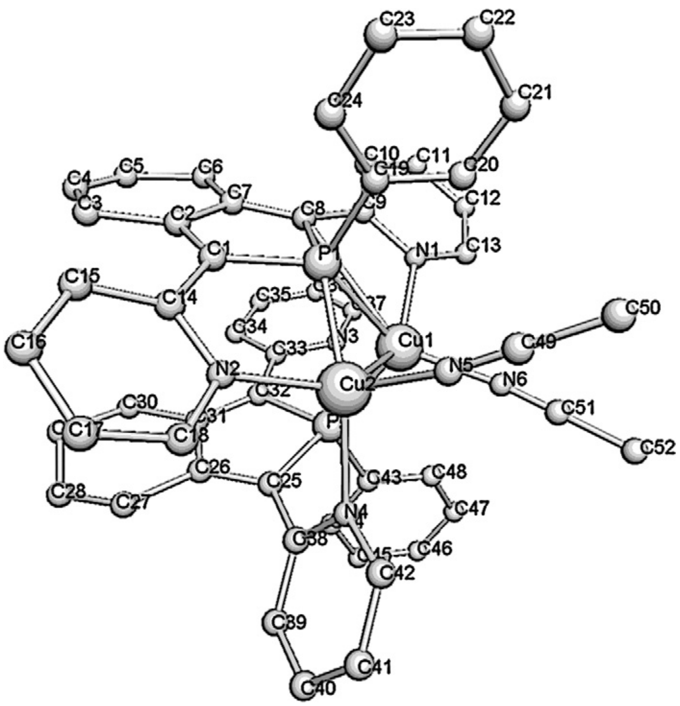

Fig. 40. Homobimetallic complex $[\{Cu(NCCH_3)\}_2(\mu\text{-}\mathbf{34}\text{-}\kappa^2 N,N',\kappa^2 P)(\mu\text{-}\mathbf{34}\text{-}\kappa N,\kappa^2 P)](PF_6)_2$ (**34b**).

Table 11) [125], and *trans*-$[(CO)Rh(\mu\text{-}\mathbf{38}\text{-}\kappa N,\kappa^2 P,P')_2Rh](BPh_4)_2$ (**38d**) (Fig. 45, Table 11). In **38a**, **38b**, **38c**, the structures show a P,P-bridging mode of the two **38** ligands with their N-donors bound to different metal centers. In **38a** and **38b** the four P-donor atoms of the two **38** ligands are almost coplanar and adopt a *trans* disposition to both the metallic centers which are at a single bond distance.

In **38c** and $[Cu_2(\mathbf{39}\text{-}\kappa N,\kappa^2 P,P')_2](BF_4)_2$ (**39a**) [126] the Cu centers adopt a distorted tetrahedral geometry. The presence of the Cu-THF binding in **38c** is probably the cause of the non-bonding Cu...Cu distance [125]. In **38d** (Fig. 45, Table 11), the two N-donor atoms of the two **38** ligands are both bonded to the same Rh center. The structure presents a *trans*, *cis*-bis(phosphine)-bridged disposition, with the four P-donor atoms of the two **38** ligands not coplanar; two of the phosphorus atoms are arranged *cis* around one Rh and *trans* around the other Rh center.

Table 10
Ligands discussed, arranged by type of additional donor atom, then number of spacer atoms.

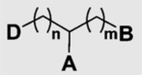	P,N-ligand
n = 0, *m* = 0, D = S	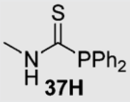 **37H**
n = 0, *m* = 1, D = P(A = P, B = N)	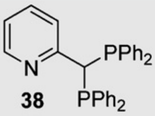 **38** 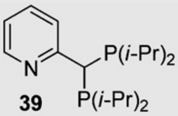 **39**
n = 0, *m* = 1, D = O (A = N, B = P)	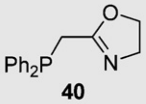 **40** 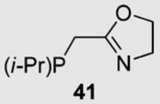 **41**
n = 1, *m* = 1, D = O(A = P, B = N)	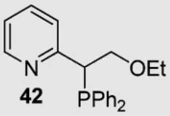 **42**

Key: A and B can be either N- or P-donor atoms but are dissimilar for the same molecule. D is a generic additional donor atom, including but not limited to P or N. Lower case *n* and *m* represent the number of spacer atoms in a particular bridge.

4.4.1.3. n = 0, 1, m = 1. In **42**, **40**, and **41** ligands, the additional donor atom is an oxygen. The ligands are usually involved in monometallic complexes as P,N-chelating ligands. The sole bimetallic complex reported with **42** is $[\{Rh(CO)\}_2(\mu\text{-}\mathbf{42}\text{-}\kappa N,\kappa O,\kappa P)_2](ClO_4)_2$ (**42a**) (Scheme 8) [118], where the ligands act as P,N-chelating and P/N,O-bridging units and no Metal–Metal bond is present.

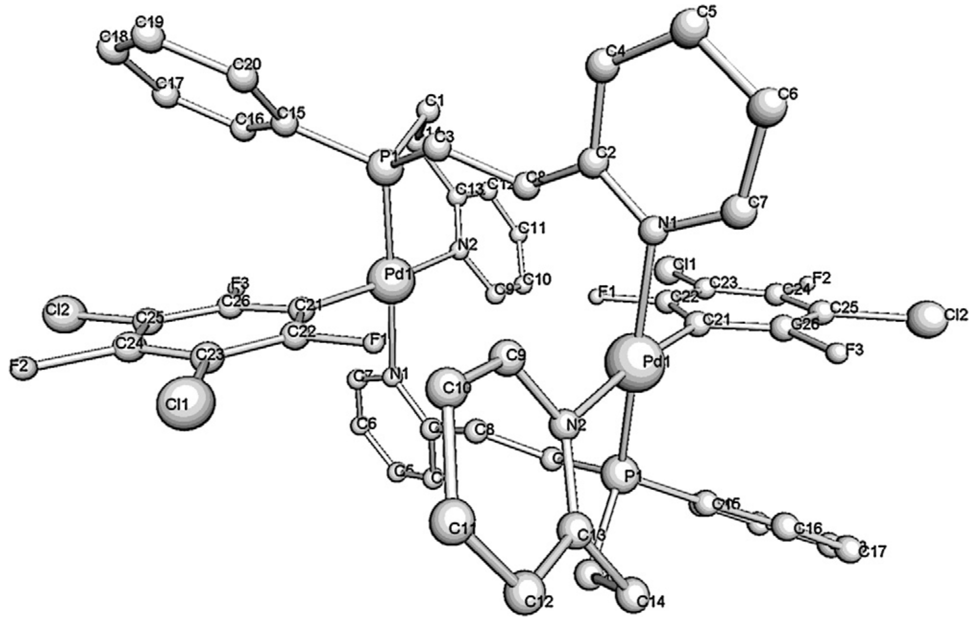

Fig. 41. Homobimetallic complex $[\{Pd(C_6Cl_2F_3)\}_2(\mu\text{-}\mathbf{36}\text{-}\kappa^2 N,N',\kappa P)_2](BF_4)_2$ (**36a**).

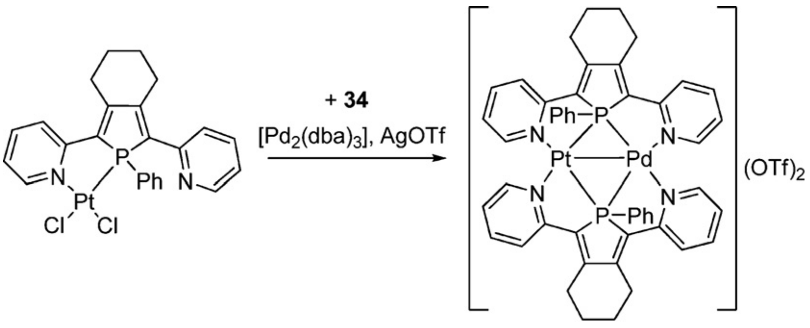

34c

Scheme 6.

Table 11
Geometric parameters of the bimetallic complexes.

Complex	P–Metal–N	N–Metal–N	P–Metal–P	Metal–Metal
38a	99°, 77°	n.a.	177°	3.05 Å
38b	101°, 99°, 73°	n.a.	171°, 172°	2.82 Å, 2.81 Å
38c	134°, 83°	n.a.	138°	3.37 Å
38d	173°, 175°, 83°, 77°	99°	130°, 170°	2.67 Å
40d	n.a.	133°	174°	2.54 Å

In [{CoCl$_2$}$_2$(μ-**L**-κ*N*,κ*P*)$_2$] (L = **40**, **41**) (**40a**, **41a**) [127], the two **40** or **41** ligands adopt a P,N-bridging mode and no O-donor coordination is observed (Scheme 9).

4.4.2. Heterobimetallic complexes

Heterobimetallic complexes were synthesized by reacting [Rh(**38**-κ^2*P*)$_2$]BF$_4$ with M(PPh$_3$)NO$_3$ (M = Au (**38e**), Ag (**38f**)) [128]. Complexes **38e** and **38f** possess a structure similar to **38d**.

Fe–Cu, Fe–Co, and Fe–Pd heterobimetallic complexes containing two **40** ligands were obtained by reacting *trans*-[Fe(CO)$_3$(μ-**40**-κ*P*)$_2$] (**40b**) with a second metallic center (Scheme 10) [129].

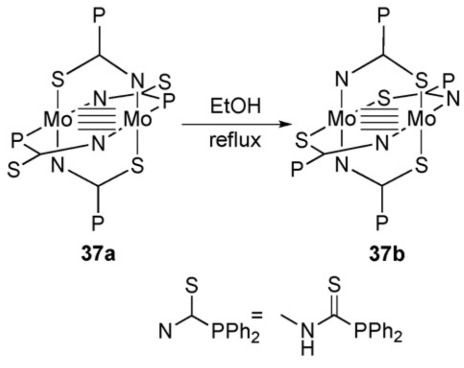

Scheme 7.

In all the complexes, a dative Metal–Metal bond is present; the P-donor of **40** is bound to the Fe and the N-donor of **40** to the other metal center. [(CO)$_3$Fe(μ-**40**-κ*N*,κ*P*)$_2$Pd(NCCH$_3$)](BF$_4$)$_2$ (**40c**) contains an electron rich metal such as Pd^{II} and presents limited stability, probably due to the poor capability of Pd^{II} to take part in

Fig. 42. Homobimetallic complex [{Rh(CO)}$_2$(μ-**38**-κ*N*,κ^2*P*,*P*′)$_2$](PF$_6$)$_2$ (**38a**).

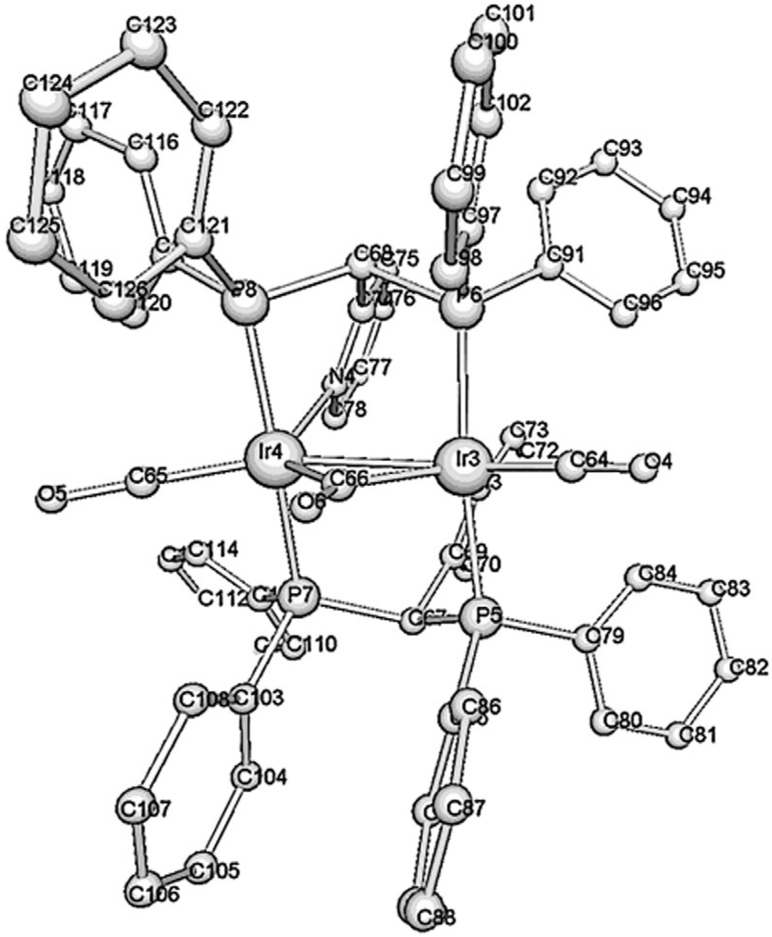

Fig. 43. Homobimetallic complex $[\{Ir(CO)\}_2(\mu\text{-}\mathbf{38}\text{-}\kappa N,\kappa^2 P,P')_2(\mu\text{-}CO)](BF_4)_2$ (**38b**).

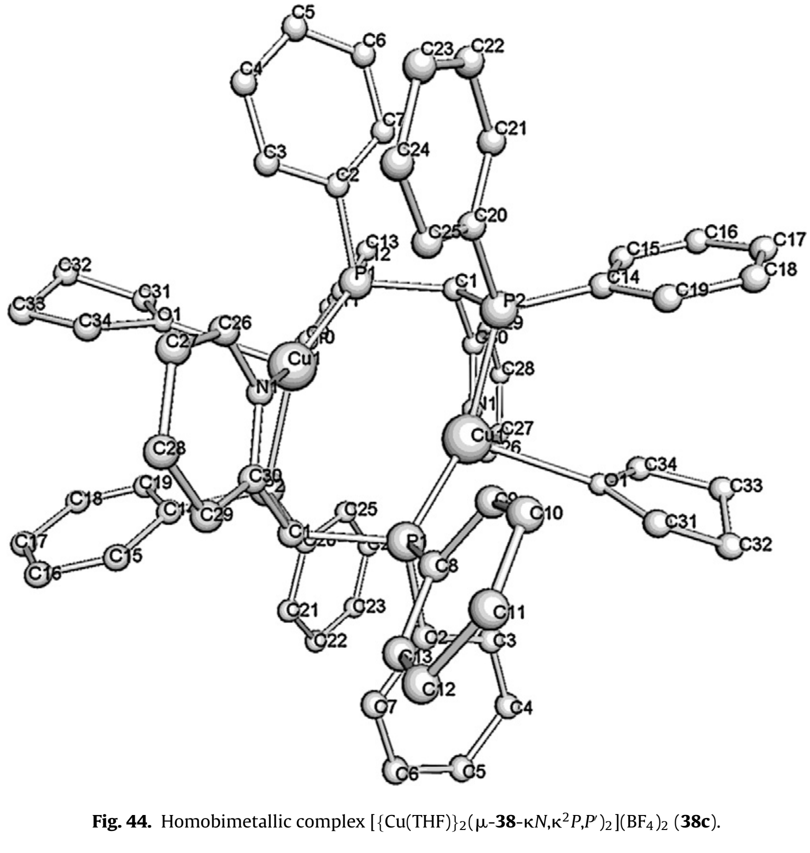

Fig. 44. Homobimetallic complex $[\{Cu(THF)\}_2(\mu\text{-}\mathbf{38}\text{-}\kappa N,\kappa^2 P,P')_2](BF_4)_2$ (**38c**).

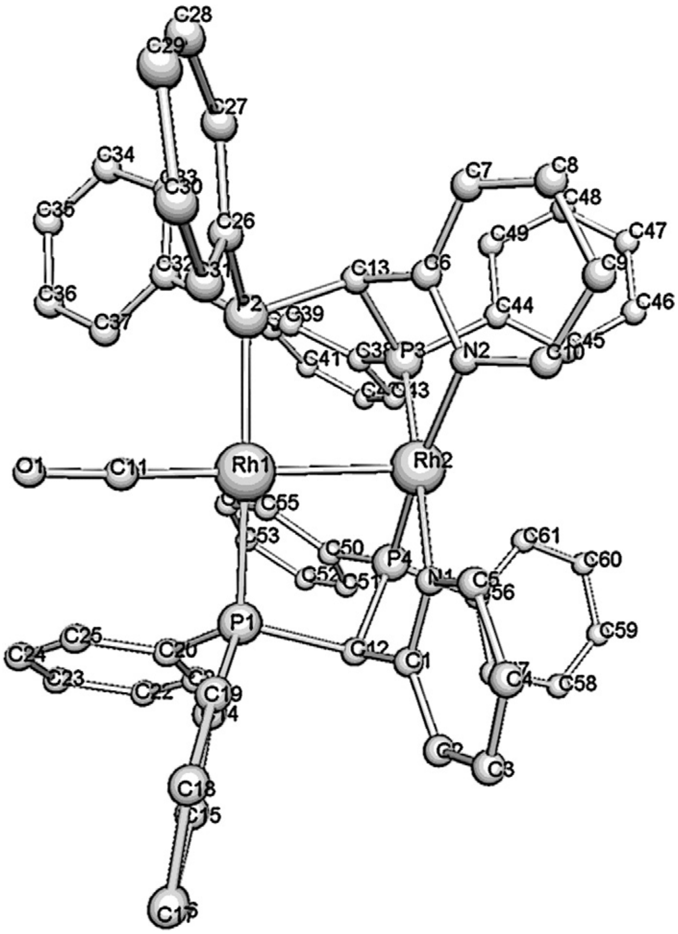

Fig. 45. Homobimetallic complex *trans*-[(CO)Rh(μ-**38**-$\kappa N,\kappa^2 P,P'$)$_2$Rh](BPh$_4$)$_2$ (**38d**).

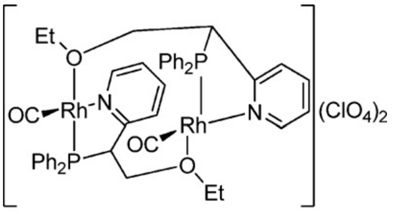

42a

Scheme 8.

a dative bond with Fe [129]. In *trans*-[(CO)$_3$Fe(μ-**40**-$\kappa N,\kappa P$)$_2$Cu]BF$_4$ (**40d**) (Fig. 46, Table 11) the Fe is in a trigonal bipyramidal geometry bond to the P-donors of the two **40** ligands in a *trans* arrange, while Cu^{I} is in a trigonal geometry. The complex possesses a cradle cavity shape with a P–Fe–Cu–N torsional angles of ∼7° [130].

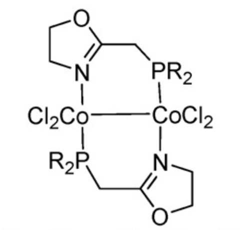

R = *i*-Pr or Ph (**40a, 41a**)

Scheme 9.

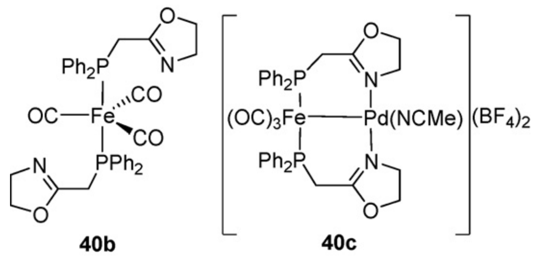

40b **40c**

Scheme 10.

4.5. Structure 5: PN$_3$ or NP$_3$ ligands

Tripodal ligands are briefly treated to highlight their use in the synthesis of heterobimetallic complexes where the B-donors bind to one metal center and the A-donor binds a second metal. This structure is interesting enough that their inclusion seemed worthwhile. However, the concept behind the bonding is different from the other ligands treated in this document and so only a brief discussion is given (Table 12 and Scheme 11).

The tripodal ligands **43H**–**45H** react with [Ti(NMe$_2$)$_4$] to generate the monometallic complex [Ti(NMe$_2$)(**L**-$\kappa^3 N,N',N''$)] (**L** = **43**, **44** (**44a**), **45**) where the N-donors chelate to the Ti center and the P-donor is available to bind a second metal. The reaction of **44a** with [Ni(CO)$_4$] produces at first the bimetallic complex [(Me$_2$N)Ti(μ-**44**-$\kappa^3 N,N'',N''',\kappa P$)Ni(CO)$_3$] (**44b**) which then gradually converts to the trimetallic complex [{Ti(NMe$_2$)}$_2$(μ-**44**-$\kappa^3 N,N'',N''',\kappa P$)$_2$Ni(CO)$_2$] (**44c**) (Scheme 11 and Fig. 47) [131].

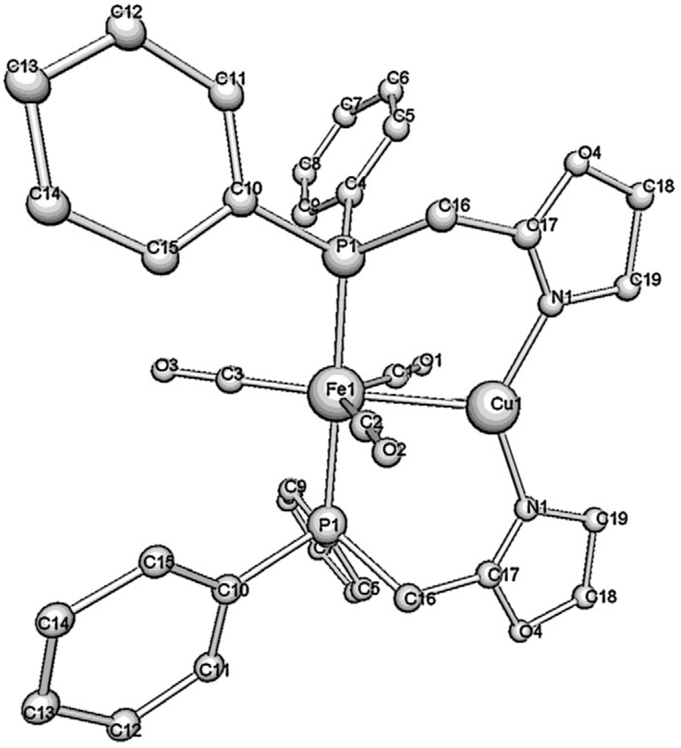

Fig. 46. Heterobimetallic complex *trans*-[(CO)$_3$Fe(μ-**40**-$\kappa N,\kappa P$)$_2$Cu]BF$_4$ (**40d**).

Table 12
Ligands discussed, classified according to donor atoms and number of spacing atoms.

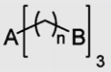	P,N-ligand
n = 1 A = P, B = N	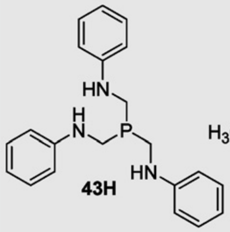 **43H** 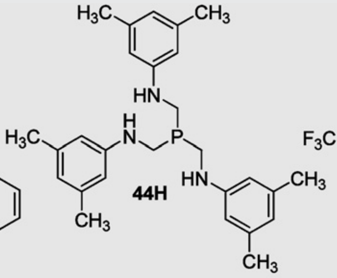 **44H** 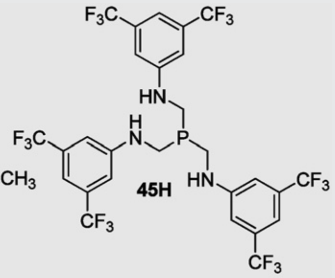 **45H**

Key: A and B can be either N- or P-donor atoms but are dissimilar for the same molecule. Lower case *n* represents the number of spacer atoms in a particular bridge.

4.6. Structure 6: two P and two N donors in a symmetric linear chain

See Table 13.

4.6.1. Homobimetallic complexes

4.6.1.1. n = 1, m = 1 (A = N and B = P). Ligand **46** commonly behaves with transition metals as a P,P-bridging ligand [132]. The only example where the ligand adopts a P,N-bridging mode is in *cis*,*cis*-[Mo$_2$(μ-**46**-κ*N*,κ*P*)$_2$(μ-O$_2$CCH$_3$-κ^2*O*,*O*′)$_2$](BF$_4$)$_2$ (**46a**) where the Mo–Mo quadruple bond is bridged by two acetate and two P,N-**46** ligands disposed in a *cis* arrangement (Fig. 48, Table 14) [133].

4.6.1.2. n = 2, m = 0, 1, 4 (A = N and B = P). When the number of atoms between the P- and N-donor is equal to two, each metal is P,N-chelated. The geometry of the spacer and its length determine the disposition of the two A,B-pockets.

In the Ni^{II}, Rh^{I}, Ir^{I}, and Pd^{II} homobimetallic complexes isolated with **47** ligand, the two metals are in close proximity but at a distance too great for Metal–Metal bond formation (Scheme 12) [134–137].

Homobimetallic complexes with an A-frame structure, such as [{PtMe}$_2$(μ-**48**-κ^2*N*,*N*′,κ^2*P*,*P*′)(μ-H)$_2$] (**48a**) (Fig. 49, Table 14) and [{PtMe}$_2$(μ-**48**-κ^2*N*,*N*′,κ^2*P*,*P*′)(μ-Cl)] (**48b**) (Fig. 50, Table 14) are easily synthesized with ligand **48** [138].

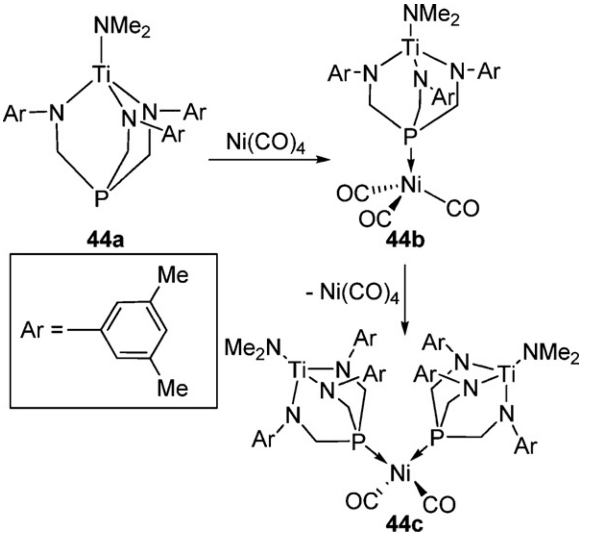

Scheme 11.

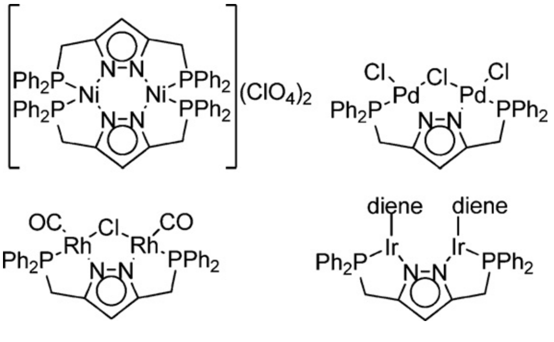

Scheme 12.

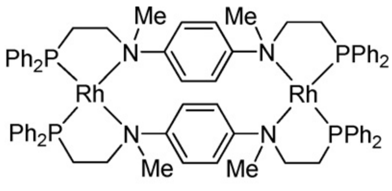

49a

Scheme 13.

In [Rh$_2$(μ-**49**-κ^2*N*,*N*′,κ^2*P*,*P*′)$_2$](BF$_4$)$_2$ (**49a**), the two metallic centers are held at a longer Metal. . .Metal distance by **49** (Scheme 13) [139].

4.6.1.3. n = 1, m = 1, 2, 3 (A = P and B = N). The three pyridylphosphine ligands: **50**, **51**, and **52** adopt in their homobimetallic complexes coordination modes **II** and **I** (Scheme 14), characterized respectively in the *rac*-[{Rh(CO)Cl}$_2$(μ-**50**-κ^2*N*,*N*′,κ^2*P*,*P*′)] (**50a**) (Fig. 51, Table 14) and *meso*-[{RhCl}$_2$(μ-**L**-κ^2*N*,*N*′,κ^2*P*,*P*′)$_2$][Rh(CO)$_2$Cl$_2$]$_2$ (L = **51**, **52** (**52a**)) complexes (Fig. 52, Table 14) [140].

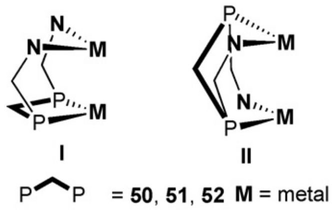

Scheme 14.

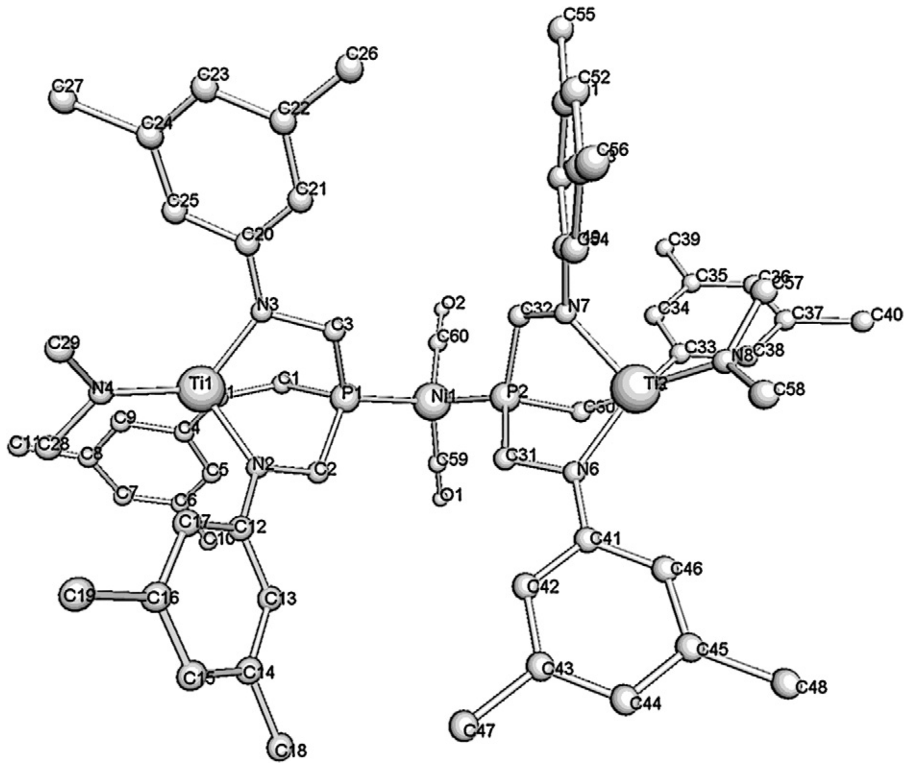

Fig. 47. Heterobimetallic complex $[\{Ti(NMe_2)\}_2(\mu\text{-}\mathbf{44}\text{-}\kappa^3N,N'',N''',\kappa P)_2Ni(CO)_2]$ (**44c**).

Table 13
Ligands discussed, arranged by donor type and then spacing atoms.

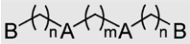	P,N-ligand
n = 1, *m* = 1 A = N, B = P	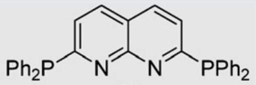 **46**
n = 2, *m* = 0, 1, 4 A = N, B = P	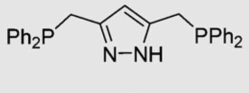 **47H** 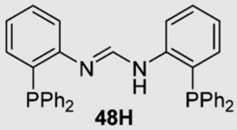 **48H** 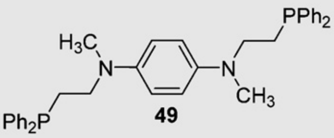 **49**
n = 1, *m* = 1, 2, 3 A = P, B = N	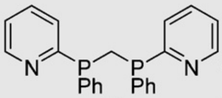 **50** 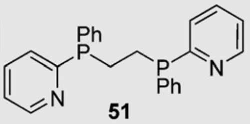 **51** 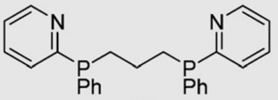 **52**
n = 3, *m* = 2, 3 A = P, B = N	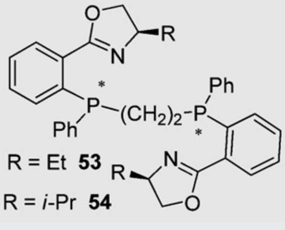 R = Et **53** R = *i*-Pr **54** 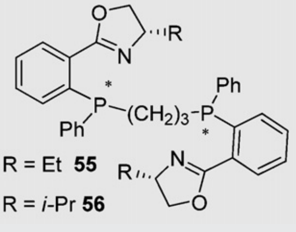 R = Et **55** R = *i*-Pr **56**

Key: A and B can be either N- or P-donor atoms but are dissimilar for the same molecule. Lower case *n* and *m* represent the number of spacer atoms in a particular bridge.

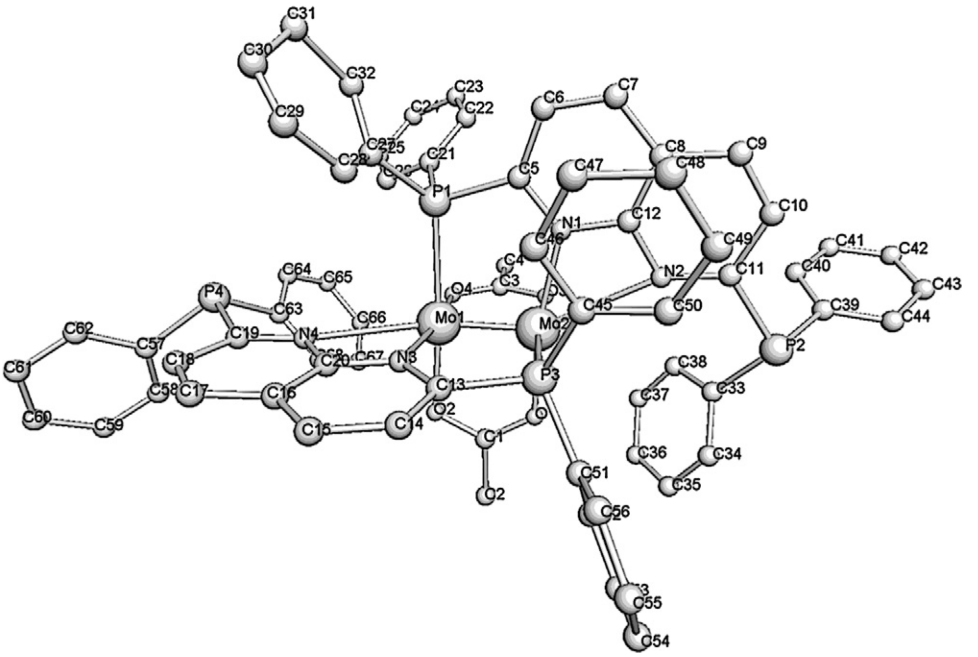

Fig. 48. Homobimetallic complex *cis*,*cis*-[Mo$_2$(μ-**46**-κ*N*,κ*P*)$_2$(μ-O$_2$CCH$_3$-κ^2*O*,*O*′)$_2$](BF$_4$)$_2$ (**46a**).

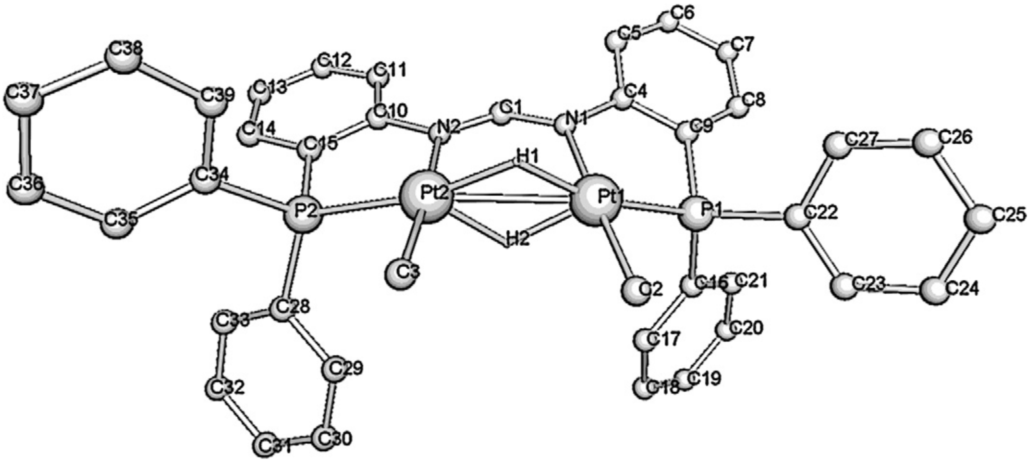

Fig. 49. Homobimetallic complex [{PtMe}$_2$(μ-**48**-κ^2*N*,*N*′,κ^2*P*,*P*′)(μ-H)$_2$] (**48a**).

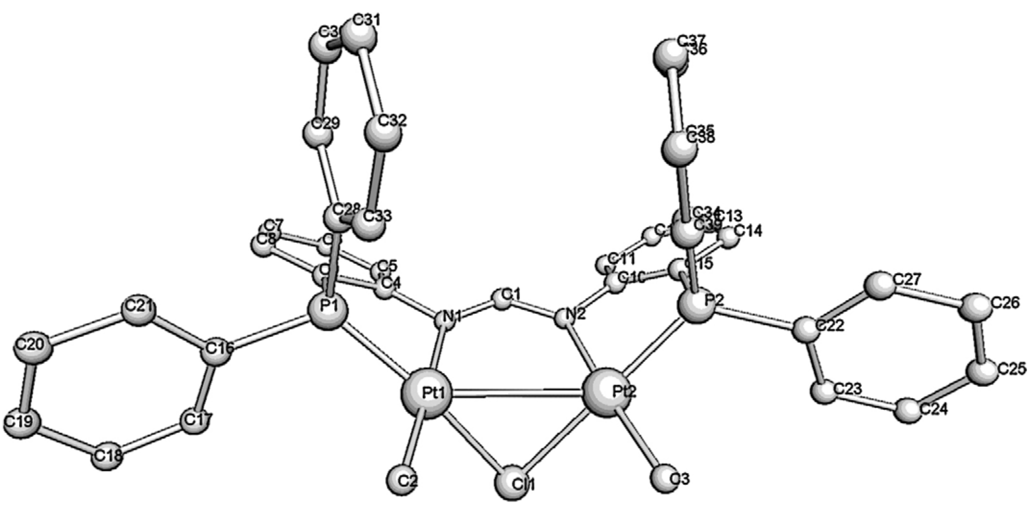

Fig. 50. Homobimetallic complex [{PtMe}$_2$(μ-**48**-κ^2*N*,*N*′,κ^2*P*,*P*′)(μ-Cl)] (**48b**).

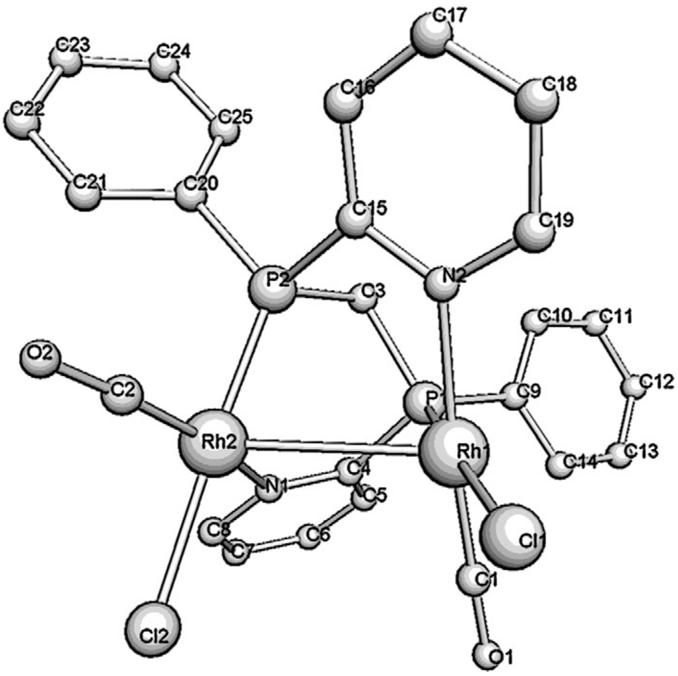

Fig. 51. Homobimetallic complex [{Rh(CO)Cl}$_2$(μ-**50**-κ^2*N*,*N′*,κ^2*P*,*P′*)] (**50a**).

Table 14
Geometric parameters of the bimetallic complexes.

Complex	P–Metal–N	N–Metal–N	P–Metal–P	Metal–Metal
46a	94°, 88°	n.a.	n.a.	2.12 Å
48a	83°	n.a.	n.a.	2.80 Å
48b	83°	n.a.	n.a.	3.16 Å
50a	93°, 92°	n.a.	n.a.	2.65 Å
52a	175°, 94°, 93°	82°	90°	3.09 Å
53a	92°,91°	n.a.	n.a.	7.03 Å

4.6.1.4. n = 3, m = 2, 3 (A = P and B = N). Bis-P,N-chelating palladium bimetallic complexes were obtained with the bis(oxazolinylphosphine) **53**–**56** ligands as the allylic palladium complex [{Pd$_2$(η^3-C$_4$H$_6$)}$_2$(μ-**53**-κ^2*N*,*N′*,κ^2*P*,*P′*)] (**53a**) (Fig. 53, Table 14). In **53a**, the two Pd centers do not interact with each other [141].

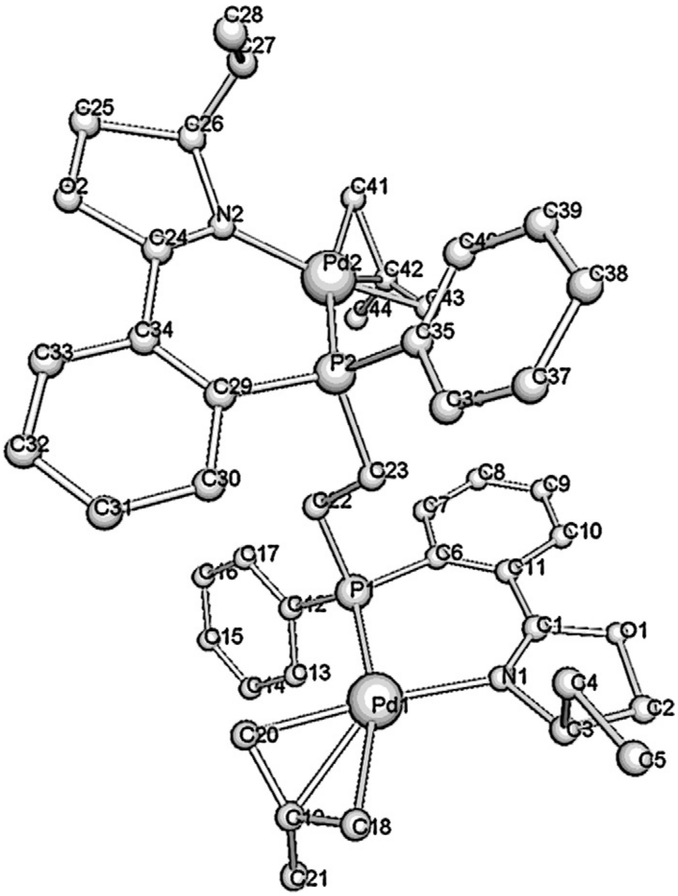

Fig. 53. Homobimetallic complex [{Pd(η^3-C$_4$H$_6$)}$_2$(μ-**53**-κ^2*N*,*N′*,κ^2*P*,*P′*)] (**53a**).

4.7. Structure 7: complex structures with multiple PNP or NPN chains

See Table 15.

4.7.1. Homibimetallic complexes

4.7.1.1. n = 2, m = 2, 5, 6 (A = N, B = P). Homobimetallic complexes containing transition metals from group 8 to group 11 were

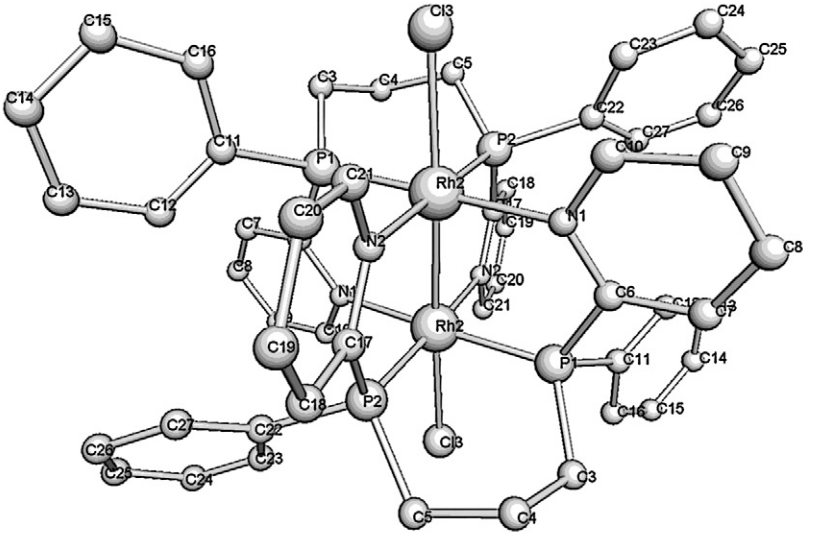

Fig. 52. Fragment [{RhCl}$_2$(μ-**52**-κ^2*N*,*N′*,κ^2*P*,*P′*)$_2$] of complex (**52a**).

Table 15
Ligands discussed, PNP then NPN.

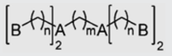	P,N-ligand
$n = 2$, $m = 2, 5, 6$ A = N, B = P	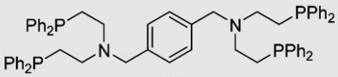 **57** 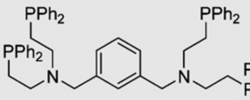 **58** 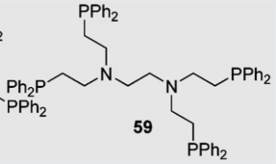 **59**
$n = 1$, $m = 2$ A = P, B = N, S	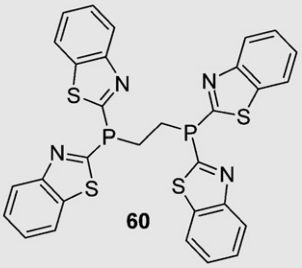 **60**
$n = 2$, $m = 1$ A = P, B = N	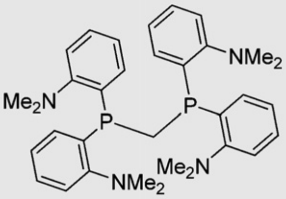 **61**

Key: A and B can be either N- or P-donor atoms but are dissimilar for the same molecule. Lower case *n* represents the number of spacer atoms in a particular bridge.

obtained with ligands **57**, **58**, and **59**. These ligands are composed of two terdentate moieties containing N- and P-donor atoms and are separated by either semi-flexible or rigid units. They support several coordination geometries: tetrahedral [142,143], square planar [142,144–146], trigonal planar [147], octahedric [144,148], trigonal-pyramidal [143], trigonal bipyramidal [142,145,146]. The majority of these complexes have been characterized spectroscopically. However, X-ray analysis was used for the characterization of $[\{CuCl\}_2(\mu$-**57**-$\kappa^4P,P',P'',P''')]$ (**57a**) (Fig. 54, Table 16) [147], $[\{CuCl\}_2(\mu$-**58**-$\kappa^2N,N',\kappa^4P,P',P'',P''')]$ (**58a**) (Fig. 55, Table 16) [143], and $[\{CuCl(PPh_3)\}_2(\mu$-**59**-$\kappa^4P,P',P'',P''')]$ (**59a**) (Fig. 56, Table 16) [143].

4.7.1.2. n = 1, m = 2 (A = P, B = N, S). In $[\{RhCl\}_2(\mu$-**60**-$\kappa N,\kappa^2P,P')_2]$ (**60a**) (Fig. 57, Table 16) and $[\{RhCl\}_2(\mu$-**60**-$\kappa^2N,N',\kappa^2P,P')_2][RhCl_4($**60**-$\kappa^2P,P')]_2$ (**60b**) (Fig. 58, Table 16), each **60** ligand P,P-chelates one Rh center and at the same time P,N-bridges both Rh centers in a head-to-tail configuration [149,150]. In

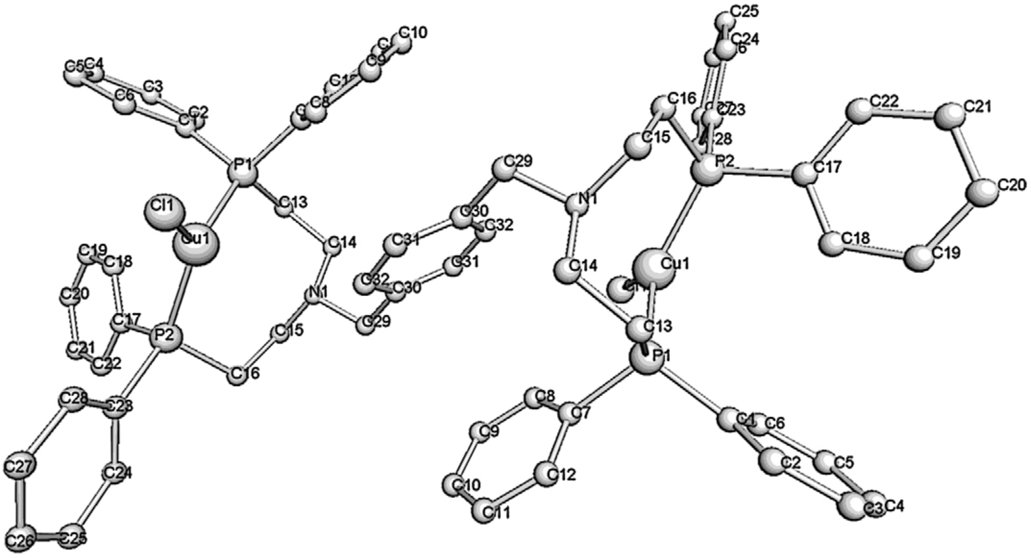

Fig. 54. Homobimetallic complex $[\{CuCl\}_2(\mu$-**57**-$\kappa^4P,P',P'',P''')]$ (**57a**).

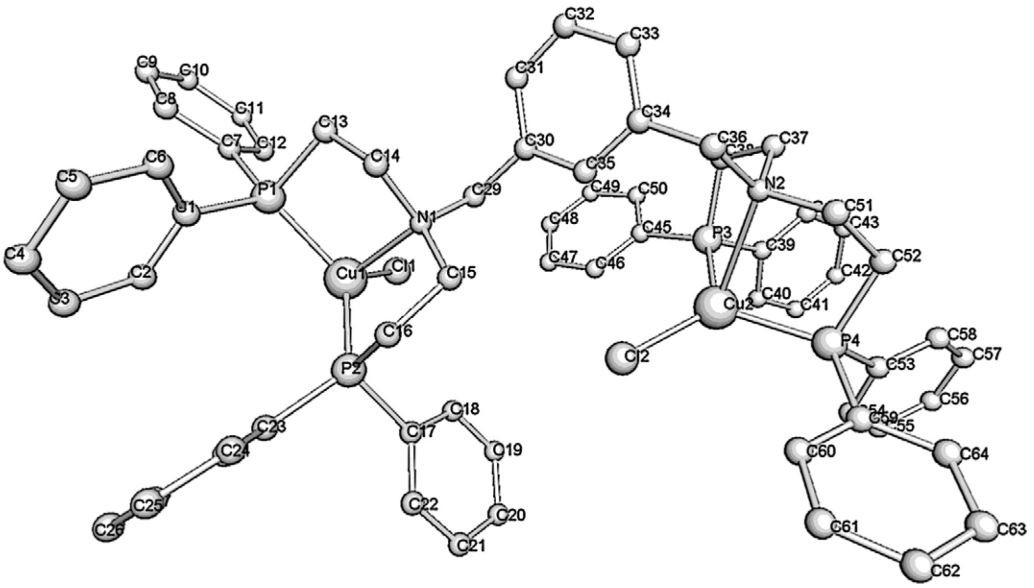

Fig. 55. Homobimetallic complex $[\{CuCl\}_2(\mu$-**58**-$\kappa^2N,N',\kappa^4P,P',P'',P''')]$ (**58a**).

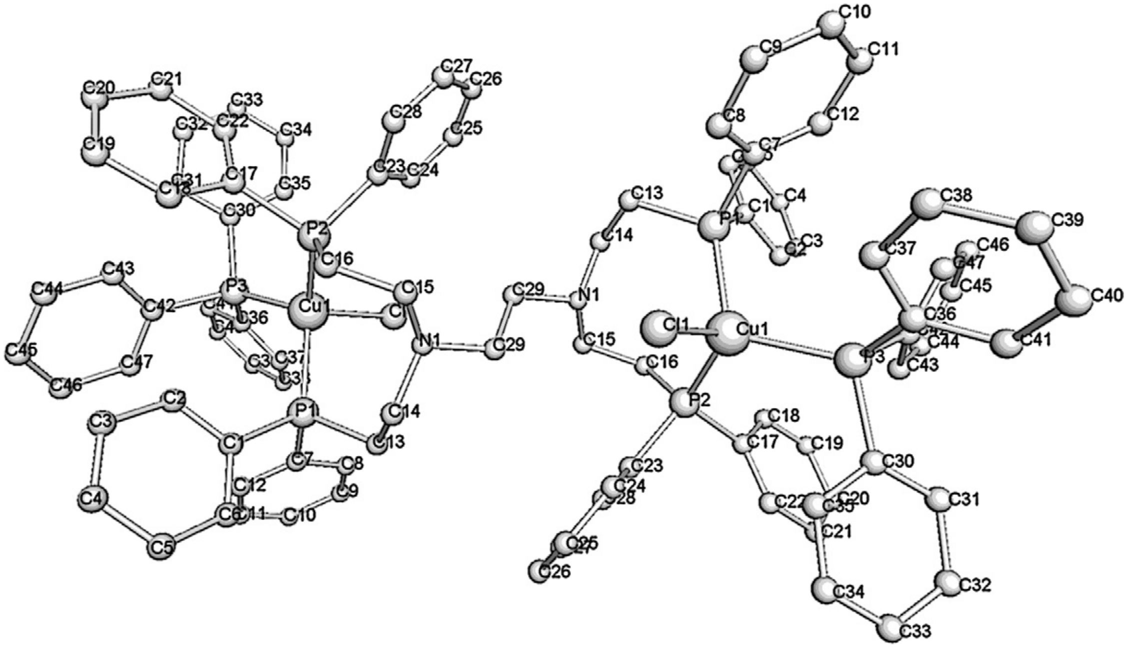

Fig. 56. Homobimetallic complex $[\{CuCl(PPh_3)\}_2(\mu$-**59**-$\kappa^4P,P',P'',P''')]$ (**59a**).

Table 16
Geometric parameters of the bimetallic complexes.

Complex	P–Metal–N	N–Metal–N	P–Metal–P	Metal–Metal
57a	n.a.	n.a.	121°	7.69 Å
58a	85°, 84°, 83°, 80°	n.a.	115°, 116°	6.78 Å
59a	n.a.	n.a.	111°	9.12 Å
60a	173°, 167°, 98°, 93°	n.a.	84°	3.07 Å
60b	179°, 173°, 95°, 89°	91°	84°	2.72 Å
61a	86°, 85°	n.a.	n.a.	4.33 Å, 4.13 Å
61b	86°	n.a.	n.a.	2.53 Å

60a there is a slight interaction between the two Rh centers while in **60b** the Rh–Rh distance corresponds to that of a single bond.

4.7.1.3. n = 2, m = 1 (A = P, B = N). Ligand **61** was used to synthesize the racemic mixtures (*R*,*R* and *S*,*S*) *rac*-$[\{IrCl(CO)\}_2(\mu$-**61**-$\kappa^2N,N',\kappa^2P,P')]$ (**61a**) [151] (Fig. 59, Table 16) and *rac*-$[\{PdCl\}_2(\mu$-**61**-$\kappa^2N,N',\kappa^2P,P')]$ (**61b**) (Fig. 60, Table 16) [152]. In both complexes, the metallic centers are in a square-planar geometry. In **61b**, the two Pd are at a single bond Pd–Pd distance.

4.7.2. Heterobimetallic complexes

As in ligands **34** and **35**, the presence in ligand **61** of two P,N-pockets allows stable heterobimetallic complexes with metals that posses a similar hard/soft character.

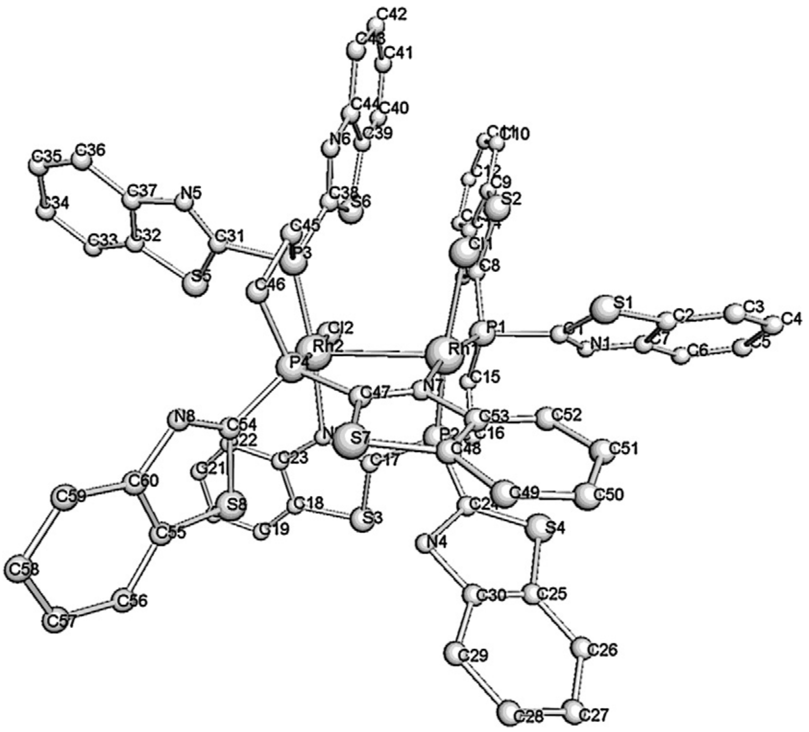

Fig. 57. Homobimetallic complex $[\{RhCl\}_2(\mu$-**60**-$\kappa N,\kappa^2P,P')_2]$ (**60a**).

Heterobimetallic complexes were prepared with ligand **61** by reacting a pre-synthesized monometallic–**61** complex with a second metallic center. A racemic mixture of *S*,*S* and *R*,*R* enantiomers of $[(CO)ClIr(\mu$-**61**-$\kappa^2N,N',\kappa^2P,P')Rh(CO)Cl]$ (**61d**) was prepared by reacting the monometallic complex $[Ir(CO)Cl($**61**-$\kappa N,\kappa P)]$ (**61c**) with ½ equivalent of $[RhCl(COD)]_2$ under an atmosphere of CO (Scheme 15) [151].

The reaction of $[PdCl_2($**61**$)]$ with K_2PtCl_4 led to $[Cl_2Pt(\mu$-**61**-$\kappa^2N,N',\kappa^2P,P')PdCl_2]$ (**61e**) which was reduced with KOH to synthesize the racemic mixture (*R*,*R*)/(*S*,*S*)-$[ClPt(\mu$-**61**-$\kappa^2N,N',\kappa^2P,P')PdCl]$ (**61f**) (Scheme 16) [153].

The highly strained structure $[Ru(CO)_3($**61**-$\kappa^2P,P')]$ (**61 g**) was also reacted with ½ equivalent of $[Rh_2Cl_2(COD)_2]$ or $[Rh_2Cl_2(C_2H_4)_4]$ to give the $[(CO)_2Ru(\mu$-$CO)(\mu$-**61**-

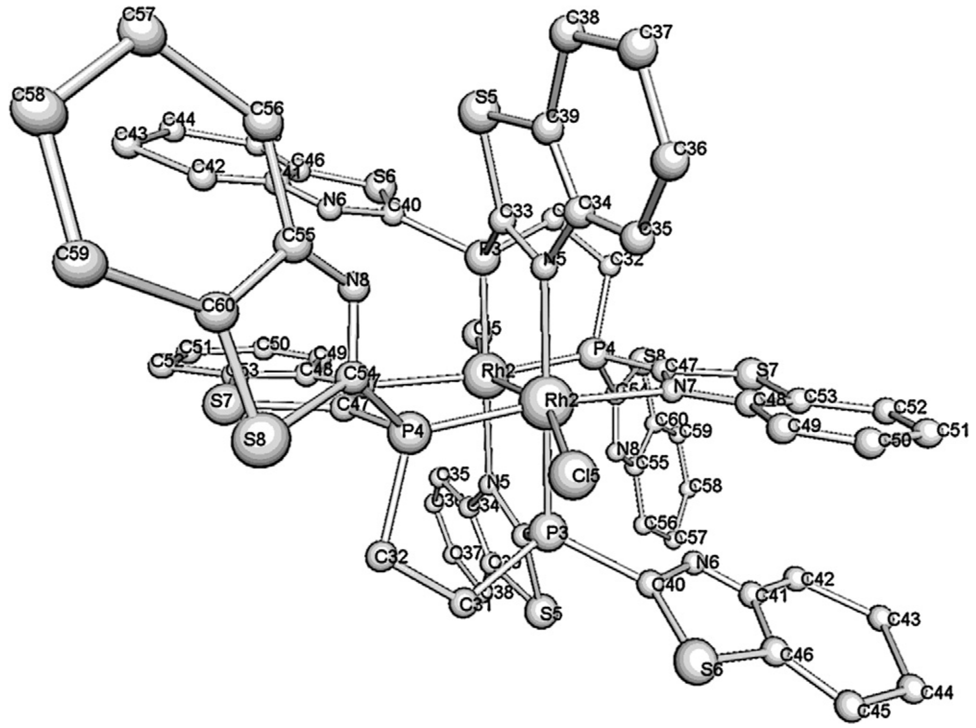

Fig. 58. Fragment $[\{RhCl\}_2(\mu$-**60**-$\kappa^2N,N',\kappa^2P,P')_2]$ of complex **60b**.

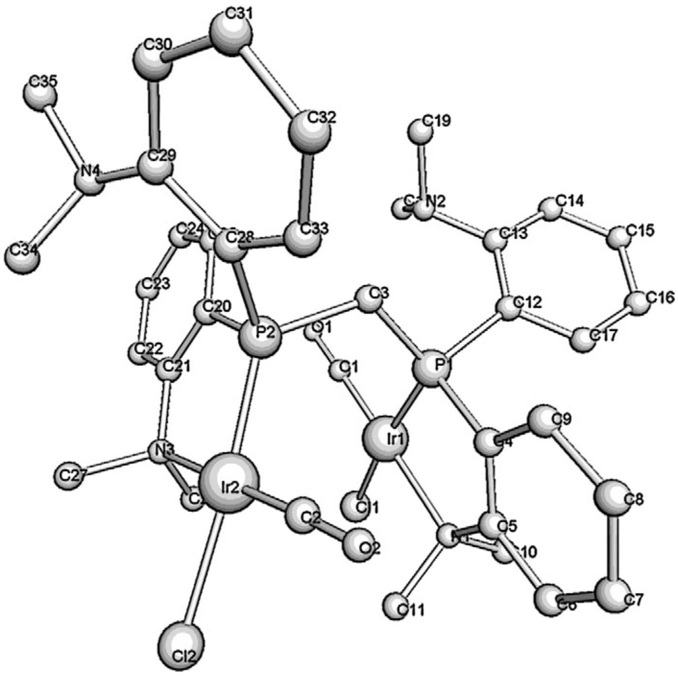

Fig. 59. Homobimetallic complex [{IrCl(CO)}$_2$(μ-**61**-κ^2*N*,*N*′,κ^2*P*,*P*′)] (**61a**).

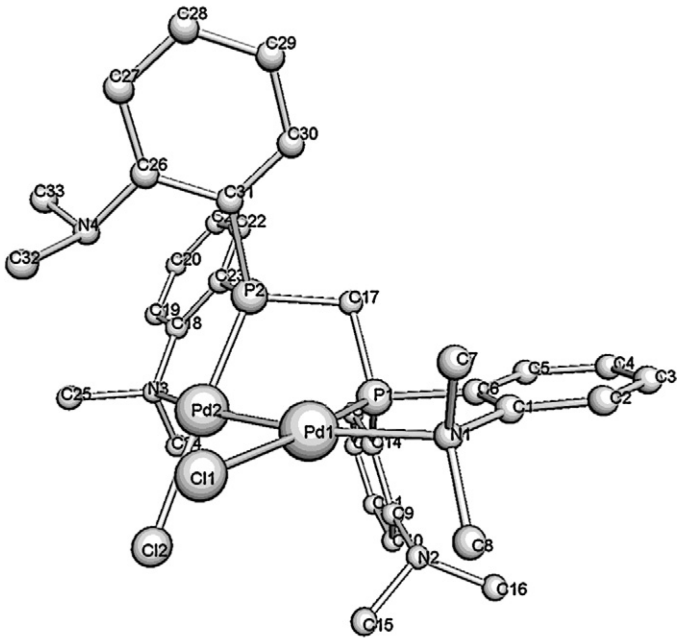

Fig. 60. Homobimetallic complex [{PdCl}$_2$(μ-**61**-κ^2*N*,*N*′,κ^2*P*,*P*′)] (**61b**).

κ^2*N*,*N*′,κ^2*P*,*P*′)RhCl] (**61h**) complex, where the two metal are bridged through the two P-donors of the **61** ligand and a CO molecule (Scheme 17) [151]. The species was characterized through spectroscopic analysis.

5. Catalysis

The application of P,N-binucleating ligands in catalysis is promising, however few of the ligands reported here were actu-

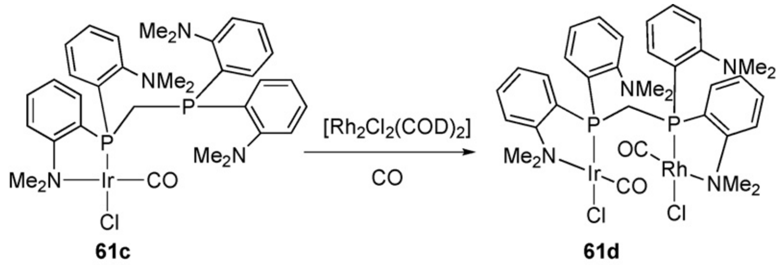

Scheme 15.

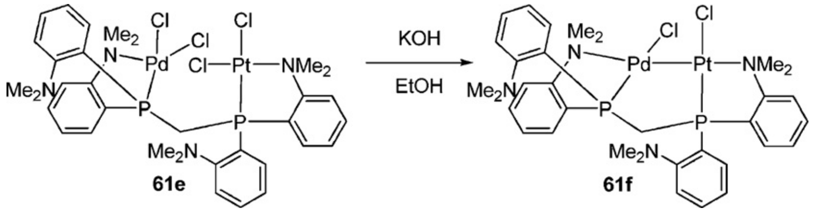

Scheme 16.

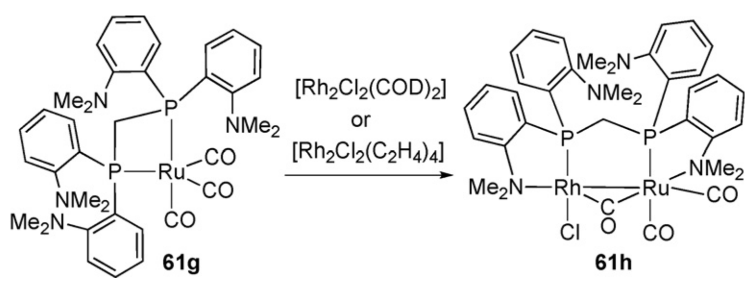

Scheme 17.

ally designed for catalysis. Some were synthesized for structural study, some for the luminescent, host–guest or other properties of their corresponding multimetallic complexes. Of the ones that were designed for catalysis, often the literature stops after their creation. It is hard to say if this was because there were not enough results to justify reporting or if the work was just not completed. In any event, only a limited number of bimetallic complexes were reported to be catalytically active.

5.1. Structure 1

5.1.1. n = 0

A patent reports Pt–Ti, Pd–Ti, and Ni–Ti heterobimetallic complexes of ligand **1** in olefin polymerisation and hydroformylation catalysis [154].

5.1.2. n = 1

A number of homo- and heterobimetallic complexes containing ligand **3** were tested in catalysis.

The homobimetallic complex $[\{Rh(BH_4)\}_2(\mu\text{-CO})(\mu\text{-}\mathbf{3}\text{-}\kappa P,\kappa N)_2]$ exhibits some catalytic activity in the hydrogenation of *tert*-butylethylene and ethylene [45].

$[ClPd(\mu\text{-CO})(\mu\text{-}\mathbf{3}\text{-}\kappa P,\kappa N)_2Mo(CO)_2Cl]$, in its heterogeneous and homogeneous forms, catalyze the hydrogenation of 1,5,9-cyclododecatriene [155].

Complexes $[\{PdX\}_2(\mu\text{-}\mathbf{3}\text{-}\kappa P,\kappa N)_2]$ (X = Cl (**3b**), Br, I, OCN, SCN, NO_2, N_3) along with a redox catalyst and an ammonium halide were excellent catalysts for the oxidative carbonylation of phenol [156]. Their performance was superior to $[\{PdX\}_2(\mu\text{-dpm-}\kappa P,P')_2]$ (dpm = bis(diphenylphosphino)methane, X = Cl, Br, I, OCN, SCN, NO_2, N_3) and the conventional $PdBr_2/Ce(trop)_4$ (trop = tropolate) system. $[\{PdX\}_2(\mu\text{-}\mathbf{3}\text{-}\kappa P,\kappa N)_2]$ (X = Cl (**3b**), NO_2) catalyze also the direct synthesis of polycarbonate from CO and Bisphenol A [157].

Complexes $[(CO)_3Fe(\mu\text{-}\mathbf{3}\text{-}\kappa P,\kappa N)_2Mo(CO)_3]$, $[(CO)_3Fe(\mu\text{-CO})(\mu\text{-}\mathbf{3}\text{-}\kappa P,\kappa N)_2RhCl]$, $[(CO)_3Fe(\mu\text{-}\mathbf{3}\text{-}\kappa P,\kappa N)_2CuCl]$, $[(CO)_3Fe(\mu\text{-}\mathbf{3}\text{-}\kappa P,\kappa N)_2Ni(NCS)_2]$, and $[(CO)_3Fe(\mu\text{-}\mathbf{3}\text{-}\kappa P,\kappa N)_2Hg(NCS)_2]$ are active catalysts for the carbonylation of ethanol to ethyl propionate [71]. At higher temperatures (200 °C), $[(CO)_3Fe(\mu\text{-CO})(\mu\text{-}\mathbf{3}\text{-}\kappa P,\kappa N)_2RhCl]$ presents a better catalytic activity than $RhCl(Ph_3P)_3$. This was explained as a synergic behaviour between the Fe and Rh metals, since the Fe atom is believed to promote migratory CO insertion at the Rh atom [158]. At lower reaction temperatures however the positive influence of the Fe atom was considered to be hidden by the rate-determining step. The oxidative addition of RI towards the Rh atom (which is the rate-determining step) is hindered by the presence of the Fe atom.

Heterobimetallic complexes $[(CO)ClIr(\mu\text{-}\mathbf{3}\text{-}\kappa P,\kappa N)_2Cu](BF_4)$ and $[(CO)ClIr(\mu\text{-}\mathbf{3}\text{-}\kappa P,\kappa N)_2Tl](PF_6)$ were tested as catalysts in the hydroformylation of styrene. Even if the reactions lead to the formation of the product, it was proven that under the experimental conditions used the Cu–N and Tl–N bonds broke giving the $[Ir(CO)Cl(\mathbf{3}\text{-}\kappa P)_2]$ monometallic complex which was the active species [82].

In general, bimetallic complexes containing ligand **3** and its derivatives present a wide range of reactive behaviours such as: ring opening, ligand exchange, ionization and oxidative addition [21]. The predominance of these types of processes and the difficulty of the reversible breaking/formation of their Metal–Metal bond is considered to be a limitation in the use of these types to bimetallic structures in catalysis.

5.1.3. n = 2

The bimetallic complex $[Pd_2(\mu\text{-}\mathbf{16}\text{-}\kappa C^{23-24},\kappa N,\kappa P)_2](BF_4)_2$ (**16a**) is kinetically stable and does not catalyze the CO/ethylene copolymerisation reaction [66].

5.1.4. n = 3

$[Cl_2Ti(\mu\text{-}\mathbf{19}\text{-}\kappa P,\kappa N)_2PdCl_2]$ complex catalyzes the Suzuki–Miyaura cross-coupling reactions between phenylboronic acid and 3,5-dimethoxybromobenzene or 4-nitrobromobenzene. Little or no catalytic activity was observed in the arylamination reactions between 4-bromoanisole and aniline.

$[Cl_2Ti(\mu\text{-}\mathbf{19}\text{-}\kappa P,\kappa N)_2PtCl_2]$, $[Cl_2Ti(\mu\text{-}\mathbf{19}\text{-}\kappa P,\kappa N)_2PdCl_2]$, and $[Cl_2Ti(\mu\text{-}\mathbf{19}\text{-}\kappa P,\kappa N)_2NiBr_2]$ are catalysts for olefin polymerisation with low activity. $[Cl_2Ti(\mu\text{-}\mathbf{19}\text{-}\kappa P,\kappa N)_2PtCl_2]$ and $[Cl_2Ti(\mu\text{-}\mathbf{19}\text{-}\kappa P,\kappa N)_2PdCl_2]$ result in a drop in activity compared to $[TiCl_2(\mathbf{19}\text{-}\kappa N)_2]$, while no polymerisation was observed with $[Cl_2Ti(\mu\text{-}\mathbf{1}\text{-}\kappa P,\kappa N)_2NiBr_2]$ [87].

5.2. Structure 2

n = 2 and D = N A = N B = P

No catalytic studies were reported with ligand **29**, but Cu^I and Ag^I homobimetallic complexes of ligand **29** undergo ligand substitution [102] and insertion reactions of various anions [103,159].

5.3. Structure 3

5.3.1. n = 2 and A = P B = N

Complex $[Pd_2(\mu\text{-}\mathbf{34}\text{-}\kappa^2N,N',\kappa P)_2](SbF_6)_2$ was an inactive species in the carbon monoxide-ethylene copolymerisation [160].

$[Pd_2(\mu\text{-}\mathbf{34}\text{-}\kappa^2N,N',\kappa P)_2](PF_6)_2$ (**34a**) did not show any reactivity with CO and PPh_3 but an insertion reaction accompanied by the rupture of the Pd–Pd bonding was observed with dimethyl acetylene dicarboxylate [114].

5.4. Structure 4

5.4.1. n = 0, m = 1 and D = P A = P B = N

No catalytic studies were reported with ligand **38** but complex $[Rh(\mu\text{-}\mathbf{38}\text{-}\kappa N,\kappa^2P,P')_2Au](BF_4)(NO_3)$ (**38e**) exhibits Metal–Metal breaking reactivity and ligand addition [128].

5.4.2. n = 0, m = 1 and D = O A = N B = P

Trans-$[(CO)_3Fe(\mu\text{-}\mathbf{40}\text{-}\kappa N,\kappa P)_2Cu]BF_4$ (**40d**) is a catalyst for the cyclopropanation of styrene with ethyl diazoacetate and the Diels–Alder reaction between cyclopentadiene and methacrolein [130]. Unfortunately, except for the reactions being catalytically tested with the correspondent monometallic $[Cu(\mathbf{40}\text{-}\kappa P)_2]BF_4$ complex for comparison, no further studied were reported.

5.5. Structure 6

5.5.1. n = 2, m = 0 and A = N B = P

$[\{Rh(NBD)\}_2(\mu\text{-}\mathbf{47}\text{-}\kappa N,N',\kappa P,P')](BF_4)$ and $[\{Ir(COD)\}_2(\mu\text{-}\mathbf{47}\text{-}\kappa N,N',\kappa P,P')](BF_4)$ catalyze the hydrogenation process of a limited number of alkenes and alkynes [135]. Hydrogenation appears to proceed via one metal at a time. A deactivation of the H_2 addition to the second metal was observed after the first H_2 was added to the first metal.

Complex $[\{Rh(CO)_2\}_2(\mu\text{-}\mathbf{47}\text{-}\kappa N,N',\kappa P,P')]BF_4$ catalyzed the disproportionation reaction of cyclohexadiene to benzene and cyclohexene as well as the dimerisation reaction of norbornadiene [136]. The weakness of the bonds of the inner CO ligands (*trans* to P atoms) in $[\{Rh(CO)_2\}_2(\mu\text{-}\mathbf{47}\text{-}\kappa N,N',\kappa P,P')]BF_4$ makes the complex an important precursor for the *cis*-divacant active species $[\{Rh(CO)\}_2(\mu\text{-}\mathbf{47}\text{-}\kappa N,N',\kappa P,P')](BF_4)$ [136,137].

The complexes obtained with ligand **47** showed a spectrum of reactivity from a single/reversible oxidative addition to irreversible/double oxidative addition according to the electron density on the two metal centers [135].

5.5.2. $n = 2$, $m = 1$ and $A = N$ $B = P$

Dinuclear palladium complexes [{Pd(*p*-tolyl)}$_2$(μ-**48**-κ^2*N*,*N*′,κ^2*P*,*P*′)(μ-OH)], [{PdMe}$_2$(μ-**48**-κ^2*N*,*N*′,κ^2*P*,*P*′)(μ-OH)] and [{Pd(*p*-tolyl)}$_2$(μ-**48**-κ^2*N*,*N*′,κ^2*P*,*P*′)(μ-I)] catalyze *cis*-hydroarylation of alkyne with monosubstituted arenas in the presence of tri(*n*-butyl)borane, giving *meta* and *para* products in statistical ratios [161]. Both electron-rich and electron poor arenes were reactive. The borane was suggested to be necessary for the formation of the hydride-bridged [{Pd(R)}$_2$(μ-**48**-κ^2*N*,*N*′,κ^2*P*,*P*′)(μ-H)] complexes (R = *p*-tolyl, Me). No products were observed using the corresponding mononuclear palladium complexes.

The hydroalkenylation of alkynes to give 1,3-dienes was also performed using the same bimetallic complexes from the *cis*-hydroarylation reaction in the presence of a metallic hydride reagent [162].

Complexes [{Pd(*p*-tolyl)}$_2$(μ-**48**-κ^2*N*,*N*′,κ^2*P*,*P*′)(μ-OH)] and [{PdMe}$_2$(μ-**48**-κ^2*N*,*N*′,κ^2*P*,*P*′)(μ-OH)] also catalyze efficiently and stereoselectively the addition of heteroarene C–H bonds to alkynes [163]. In the cross-addition of triisopropylsilylacetylene to internal and terminal alkynes, comparable results were obtained with the previous complexes and the mononuclear complexes [Pd(*p*-tolyl)(**48**-κ*N*,κ^2*P*)] and [PdMe(**48**-κ*N*,κ^2*P*)] [164].

[{PdMe}$_2$(μ-**48**-κ^2*N*,*N*′,κ^2*P*,*P*′)(μ-Cl)] (**48b**), [{PdCl}$_2$(μ-**48**-κ^2*N*,*N*′,κ^2*P*,*P*′)(μ-Cl)], [{PdI}$_2$(μ-**48**-κ^2*N*,*N*′,κ^2*P*,*P*′)(μ-*p*-tolyl)], and [MePd(μ-**48**-κ^2*N*,*N*′,κ^2*P*,*P*′)(μ-Cl)PtMe] are efficient and selective catalysts for the double carbonylation of iodobenzene [165]. At higher loading concentrations, complex [{PdMe}$_2$(μ-**48**-κ^2*N*,*N*′,κ^2*P*,*P*′)(μ-Cl)] (**48b**) was more active and selective than its correspondent monometallic complex [PdMe(**48**-κ*N*,κ^2*P*)(μ-Cl)].

5.5.3. $n = 2$, $m = 4$ and $A = N$ $B = P$

No catalytic studies were reported with ligand **49**, however [Rh$_2$(μ-**49**-κ^2*N*,*N*′,κ^2*P*,*P*′)$_2$](BF$_4$)$_2$ (**49a**) complex has shown reactivity with small molecules to give substitution reactions that involve the breaking of the Rh–N bond [139].

5.5.4. $n = 3$, $m = 2, 3$ and $A = P$ $B = N$

Allylic palladium complexes [Pd$_2$(η^3-allyl)$_2$(L)](PF$_6$)$_2$ (L = **53**–**56**) catalyze the allylic alkylation of rac-3-acetoxy-1,3-diphenyl-1-propene with dimethyl malonate. Similarities to the monometallic P,N-palladium catalytic systems used in allylic substitutions were observed on the steric and electronic factors: the enantioselectivity was enhanced by bulky substituents on the oxazoline moiety but not by the configuration of the stereogenic phosphorus atom. In the case of the bimetallic complexes, higher enantioselectivity was observed at higher loading of catalysts [141].

5.6. Structure 7

5.6.1. $n = 2$, $m = 2, 5, 6$ and $A = N$ $B = P$

No catalytic studies were reported with ligands **57**–**59**, but their bimetallic complexes take part in ligand substitution [146] and reductive/oxidative addition processes [166,145]. Two reversible or quasi-reversable oxidation–reduction processes were observed in electrochemical studies with Cu$^{\mathrm{I}}$ [167], Ru$^{\mathrm{II}}$ [148], Ni$^{\mathrm{II}}$ and Co$^{\mathrm{II}}$ homobimetallic complexes synthesized with ligands **59** and **58** [142].

5.6.2. $n = 2$, $m = 1$ and $A = P$ $B = N$

rac-[{PdCl}$_2$(μ-**61**-κ^2*N*,*N*′,κ^2*P*,*P*′)] (**61a**) and *rac*-[Cl$_2$Pt(μ-**61**-κ^2*N*,*N*′,κ^2*P*,*P*′)PdCl$_2$] (**61e**) were effective catalysts for the Heck reaction of iodobenzene and styrene [168]. Although the bimetallic complexes are more active than predicted from the sum of the activities of the mono-metallic chosen to mimic their half units (leading to suppose a possible metal–metal cooperation), kinetic data imply that these bimetallic complexes dissociate into active monometallic catalysts.

rac-[{PdCl}$_2$(μ-**61**-κ^2*N*,*N*′,κ^2*P*,*P*′)] (**61a**) exhibits Metal–Metal breaking reactivity [152], reversible insertion of small molecules [153], and ligand substitution reactions [153].

6. Conclusion

The available literature indicates some general considerations to take into account about when different types of P,N-ligands are likely to give bimetallic structures.

In the prediction of the coordination mode of a P,N-ligand to one or two metal centers, consideration of the length and the flexibility of the P,N-ligand backbone is crucial. If the coordination mode of the P,N-ligand is not obviously determined by constraints imposed by the ligand backbone, the determining factor for the metal(s)/P,N-ligand structure is the stability of the monometallocycle versus the bimetallocycle. These are obtained respectively with the coordination of the P,N-ligand to one or two metallic centers.

Generally, 5-membered ring cycles are the most stable, followed by the 6-membered rings, while smaller ring sizes are less favoured because of the strain of the bond angles involved.

The stability of the 5-membered bimetallocycle explains the large number of bimetallic complexes synthesized with P,N-ligands where P- and N-donor are separated by one atom. In these complexes, the formation of a Metal–Metal bond is usually favoured due to the short distance between the P- and N-donor.

When P- and N-donor are separated by two or three atoms, the formation of a monometallic P,N-ligand complex is often preferred since 5- and 6-membered ring metallocycles are obtained in these cases. However, the formation of bimetallic complexes can be induced by the geometry of the P,N-ligand backbone, the preferred metal bite angle, the formation of a Metal–Metal bond that stabilizes the resulting bimetallic complex or when the synthesis of the complex involves a pre-formed Metal–Metal multiple bonded core.

When there are more than three atoms between the P- and N-donor then the rigidity of the P,N-ligand backbone becomes very important since larger ring sizes are much less stable. Only by limiting the possibility of bond rotation and having the donor atoms already tied into the optimal positions is the formation of large metallo- or bimetallocycles enhanced. Intramolecular forces such as π–π bonding, hydrogen bonding, or hydrogen–halogen interaction play an important role for the stabilization of bimetallic structures.

In the case of P,N-ligands containing additional donor atom/s, the two main considerations are the number of additional donors and its/their affinity with the metallic centers. Then, similar prediction paths as for the simpler P,N-ligands can be used. A classification of these ligands according to the type and number of additional donors and their disposition on linear or branched chains helps to predict/explain the structure of the mono/bimetallic complexes formed.

The synthesis of heterobimetallic complexes has some additional considerations. If the two metals both have a soft character then synthesis of bimetallic complexes can be not trivial. Successful synthesis in this case usually involves P,N-ligands capable of chelating each metal center through a P and an N donor.

The synthesis of early–late heterobimetallic complexes is helped by the different hard/soft character of the P- and N-donors. In some cases, P,N-ligands that would not form homobimetallic complexes can give heterobimetallic complexes of this type. The use of two metallic centers that can adopt different coordination geometries can also facilitate the formation of the bimetallic structure.

Bimetallic complexes containing rigid ligands with a short bite angle have found application in catalysis. Their reactivity is strongly influenced by the limited flexibility of the ligand that holds the two metals at a tight distance.

Ligands with two P,N-chelating coordination sites in close proximity appear to be promising ligands for the construction of catalytically active bimetallic complexes where the two metals can cooperate.

Acknowledgments

I would like to thank Dr. J.M. Brown for the critical review and suggestions, Dr. T. Archibald for his comments, and J.K. Thiessen for his precious help in proofreading.

Appendix A. Abbreviations

Ac	acetate
Bz	benzyl
COD	cycloocta-l,5-diene
Cy	cyclohexyl
Cp^*	pentamethylcyclopentadiene
Me	methyl
NBD	norbornadiene or bicyclo[2.2.1] hepta-2,5-diene
OTf	trifluoromethanesulfonate
Ph	phenyl
THF	tetrahydrofuran

References

[1] E. Jacobsen, A. Pfaltz, H. Yamamoto, Comprehensive Asymmetric Catalysis I-III, Springer.
[2] H. Steinhagen, G. Helmchen, Angew. Chem. Int. Ed. 35 (1996) 2339.
[3] G.J. Rowlands, Tetrahedron 57 (2001) 1865.
[4] J.A. Ma, D. Cahard, Angew. Chem. Int. Ed. 43 (2004) 4566.
[5] E.K. Van den Beuken, B.L. Feringa, Tetrahedron 54 (1998) 12985.
[6] A.L. Gavrilova, B. Bosnich, Chem. Rev. 104 (2004) 349.
[7] T. Miyake, T. Asakawa, Appl. Catal. A 208 (2005) 47.
[8] R.-J. Wang, X.K. Yao, Z.Z. Zhang, H.K. Wang, Chin. J. Struct. Chem. 8 (1989) 184.
[9] T. Suzuki, N. Iitaka, S. Kurachi, M. Kita, K. Kashiwabara, S. Ohba, J. Fujita, Bull. Chem. Soc. Jpn. 65 (1992) 1817.
[10] L. Párkányi, G. Szalontai, G. Besenyei, Inorg. Chim. Acta 359 (2006) 2933–2941.
[11] Z.Z. Zhang, H.K. Wang, Z. Xi, X.K. Yao, R.J. Wang, J. Organomet. Chem. 376 (1989) 123.
[12] M. Rashidi, M.C. Jennings, R.J. Puddephatt, Organometallics 22 (2003) 2612.
[13] S. Jaaskelainen, M. Haukka, H. Riihimaki, J.T. Pursiainen, T.A. Pakkanen, J. Organomet. Chem. 689 (2004) 1064.
[14] A. Dervisi, P.G. Edwards, P.D. Newman, R.P. Tooze, S.J. Coles, M.B. Hursthouse, J. Chem. Soc., Dalton Trans. (1998) 3771.
[15] S.-M. Kuang, P.E. Fanwick, R.A. Walton, Inorg. Chim. Acta 305 (2000) 102.
[16] S. Wingerter, M. Pfeiffer, F. Baier, T. Stey, D. Stalke, Z. Anorg. Allg. Chem. 626 (2000) 1121.
[17] D. Fenske, B. Maczek, K. Maczek, Z. Anorg. Allg. Chem. 623 (1997) 1113.
[18] J.P. Farr, M.M. Olmstead, A. Balch, J. Am. Chem. Soc. 102 (1980) 6654.
[19] J.P. Farr, M.M. Olmstead, C.H. Hunt, A. Balch, Inorg. Chem. 20 (1981) 1182.
[20] G.R. Newkome, Chem. Rev. 93 (1993) 2067.
[21] Z.Z. Zhang, H. Cheng, Coord. Chem. Rev. 147 (1996) 1.
[22] P. Espinet, K. Soulantica, Coord. Chem. Rev. 193–195 (1999) 499.
[23] C.G. Arena, G. Bruno, G. De Munno, E. Rotondo, D. Drommi, F. Faraone, Inorg. Chem. 32 (1993) 1601.
[24] W.W. Yam, L.P. Chan, T.F. Lai, J. Chem. Soc., Dalton Trans. (1993) 2075.
[25] G.A. Abakumov, V.K. Cherkasov, V.I. Nevodchikov, I.A. Teplova, L.N. Zakharov, G.K. Fukin, Y.T. Struchkov, Izv. Akad. Nauk. SSSR, Ser. Khim. (Russ.) (Russ. Chem. Bull.) (1996) 464.
[26] M. Maekawa, M. Munakata, S. Kitagawa, T. Yonezawa, Bull. Chem. Soc. Jpn. 64 (1991) 2286.
[27] C.G. Avena, E. Rotondo, F. Faraone, M. Lanfranchi, A. Tiripicchio, Organometallics 10 (1991) 3877.
[28] A. Ecke, W. Keim, M.C. Bonnet, I. Tratchenko, F. Dahan, Organometallics 14 (1995) 5302.
[29] N.W. Alcock, P. Moore, P.A. Lampe, K.F. Mok, J. Chem. Soc., Dalton Trans. (1982) 207.
[30] E. Lastra, M.P. Gamasa, J. Gimeno, M. Lanfranchi, A. Tiripicchio, J. Chem. Soc., Dalton Trans. (1989) 1499.
[31] A. Cingolani, Effendy, D. Martini, C. Pettinari, B.W. Skelton, A.H. White, Inorg. Chim. Acta 359 (2006) 2183.
[32] L. Wei, L. Haifeng, Z. Lansun, W. Dingming, Z. Honghui, Dax. Xiamen, Xuebau, Zir. Kex. (Chin.)(J. Xiamen Univ. (Nat. Sci.) 34 (1995) 946.
[33] A. Del Zotto, E. Zangrando, Inorg. Chim. Acta 277 (1998) 111.
[34] Q.M. Wang, Y.A. Lee, O. Crespo, J. Deaton, C. Tang, H.J. Gysling, M.C. Gimeno, C. Larraz, M.D. Villacampa, A. Laguna, R. Eisenberg, J. Am. Chem. Soc. 126 (2004) 9488.
[35] T.J. Barder, F.A. Cotton, G.L. Powell, S.M. Tetrick, R.A. Walton, J. Am. Chem. Soc. 106 (1984) 1323.
[36] F.A. Cotton, K.R. Dunbar, M. Matusz, Polyhedron 5 (1986) 903.
[37] F.A. Cotton, M. Matusz, Polyhedron 7 (1988) 2201.
[38] F.A. Cotton, M. Matusz, Inorg. Chim. Acta 157 (1989) 223.
[39] R.J. Wang, X.-K. Yao, Z.Z. Zhang, H.K. Wang, J. Struct. Chem. 8 (1989) 184.
[40] T. Suzuki, J. Fujita, Chem. Lett. (1992) 1067.
[41] A.L. Balch, M.M. Olmstead, S.P. Rowley, Inorg. Chim. Acta 168 (1990) 255.
[42] A.M. Larsonneur, R. Turpin, P. Castan, G. Bernardinelli, Inorg. Chim. Acta 227 (1994) 85.
[43] A.M. Larsonneur, R. Turpin, P. Ferte, P. Castan, G. Bernardinelli, Transition Met. Chem. 19 (1994) 548.
[44] L.J. Tortorelli, C.A. Tucker, C. Woods, J. Bordner, Inorg. Chem. 25 (1986) 3534.
[45] F. Shafiq, R. Eisenberg, Inorg. Chem. 32 (1993) 3287.
[46] R.E. Marsh, Acta Crystallogr., Sect. B: Struct. Sci. 53 (1997) 317.
[47] F.A. Cotton, M. Matusz, Inorg. Chim. Acta 143 (1988) 45.
[48] E. Rotondo, G. Bruno, F. Nicolo, S.L. Schiavo, P. Piraino, Inorg. Chem. 30 (1991) 1195.
[49] J.S. Field, R.J. Haines, C.J. Parry, J. Chem. Soc., Dalton Trans. (1997) 2843.
[50] G. Espino, F.A. Jalón, M. Maestro, B.R. Manzano, M. Pérez-Manrique, A.C. Bacigalupe, Eur. J. Inorg. Chem. (2004) 2542.
[51] S. Jaaskelainen, M. Haukka, H. Riihimaki, J.T. Pursiainen, J. Organomet. Chem. 689 (2004) 1064.
[52] C. Tejel, M.A. Ciriano, R. Bravi, L.A. Oro, C. Graiff, R. Galassi, A. Burini, Inorg. Chim. Acta 347 (2003) 129.
[53] V. Díez, G. Espino, F.A. Jalón, B.R. Manzano, M. Pérez-Manrique, J. Organomet. Chem. 692 (2007) 1482.
[54] J.P. Farr, F.E. Wood, A.L. Balch, Inorg. Chem. 22 (1983) 3387.
[55] Y. Inoguchi, B. Milewski-Mahrla, H. Schmidbaur, Chem. Ber. 115 (1982) 3085.
[56] F. Bachechi, A. Burini, M. Fontani, R. Galassi, A. Macchioni, B.R. Pietroni, P. Zanello, C. Zuccaccia, Inorg. Chim. Acta 323 (2001) 45.
[57] M.A. Jalil, T. Yamada, S. Fujinami, T. Honjo, H. Nishikawa, Polyhedron 20 (2001) 627.
[58] F. Bachechi, A. Burini, R. Galassi, A. Macchioni, B.R. Pietroni, F. Ziarelli, C. Zuccaccia, J. Organomet. Chem. 593–594 (2000) 392.
[59] F. Bachechi, A. Burini, R. Galassi, B.R. Pietroni, M. Ricciutelli, Inorg. Chim. Acta 357 (2004) 4349.
[60] V.J. Catalano, S.J. Horner, Inorg. Chem. 42 (2003) 8430.
[61] C.R. Johnson, R.E. Shepherd, Inorg. Chem. 22 (1983) 3506.
[62] K.K. Klausmeyer, F. Hung-Low, Acta Crystallogr., Sect. E: Struct. Rep. Online 63 (2007) m1931.
[63] O. Crespo, E.J. Fernández, M. Gil, M.C. Gimeno, P.G. Jones, A. Laguna, J.M. López-de-Luzuriaga, M.E. Olmos, J. Chem. Soc., Dalton Trans. (2002) 1319.
[64] K.M. Cooper, G.J. Organ, J. Chem. Soc., Dalton Trans. (1988) 2287.
[65] V.D. Fester, P.J. Houghton, L. Main, B.K. Nicholson, Polyhedron 26 (2007) 430.
[66] S.I. Pascu, G.D.W. Anderson, M.L.H. Green, J.C. Green, N.H. Rees, A.R. Cowley, Inorg. Chim. Acta 359 (2006) 3677.
[67] L. Hirsivaara, M. Haukka, J. Pursiainen, J. Organomet. Chem. 633 (2001) 66.
[68] M. Hatano, T. Asai, K. Ishihara, Chem. Lett. 35 (2006) 172.
[69] H. Nagashima, T. Sue, T. Oda, A. Kanemitsu, T. Matsumoto, Y. Motoyama, Y. Sunada, Organometallics 25 (2006) 1987.
[70] Y. Sunada, T. Sue, T. Matsumoto, H. Nagashima, J. Organomet. Chem. 691 (2006) 3176.
[71] Z.-Z. Zhang, H.-P. Xi, W.-J. Zhao, K.-Y. Jiang, R.-J. Wang, H.-G. Wang, Y. Wu, J. Organomet. Chem. 454 (1993) 221.
[72] Z.Z. Zhang, H. Cheng, S.M. Kuang, Y.Q. Zhou, Z.X. Liu, J.K. Zhang, H.G. Wang, J. Organomet. Chem. 516 (1996) 1.
[73] S.M. Kuang, F. Xue, C.Y. Duan, T.C.W. Mak, Z.Z. Zhang, J. Organomet. Chem. 534 (1997) 15.
[74] S.L. Li, C.W. Mak, Z.Z. Zhang, J. Chem. Soc., Dalton Trans. (1996) 3475.
[75] S.M. Kuang, Z.Z. Zhang, K. Chinnakali, H.K. Fun, T.C.W. Mak, Inorg. Chim. Acta 293 (1999) 106.
[76] S.M. Kuang, H. Cheng, L.J. Sun, Z.Z. Zhang, Z.Y. Zhou, B.M. Wu, T.C.W. Mak, Polyhedron 15 (1996) 3417.
[77] S.M. Kuang, Z.Z. Zhang, B.M. Wu, T.C.W. Zhang, J. Organomet. Chem. 540 (1997) 55.
[78] W.H. Chan, Z.Z. Zhang, T.C.W. Mak, C.M. Che, J. Chem. Soc., Dalton Trans. (1998) 803.
[79] H.B. Song, Z.Z. Zhang, T.C.W. Mak, New J. Chem. 26 (2002) 113.
[80] S.M. Kuang, F. Xue, Z.Z. Zhang, W.M. Xue, C.M. Che, T.C.W. Mak, J. Chem. Soc., Dalton Trans. (1997) 3409.
[81] S.-M. Kuang, F. Xue, T.C.W. Mak, Z.-Z. Zhang, Inorg. Chim. Acta 284 (1999) 119.
[82] G. Francio', R. Scopelliti, C.G. Arena, G. Bruno, D. Drommi, F. Faraone, Organometallics 17 (1998) 338.
[83] J.P. Farr, M.M. Olmstead, A.l. Balch, Inorg. Chem. 22 (1983) 1229.
[84] A. Maisonnet, J.P. Farr, M.M. Olmstead, C.T. Hunt, A.L. Balch, Inorg. Chem. 21 (1982) 3961.
[85] J.R. Sowa, V. Zanotti, G. Facchin, R. Angelici, J. Am. Chem. Soc. 113 (1991) 9185.
[86] T. Suzuki, J. Fujita, Bull. Chem. Soc. Jpn. 65 (1992) 1016.
[87] Q.F. Mokuolu, P.A. Duckmanton, P.B. Hitchcock, C. Wilson, A.J. Blake, L. Shukla, J.B. Love, Dalton Trans. (2004) 1960.
[88] R.J. Haines, J.S. Field, B. Warwick, M.M. Zulu, Polyhedron 15 (1996) 3741.

[89] A.L. Balch, L.A. Fossett, M.M. Olmstead, Inorg. Chem. 25 (1986) 4526.
[90] F.A. Cotton, E.V. Dikarev, G.T. Jordan IV, C.A. Murillo, M.A. Petrukhina, Inorg. Chem. 37 (1998) 4611.
[91] H.B. Song, Z.Z. Zhang, T.C.W. Mak, Inorg. Chem. Commun. 5 (2002) 442.
[92] H.B. Song, Z.Z. Zhang, T.C.W. Mak, J. Chem. Soc., Dalton Trans. (2002) 1336.
[93] Z. Galdecki, E. Galdcki, A. Kowalski, F.P. Pruchnik, K. Wajda-Hermanowicz, R. Starosta, Pol. J. Chem. 73 (1999) 859.
[94] M. Driess, F. Franke, K. Merz, Eur. J. Inorg. Chem. (2001) 2661.
[95] T. Zhang, C. Chen, Y. Qin, X. Meng, Inorg. Chem. Commun. 9 (2006) 72.
[96] K. Mashima, H. Nakano, T. Mori, H. Takaya, A. Nakamura, Chem. Lett. (1992) 185.
[97] K. Mashima, M. Tanaka, K. Tani, J. Am. Chem. Soc. 119 (1997) 4307.
[98] S.M. Kuang, P.E. Fanwick, R.A. Walton, J. Chem. Soc., Dalton Trans. (2002) 2501.
[99] K. Mashima, M. Tanaka, K. Tani, H. Nakano, A. Nakamura, Inorg. Chem. 35 (1996) 5244.
[100] T.C.W. Mak, K.S. Chan, H.-B. Song, Z.Z. Zhang, Private Communication, 2003.
[101] R.A. Walton, S.M. Kuang, P.E. Fanwick, Inorg. Chim. Acta 305 (2000) 102.
[102] S.M. Kuang, Z.Z. Zhang, Q.G. Wang, T.C.W. Mak, J. Chem. Soc., Dalton Trans. (1998) 2927.
[103] S.M. Kuang, Z.Z. Zhang, Q.G. Wang, T.C.W. Mak, J. Chem. Soc., Dalton Trans. (1998) 1115.
[104] S.M. Kuang, Z.Z. Zhang, Q.-G. Wang, T.C.W. Mak, J. Organomet. Chem. 558 (1998) 131.
[105] Z.Z. Zhang, S.M. Kuang, Q.G. Wang, T.C.W. Mak, J. Chem. Soc., Dalton Trans. (1997) 4477.
[106] J.S. Field, R.J. Haines, C.J. Parry, S.H. Sookraj, Polyhedron (1993) 2425.
[107] H.B. Song, Q.M. Wang, Z.Z. Zhang, T.C.W. Mak, J. Organomet. Chem. 605 (2000) 15.
[108] D.-J. Cui, Q.S. Li, F.B. Xu, X.B. Leng, Z.Z. Zhang, Organometallics 20 (2001) 4126.
[109] T. Zhang, Y. Qin, D. Wu, C. Wang, C. Liu, J. Coord. Chem. 58 (2005) 1485.
[110] A.R.H. Al-Soudani, A.S. Batsanov, P.G. Edwards, J.A.K. Howard, J. Chem. Soc., Dalton Trans. (1994) 987.
[111] A.R.H. Al-Soudani, P.G. Edwards, M.B. Hursthouse, K.M.A. Malik, J. Chem. Soc., Dalton Trans. (1995) 335.
[112] S.B. Harkins, J.C. Peters, J. Am. Chem. Soc. 127 (2005) 2030.
[113] M. Sauthier, B. Le Guennic, V. Deborde, L. Toupet, J.-F. Halet, R. Réau, Angew. Chem. Int. Ed. 40 (2001) 228.
[114] F. Leca, M. Sauthier, V. Deborde, L. Toupet, R. Réau, Chem. Eur. J. 9 (2003) 3785.
[115] F. Leca, C. Lescop, E. Rodriguez-Sanz, K. Costuas, J.-F. Halet, R. Réau, Angew. Chem. Int. Ed. 44 (2005) 4362.
[116] B. Nohra, S. Graule, C. Lescope, R. Réau, J. Am. Chem. Soc. 128 (2006) 3520.
[117] M.A. Alonso, J.A. Casares, P. Espinet, K. Soulantica, J.P.H. Charmant, A.G. Orpen, Inorg. Chem. 39 (2000) 705.
[118] M. Alvarez, N. Lugan, R. Mathieu, J. Chem. Soc., Dalton Trans. (1994) 2755.
[119] A. Del Zotto, P. Rigo, G. Nardin, Inorg. Chim. Acta 247 (1996) 183.
[120] J.A. Casares, P. Espinet, K. Soulantica, I. Pascual, A.G. Orpen, Inorg. Chem. 36 (1997) 5251.
[121] H.P.M.M. Ambrosius, F.A. Cotton, L.R. Falvello, H.T.J.M. Hintzen, T.J. Melton, W. Schwotzer, Inorg. Chem. 23 (1984) 1611.
[122] J.T. Mague, J.L. Krinsky, Inorg. Chem. 40 (2001) 1962.
[123] M.P. Anderson, C.C. Tso, B.M. Mattson, L.H. Pignolet, Inorg. Chem. 22 (1983) 3267.
[124] M.P. Anderson, B.M. Mattson, L.H. Pignolet, Inorg. Chem. 22 (1983) 2644.
[125] J.T. Mague, S.W. Hawbaker, J. Chem. Crystallogr. 27 (1997) 603.
[126] H.F. Lang, P.E. Fanwick, R.A. Walton, Inorg. Chim. Acta 328 (2002) 232.
[127] S. Jie, M. Agostinho, A. Kermagoret, C.S. Cazin, P. Braunstein, Dalton Trans. (2007) 4472.
[128] R.J. McNair, P.V. Nilsson, L.H. Pignolet, Inorg. Chem. 24 (1985) 1935.
[129] P. Braunstein, G. Clerc, X. Morise, R. Welter, G. Mantovani, J. Chem. Soc., Dalton Trans. (2003) 1601.
[130] P. Braunstein, G. Clerc, X. Morise, New J. Chem. 27 (2003) 68.
[131] H. Han, M. Elsmaili, S.A. Johnson, Inorg. Chem. 45 (2006) 7435.
[132] R. Ziessel, Tetrahedron Lett. 30 (1998) 463.
[133] T. Tanase, T. Igoshi, K. Kobayashi, Y. Yamamoto, J. Chem. Res. (1998) 538.
[134] T.G. Shenck, J.M. Downes, C.R.C. Milne, P.B. Mackenzie, H. Boucher, J. Whelan, B. Bosnich, Inorg. Chem. 24 (1985) 2334.
[135] T.G. Schenck, C.R.C. Milne, J.F. Sawyer, B. Bosnich, Inorg. Chem. 24 (1985) 2338.
[136] S. Tanaka, C. Dubs, A. Inagaki, M. Akita, Organometallics 24 (2005) 163.
[137] S. Tanaka, C. Dubs, A. Inagaki, M. Akita, Organometallics 23 (2004) 317.
[138] N. Tsukada, O. Tamura, Y. Inoue, Organometallics 21 (2002) 2521.
[139] X. Liu, A.H. Eisenberg, C.L. Stern, C.A. Mirkin, Inorg. Chem. 40 (2001) 2940.
[140] P.H.M. Budzellaar, J.H.G. Frijns, A.G. Orpen, Organometallics 9 (1990) 1222.
[141] M. Gómez, S. Jansat, G. Muller, D. Panyella, P.W.N.M. van Leeuwen, P.C.J. Kamer, K. Goubitz, J. Fraanje, Organometallics 18 (1999) 4970.
[142] P. Paul, K. Venkatasubramanian, S. Purohit, J. Coord. Chem. 28 (1993) 279.
[143] M.M.T. Khan, P. Paul, K. Venkatasubramanian, S. Purohit, J. Chem. Soc., Dalton Trans. (1991) 3405.
[144] M.M.T. Khan, B. Swamy, Inorg. Chem. 26 (1987) 178.
[145] P. Paul, B. Tyagi, J. Coord. Chem. 10 (1996) 213.
[146] P. Paul, B. Tyagi, Polyhedron 15 (1996) 675.
[147] M.M.T. Khan, C. Sreelatha, P. Paul, K. Venkatasubramanian, Indian J. Chem. 32 (1993) 143–146.
[148] M.M.T. Khan, P. Paul, S. Purohit, Inorg. Chim. Acta 189 (1991) 165.
[149] M.F.M. Al-Dulaymmi, A. Hills, P.B. Hitchcock, D.L. Hughes, R.L. Richards, J. Chem. Soc., Dalton Trans. (1992) 241.
[150] M.F.M. Al-Dulaymmi, P.B. Hitchcock, R.L. Richards, J. Organomet. Chem. 338 (1988) C31.
[151] J.N.L. Dennett, M. Bierenstiel, M.J. Ferguson, R. McDonald, M. Cowie, Inorg. Chem. 45 (2006) 3705.
[152] S.J.L. Foo, N.D. Jones, B.O. Patrick, B.R. James, Chem. Commun. (2003) 988.
[153] N.D. Jones, S.J.L. Foo, B.O. Patrick, B.R. James, Inorg. Chem. 43 (2004) 4056.
[154] H. Nagashima, K. Matsubara, T. Oda, Vol. JKXXAF JP 2004067511 A 20040304 (Ed.: Japan, Japan Science and Technology Corporation), 2004.
[155] W.J. Zhao, Y.Q. Fang, S.J. Zhang, Y. Li, Z. Z: Zhang, X.K. Wang, Ion Exch. Adsorp. 8 (1992) 39.
[156] H. Ishii, M. Goyal, M. Ueda, K. Takeuchi, M. Asai, J. Mol. Catal. A: Chem. 148 (1999) 289.
[157] H. Ishii, M. Goyal, M. Ueda, K. Takeuchi, M. Asai, Macromol. Rapid Commun. 22 (2001) 376.
[158] A. Fukuoka, M. Ichikawa, J.A. Hriljac, D.F. Shriver, Inorg. Chem. 26 (1987) 3643.
[159] S.M. Kuang, F. Xue, Z.Y. Zhang, T.C.W. Mak, Z.-Z. Zhang, Q.G. Wang, J. Chem. Soc., Dalton Trans. (1998) 2927.
[160] M. Sauthier, F. Leca, L. Toupet, R. Rau, Organometallics 21 (2002) 1591.
[161] N. Tsukada, T. Mitsuboshi, H. Setoguchi, Y. Inoue, J. Am. Chem. Soc. 125 (2003) 12102.
[162] N. Tsukada, H. Setoguchi, T. Mitsuboshi, Y. Inoue, Chem. Lett. 35 (2006) 1164.
[163] N. Tsukada, K. Murata, Y. Inoue, Tetrahedron Lett. 46 (2005) 7515.
[164] N. Tsukada, S. Ninomiya, Y. Aoyama, Y. Inoue, Org. Lett. 9 (2007) 2919.
[165] N. Tsukada, Y. Ohba, Y. Inoue, J. Organomet. Chem. 687 (2003) 436.
[166] P. Paul, Polyhedron 12 (1993) 2057.
[167] M.M.T. Khan, P. Paul, Polyhedron 11 (1992) 805.
[168] N.D. Jones, B.R. James, Adv. Synth. Catal. 344 (2002) 1126.